Matter-Only Cosmology: A Unified Origin for Inflation and Dark Energy

Hyoyoung Choi[1⋆]

1 Independent Researcher, Seoul, Republic of Korea.

⋆ email

Abstract

The standard cosmological model, ΛCDM, successfully describes cosmic acceleration but treats dark energy as an independent and poorly understood component of the universe. This paper instead demonstrates that dark energy is not a fundamental entity separate from matter, but rather arises as Gravitational Self-Energy (GSE) inherent to matter itself. This model, called Matter-Only Cosmology (MOC), shows that the observed matter density ($\Omega_m \approx 0.315$) naturally generates a dark energy density that is more than twice as large ($\Omega_\Lambda \approx 0.685$), driving late-time cosmic acceleration. This is made possible by the dynamic interplay of two competing GSE-induced terms: a negative self-energy component ($-\rho_{gs}$) and a positive interaction component (ρ_{m-gs}), all within standard General Relativity and without the need for fine-tuning or new fundamental fields. This unified framework provides a coherent resolution to several long-standing problems in cosmology and gravitational physics. It not only provides a concrete physical origin for dark energy, but also predicts its entire life cycle, showing that it is predicted to have been attractive in the early universe, enhancing structure formation, before transitioning to a repulsive phase that drives cosmic acceleration. In doing so, it naturally explains the Hubble tension, the existence of massive galaxies in the early universe, recent indications of a weakening dark energy component, and offers a natural explanation of the cosmological constant coincidence problem. Moreover, MOC unifies the physics of primordial inflation and late-time acceleration as the same GSE dynamics, each with a natural, built-in end mechanism. Finally, by predicting stable, non-singular black hole interiors, MOC offers a physically motivated resolution to the black hole information paradox. By expressing dark energy as an explicit function of the matter density ρ_m and the horizon scale R, the MOC framework transforms it from a phenomenological parameter into an explicitly defined, predictive, and falsifiable physical quantity.

Contents

1 Introduction

The discovery of the accelerated expansion of the universe [1,2] marked a monumental turning point in modern cosmology. To account for this unexpected cosmic acceleration, the standard cosmological model, ΛCDM, introduced an additional component commonly referred to as dark energy [3,4]. Characterized phenomenologically by a positive energy density and a negative pressure, the cosmological constant Λ has proven remarkably successful in reproducing the observed large-scale dynamics of the universe [5].

However, despite its empirical success, the ΛCDM framework faces several deep and persistent conceptual challenges [6,7]. In particular, the physical origin of dark energy remains unknown, indicating that our current description of the cosmic energy budget may be incomplete.

In this work, we argue that the origin of these difficulties does not necessarily require the introduction of new particles, exotic fields, or modifications of gravity, but instead points to an incomplete accounting of the total energy density in gravitating systems, whose consequences become manifest in the Friedmann equations.

Within the standard cosmological framework, dark energy is modeled as a perfect fluid with a constant equation-of-state parameter $w = -1$ [3,4]. While this assumption provides an excellent phenomenological fit to current data, it is not derived from first principles. The most

widely discussed candidate, vacuum energy, leads to the well-known cosmological constant problem, namely a discrepancy of order 10^{60}–10^{120} between theoretical expectations from quantum field theory and the observed value of Λ [7,8]. In addition, the model suffers from the so-called coincidence problem, which asks why the dark energy density becomes dynamically relevant only in the current cosmological epoch [9, 10].

Beyond these theoretical concerns, a growing body of observational evidence suggests that the simplest ΛCDM scenario may be incomplete [11–14]. In particular.

1) **The Hubble tension:** A persistent discrepancy exists between the Hubble constant inferred from early-universe observations of the cosmic microwave background (CMB) and that measured directly in the local universe. This tension may indicate physics beyond a strictly constant dark energy component [11,15]. Quantitatively, $H_0(\mathrm{CMB}) \approx 67.4 \mathrm{kms}^{-1}$ Mpc^{-1} compared to $H_0(\mathrm{local}) \approx 74.0\,\mathrm{km\,s}^{-1}\,\mathrm{Mpc}^{-1}$.

2) **Supernova data anomalies:** Recent analyses of nearly 1500 Type Ia supernovae by the Dark Energy Survey (DES) collaboration suggest that a time-independent cosmological constant may not provide the best fit to the data, allowing room for a dynamical dark energy component [13].

3) **Spectroscopic measurements:** Independent results from the Dark Energy Spectroscopic Instrument (DESI) likewise favor models with evolving dark energy, further challenging the assumption of a strictly constant Λ [12].

Taken together, these theoretical and observational tensions motivate a reassessment of the physical origin of cosmic acceleration. In this paper, we propose that these issues arise from a long-standing omission in the standard treatment of gravitating systems: the failure to explicitly account for gravitational self-energy (GSE) as a contribution to the gravitational source term, as required by the equivalence principle of General Relativity.

1.1 Components of total mass or equivalent mass in a gravitational system

In gravitational physics, it is customary to characterize a gravitating system by an effective or equivalent energy (or mass) that reproduces its external gravitational influence. Even when the detailed composition of the source's internal energy is unknown, one may treat the system as possessing an equivalent mass parameter that implicitly incorporates all internal energy contributions, thereby enabling a consistent description of its external gravitational interactions within a given approximation scheme [16].

Because this equivalent energy–mass framework has been remarkably successful for analyzing external gravitational fields, it is often unnecessary to specify how the equivalent mass is decomposed into its microscopic or internal energy components.

However, this simplification becomes conceptually insufficient when one attempts to analyze the internal energy composition of a gravitating system itself, rather than merely its external gravitational influence.

In cosmology, this distinction becomes particularly important. The system under consideration is not an isolated object embedded in an external spacetime, but the universe itself, within which matter and galaxies reside. Consequently, questions concerning the internal energy structure and self-gravitating dynamics of the cosmic matter distribution can no longer be avoided when interpreting the total gravitating energy budget.

For a generic bound system, the total mass, or more precisely the total energy E_T, can be expressed as the sum of the free-state rest-mass energy of its constituents and all internal binding and interaction energies.

$$E_T = M_{fr}c^2 + \sum_i U_{\mathrm{BE},i} + \sum_{i>j} U_{\mathrm{int},ij} \tag{1}$$

Here $M_{fr}c^2$ denotes the sum of the rest-mass energies of the constituents in their free states. The terms $U_{\mathrm{BE},i}$ represent binding energies associated with composite structures, including gravitational, electromagnetic, weak, and strong interactions. The quantities $U_{\mathrm{int},ij}$ denote interaction energies between different constituents or subsystems.

Dividing by c^2 yields the corresponding total equivalent mass $M_T \equiv E_T/c^2$, which is the quantity that acts as the effective gravitational source in many external-field problems.

1.2 A conceptual analogy: Binding energy in the hydrogen atom and a missing term in the Friedmann equation

A useful analogy for understanding the role of GSE in cosmology is provided by the hydrogen atom. A hydrogen atom is a composite system consisting of a proton and an electron bound together by electromagnetic interaction. Likewise, the universe may be regarded as a composite gravitating system composed of many constituents, such as matter, galaxies, and large-scale structures, which interact gravitationally over cosmological scales.

The total energy of a hydrogen atom is given by

$$E_H = E_p + E_e + U_{\mathrm{binding}} \tag{2}$$

Here E_p and E_e are the rest-mass energies of the proton and electron in their free states.

The quantity $U_{\mathrm{binding}} < 0$ denotes the electromagnetic binding energy. Because the binding energy is negative, the total energy and hence the invariant mass of the hydrogen atom is smaller than the sum of the free-state particle masses. When a hydrogen atom acts as a gravitational source, the gravitating mass is, in principle, determined by its total energy content, including the contribution from binding energy, rather than by the free-state particle masses alone [16].

Correspondingly, one may express the total equivalent mass density schematically as

$$\rho_T = \rho_p + \rho_e + \rho_{\mathrm{binding}} \tag{3}$$

Here $\rho_{\mathrm{binding}} \equiv U_{\mathrm{binding}}/(Vc^2)$ represents the contribution of binding energy per unit volume V. This viewpoint, namely that internal binding energy contributes to the total mass-energy of a bound system, is standard in atomic, nuclear, and particle physics.

Let us now examine what is effectively assumed in standard cosmology. Neglecting the spatial curvature term for simplicity, the Friedmann equation is written as

$$H^2 = \frac{8\pi G}{3}\rho_T = \frac{8\pi G}{3}(\rho_m + \rho_\Lambda) \tag{4}$$

Here ρ_m denotes the matter density.

The quantity ρ_Λ is introduced as a separate dark energy component [3, 5]. In practice, ρ_m is constructed from the free-state mass densities of matter constituents (baryons and dark matter), analogous to using $\rho_p + \rho_e$ for the hydrogen atom. Observationally, however, the inferred matter density alone is subcritical at late times, while the expansion history indicates a total energy density close to the critical value. This motivates the introduction of an additional energy-density component ρ_Λ within the standard cosmological interpretation [1, 2, 8].

We argue that this procedure may reflect an incomplete accounting of the total gravitating energy budget. From the standpoint of General Relativity, the source term governing cosmic

expansion is the total stress-energy content, which suggests that all relevant contributions to the system's energy, including those associated with self-gravitating interactions, should in principle be taken into account [16–18].

In a cosmological context, this motivates considering a decomposition of the form

$$\rho_T = \rho_{\text{free}} + \rho_{\text{GSE}} \tag{5}$$

Here ρ_{GSE} represents an effective contribution associated with GSE. This term arises from the mutual gravitational interactions of matter within the causally connected region.

By omitting such a contribution and modeling the additional required energy density as an independent fluid component, standard cosmology introduces ρ_Λ phenomenologically. We argue that the physical origin of dark energy lies in GSE itself, and that the introduction of ρ_Λ in standard cosmology reflects a systematic omission of this contribution from the total gravitating energy density.

Finally, we note an important conceptual point. Gravitational binding energy is conventionally negative, as it represents the energy required to disassemble a bound system into free components. However, as will be shown in the following sections, the self-gravitating contribution to the cosmological energy budget is not restricted to being purely negative. Depending on the scale and compactness of the causally connected system, the net contribution associated with GSE can become positive and thereby act as a source of repulsive cosmic dynamics.

This perspective suggests that what is conventionally identified as dark energy may instead reflect an intrinsic manifestation of GSE, consistently included in the total energy accounting as required by the principles of General Relativity.

1.3 Gravitational field energy vs. gravitational self-energy

A frequent source of confusion in discussions of GSE arises from conflating it with the energy of the gravitational field itself. In General Relativity, it is well established that the energy of the gravitational field cannot be localized in a coordinate independent manner [16, 18]. Because the gravitational field extends beyond the material source and depends on the choice of coordinates, no unique local energy density can be assigned to it. For this reason, gravitational field energy does not appear explicitly as a source term in the Einstein field equations, but is instead encoded implicitly through their nonlinear structure [17, 18].

GSE, however, represents a conceptually distinct physical quantity. It does not correspond to the energy of the gravitational field in empty space, but rather to the gravitational potential energy associated with interactions among the constituents of a gravitating system [16]. As such, GSE is defined with respect to the finite mass distribution and finite spatial extent of the system itself.

In contrast to gravitational field energy, GSE is defined with respect to the finite mass distribution and finite spatial extent of the system, and therefore contributes to the total energy characterizing that system in a well defined manner [16].

> *The mass energy of a gravitating system includes the negative binding energy, such that the total gravitational mass is less than the sum of the constituent rest masses.* [19]

This distinction is familiar in other areas of physics. In atomic physics, for example, the mass of a hydrogen atom is smaller than the sum of the rest masses of a free proton and electron. The difference corresponds to the negative electromagnetic binding energy, which contributes to the invariant mass of the bound system [16, 18]. The atom is therefore treated as a single object whose total mass already incorporates its internal binding energy.

There is no compelling physical reason to treat gravity differently in this respect. Although gravitational field energy itself cannot be represented as a local density, the binding energy associated with gravitational interactions among matter constituents contributes to the total energy of a self gravitating system. In a cosmological setting, this contribution is therefore relevant to the effective energy density that governs the expansion dynamics. Neglecting GSE in this context corresponds to describing the system using only free state mass densities, rather than the total equivalent mass required by a consistent accounting of energy in General Relativity.

2 Gravitational Self-Energy as the Origin of Dark Energy

In a cosmological context, the binding energies associated with the strong, weak, and electromagnetic interactions are confined to microscopic and effectively time independent scales, and may therefore be regarded as part of the free state mass M_{fr}. In contrast, GSE is determined by the macroscopic distribution of matter M and by the evolving spatial scale of the universe R. As cosmic expansion proceeds, GSE is not constant but evolves dynamically, actively participating in the global energy budget of the universe. This observation leads to the central thesis of this work, namely that the phenomenon conventionally labeled as dark energy is not a new exotic component, but rather the manifestation of the universe's own dynamical GSE.

2.1 The equivalent gravitational source

The calculation of gravitational potential energy involves integrating the contributions of infinitesimal mass elements dm as they are assembled within the gravitational field generated by the interior mass $M'(r)$. In its standard form, the differential contribution is written as

$$dU_{gs} = -G\frac{M'(r)}{r}dm \tag{6}$$

A fundamental principle of General Relativity is that all forms of energy contribute to gravitation [17, 18]. It follows that gravitational potential energy, or GSE, must itself contribute to the effective gravitational source. In conventional treatments, however, the gravitational influence of self-energy is not incorporated explicitly, since the source mass is taken to be the free state mass alone.

The central postulate of this work is that the interior source term $M'(r)$ should instead be replaced by an equivalent gravitational source $M_{\rm eq}(r)$, which includes both the material mass and the equivalent mass associated with GSE, denoted by $M'_{gs}(r)$.

$$M_{\rm eq}(r) = M'(r) - M'_{gs}(r) \tag{7}$$

For a general mass distribution, the GSE of the interior sphere of radius r and mass $M'(r)$ is parameterized by a structural coefficient β, which encapsulates the effects of mass geometry and relativistic corrections. For a uniform sphere in Newtonian gravity, $\beta = 3/5$, while more compact or relativistic configurations admit values in the range $\beta \approx 1.0$ to 2.0 [20, 21].

$$U_{gs}(r) = -\beta\frac{GM'(r)^2}{r} \tag{8}$$

The equivalent mass associated with this self-energy is therefore given by

$$-M'_{gs}(r) = \frac{U_{gs}(r)}{c^2} = -\beta\frac{GM'(r)^2}{rc^2} \tag{9}$$

Substituting this back into the equivalent source equation yields [22].

$$M_{\text{eq}}(r) = M'(r)\left(1 - \beta \frac{GM'(r)}{rc^2}\right) \tag{10}$$

The **total GSE,** $U_{\text{gs-T}}$, is the integral of the differential energy contributions from $r = 0$ to the final radius R.

$$U_{\text{gs-T}} = \int_0^R dU_{\text{gs-T}} = \int_0^R -G\frac{M_{\text{eq}}(r)}{r} dm \tag{11}$$

Assuming a uniform density ρ for analytical clarity, we have $M'(r) = \frac{4}{3}\pi r^3 \rho$ and the differential mass shell is $dm = 4\pi r^2 \rho\, dr$. Substituting these into the integral.

$$U_{\text{gs-T}} = \int_0^R -G\frac{1}{r}\left[M'(r)\left(1 - \beta \frac{GM'(r)}{rc^2}\right)\right](4\pi r^2 \rho\, dr) \tag{12}$$

$$= -4\pi G\rho \int_0^R r\left[M'(r) - \frac{\beta G}{c^2}\frac{M'(r)^2}{r}\right] dr \tag{13}$$

We now substitute $M'(r) = \frac{4}{3}\pi r^3 \rho$.

$$U_{\text{gs-T}} = -4\pi G\rho \int_0^R r\left[\left(\frac{4\pi}{3}\rho r^3\right) - \frac{\beta G}{c^2 r}\left(\frac{4\pi}{3}\rho r^3\right)^2\right] dr \tag{14}$$

$$= \int_0^R \left(-\frac{16\pi^2 G\rho^2}{3} r^4 + \frac{64\pi^3 \beta G^2 \rho^3}{9c^2} r^6\right) dr \tag{15}$$

$$U_{\text{gs-T}} = \frac{3}{5}\left[-\frac{16\pi^2 G\rho^2 R^5}{9} + \frac{320\pi^3 \beta G^2 \rho^3 R^7}{189c^2}\right] \tag{16}$$

To account for the relativistic contributions and the geometric distribution of mass in a general self-gravitating system, we generalize the Newtonian coefficient 3/5 to the structural parameter β.

$$U_{\text{gs-T}} = \beta\left[-\frac{16\pi^2 G\rho^2 R^5}{9} + \frac{320\pi^3 \beta G^2 \rho^3 R^7}{189c^2}\right] \tag{17}$$

Performing the definite integration yields the final expression for the total GSE or total GSE [22].

$$U_{\text{gs-T}} = -\beta\frac{GM^2}{R} + \frac{5}{7}\beta^2\frac{G^2M^3}{c^2R^2} = -\beta\frac{GM^2}{R}\left(1 - \frac{5\beta}{7}\frac{GM}{c^2R}\right) \tag{18}$$

This can also be written in a factored form to highlight the repulsive correction.

$$\boxed{U_{\text{gs-T}} = \beta\frac{GM^2}{R}\left(\frac{5\beta}{7}\frac{GM}{c^2R} - 1\right)} \tag{19}$$

2.2 Connection to post-Newtonian gravity: Validation and reinterpretation

It is important to emphasize that the functional form of the self-energy correction derived in Eq. (19) is not an ad hoc assumption, but is structurally consistent with results obtained within General Relativity. In the post-Newtonian approximation, the total energy of a self-gravitating system contains relativistic corrections arising from the nonlinear structure of the Einstein field equations. Chandrasekhar [23] and Weinberg [18] showed that the gravitational

potential energy of a static spherical mass distribution, evaluated to first post-Newtonian order at order $1/c^2$, can be written in the form

$$U_{PN} \approx -\frac{3}{5}\frac{GM^2}{R}\left(1-\kappa\frac{GM}{Rc^2}\right) \tag{20}$$

Here κ is a dimensionless coefficient of order unity. Its value depends on the internal structure and pressure distribution of the system.

The close correspondence between the nonperturbative GSE resummation $U_{\text{gs-T}}$ and the formal post-Newtonian expansion U_{PN} serves two essential roles.

1) **Validation:** It demonstrates that treating GSE as an effective contribution to the gravitational source captures the leading nonlinear corrections predicted by General Relativity, without requiring an explicit tensorial expansion.

2) **Reinterpretation in a cosmological context:** In standard post-Newtonian theory, this term is interpreted as a small correction to the binding energy relevant for stellar structure. In contrast, we identify the total GSE as the physical origin of dark energy. When applied to cosmology, where M represents the mass contained within the causally connected region, the cumulative GSE is no longer negligible and can dominate the large scale dynamics, thereby driving accelerated expansion.

By deriving this contribution from a physical principle rather than from a truncated perturbative expansion, the GSE framework elevates what appears as a small correction in the post-Newtonian approach to a central dynamical ingredient. This provides a transparent mechanism for effective repulsive gravity that remains implicit in the standard post-Newtonian formulation.

1) **Approximation versus principle:** Chandrasekhar's result is obtained through a perturbative expansion of the Einstein field equations and is strictly valid only in the weak field regime where $GM/(Rc^2) \ll 1$ and in the slow motion limit. Higher order contributions are therefore systematically neglected [23–25]. In contrast, the present derivation is nonperturbative and self consistent, arising from a closed form resummation of GSE based on energy conservation rather than on a truncated weak field expansion. This suggests that the framework may remain applicable in regimes where standard post-Newtonian methods lose accuracy, including the early universe or strongly gravitating environments.

2) **Static versus dynamic applicability:** Post-Newtonian analyses typically assume quasi static equilibrium, such as hydrostatic or virial balance, which is appropriate for stellar configurations [23–25]. The core mechanism of the GSE framework, namely the replacement of bare mass by equivalent mass through $M \to M_{\text{eq}}$, relies instead on local energy conservation and does not require static equilibrium. The approach is therefore naturally suited to dynamic cosmological settings, including phases of rapid expansion or contraction where hydrostatic assumptions are invalid.

Accordingly, the present result should not be regarded as a mere reproduction of the post-Newtonian approximation, but rather as an effective resummation that captures the essential physics of gravitational self-repulsion in a compact analytical form applicable across a wide range of cosmic epochs.

2.3 The necessity of the GSE framework in cosmology

A common critique of semiclassical approaches is that they are not derived directly from the full formalism of General Relativity. This critique, however, overlooks the practical and mathematical limitations of exact General Relativistic solutions in a cosmological setting.

It is a well established mathematical result that no closed form analytic solution of the Einstein field equations exists for the interior of a gravitating system with nonzero density [24, 25]. While numerical methods such as solutions of the Tolman-Oppenheimer-Volkoff (TOV) equations provide accurate descriptions of static compact objects, these approaches are both mathematically and physically unsuitable for cosmological systems, which are characterized by low density and dynamical expansion rather than hydrostatic equilibrium.

As a consequence, there currently exists no analytic solution derived from exact General Relativity for the total GSE of the universe [25].

In contrast, the GSE framework provides a closed form analytic expression for an effective energy contribution that incorporates self-gravitating interactions on cosmological scales. By basing the derivation on the principle of source renormalization through self-energy, the framework bypasses the intractability of the full field equations while remaining physically testable. Its consistency with the first order post-Newtonian results derived by Chandrasekhar provides an important cross check of validity [23]. Moreover, the framework is conceptually aligned with the fact that the Friedmann equation itself admits a derivation from energy conservation arguments within Newtonian mechanics [16, 26, 27].

At present, the GSE framework therefore represents a viable and analytically tractable approach for investigating the role of self-gravitating energy in the dynamical evolution of the universe.

2.4 The two components of total GSE

The result derived in Eq. (19) constitutes a central element of the present framework. It shows that when GSE is computed self-consistently, it is not a single monolithic contribution, but naturally separates into two distinct components with opposite signs. This decomposition provides the physical basis for identifying GSE as the origin of dark energy.

For clarity and consistent usage throughout this paper, we explicitly define these two components according to their physical origin.

1) **Negative equivalent mass component ($-\rho_{gs}$):** This term corresponds to the GSE obtained at the Newtonian level. The structural parameter β is included to account for the geometry of the mass distribution and relativistic corrections relevant on cosmological scales.

$$-\rho_{gs} \equiv \frac{1}{Vc^2}\left(-\beta\frac{GM^2}{R}\right) < 0 \tag{21}$$

Using $V = \frac{4}{3}\pi R^3$, this expression may be written as

$$-\rho_{gs} = -\frac{3\beta}{4\pi}\frac{GM^2}{c^2R^4} = -\frac{4\pi\beta G}{3c^2}\rho_m^2 R^2 \tag{22}$$

2) **Positive equivalent mass component ($\rho_{m\text{-}gs}$):** This term arises from the interaction between matter and its own GSE. It represents a relativistic correction associated with the fact that GSE itself contributes to the effective gravitational source. In this sense, it is post-Newtonian in character, while remaining fully consistent with the nonperturbative

formulation developed here.

$$\rho_{m\text{-}gs} \equiv \frac{1}{Vc^2}\left(\frac{5\beta^2}{7}\frac{G^2M^3}{c^2R^2}\right) > 0 \tag{23}$$

Using again $V = \frac{4}{3}\pi R^3$, one finds

$$\rho_{m\text{-}gs} = \frac{15\beta^2}{28\pi}\frac{G^2M^3}{c^4R^5} = \frac{80\pi^2\beta^2G^2}{63c^4}\rho_m^3R^4 \tag{24}$$

The total mass energy density of the universe ρ_T is therefore given by the sum of the matter density and the net contribution from GSE. [1]

$$\rho_T = \rho_m + \rho_{\Lambda_m} = \rho_m + \rho_{m\text{-}gs} - \rho_{gs} \tag{25}$$

We therefore identify the total GSE density with the dark energy density,

$$\boxed{\rho_{\Lambda_m} = \rho_{m\text{-}gs} - \rho_{gs}} \tag{26}$$

Expressed explicitly in terms of M and R, this yields

$$\rho_{\Lambda_m} = \frac{3\beta}{4\pi}\frac{GM^2}{c^2R^4}\left(\frac{5\beta}{7}\frac{GM}{c^2R} - 1\right) \tag{27}$$

In terms of the matter density ρ_m and the scale R, the same quantity may be written as

$$\rho_{\Lambda_m}(\rho_m, R) = \frac{4\pi\beta G}{3c^2}\rho_m^2R^2\left[\left(\frac{20\pi\beta G}{21c^2}\right)\rho_mR^2 - 1\right] \tag{28}$$

Defining the constants

$$c_1 \equiv \frac{4\pi G}{3c^2}, \qquad c_2 \equiv \frac{20\pi G}{21c^2}, \qquad R_S \equiv \frac{2GM}{c^2} \tag{29}$$

the dark energy density can be written compactly as

$$\boxed{\rho_{\Lambda_m}(\rho_m, R) = c_1\beta\rho_m^2R^2\left(c_2\beta\rho_mR^2 - 1\right)} \tag{30}$$

Equivalently, in terms of M and R, one obtains

$$\boxed{\rho_{\Lambda_m}(M, R) = \frac{3\beta}{4\pi}\frac{GM^2}{c^2R^4}\left(\frac{5\beta}{14}\frac{R_S}{R} - 1\right)} \tag{31}$$

2.5 Cosmological interpretation: Attraction and repulsion

Having defined the fundamental components of GSE, we now turn to their cosmological interpretation. The dynamical role of each energy or mass component in cosmic expansion is determined by its contribution to the Friedmann acceleration equation,

$$\frac{\ddot{a}}{a} = -\frac{4\pi G}{3}\sum_i(\rho_i + 3P_i) = -\frac{4\pi G}{3}\sum_i\rho_i(1 + 3w_i) \tag{32}$$

In the standard ΛCDM framework, the dark energy component is observationally consistent with an equation of state parameter $w \approx -1$ and a positive energy density, which together imply a negative pressure [3, 4]. It is under this specific cosmological condition that the two components of GSE acquire their distinct roles as sources of attraction and repulsion.

[1] In the Appendix, we present an alternative but equivalent formulation in which the total GSE is explicitly decomposed into a pure self-energy term and a matter self-interaction term, leading to the almost same dark energy contribution.

- **Positive equivalent mass density $\rho_{m\text{-}gs}$:** This component has a positive equivalent energy density, $\rho > 0$. When its effective pressure satisfies $P \approx -\rho$, its contribution to the acceleration equation becomes $(\rho + 3P) \approx -2\rho < 0$. As a result, this term yields $\ddot{a} > 0$ and acts as a source of cosmic repulsion, driving accelerated expansion.

- **Negative equivalent mass density $-\rho_{gs}$:** This component corresponds to a negative equivalent energy density, $\rho < 0$. With the same effective pressure relation $P \approx -\rho$, its contribution becomes $(\rho + 3P) \approx -2\rho > 0$. Consequently, this term yields $\ddot{a} < 0$ and acts as a source of cosmic attraction, contributing to decelerated expansion.

The fundamental entities are therefore the two GSE components, $\rho_{m\text{-}gs}$ and $-\rho_{gs}$.

A point of caution in a cosmological context is that the two quantities $\rho_{m\text{-}gs}$ and $-\rho_{gs}$ should not be interpreted as independent energy components. Although these terms arise naturally from the decomposition of the total GSE, only their combined contribution corresponds to a physically meaningful and observationally relevant energy density. In cosmology, the dark energy component is therefore identified with the total GSE density, $\rho_{\Lambda_m} = \rho_{m\text{-}gs} - \rho_{gs}$.

Accordingly, the appropriate interpretation of the Friedmann acceleration equation is obtained by considering the sign and magnitude of the total equivalent mass density associated with GSE. The resulting cosmic acceleration or deceleration is therefore determined by the net contribution of the total GSE, rather than by the isolated effects of its individual constituents.

This framework, which follows directly from a consistent accounting of GSE, is referred to as **Matter-Only Cosmology (MOC)**. [2] The designation reflects the core premise of the model, namely that cosmic acceleration and the phenomenon attributed to dark energy arise from the GSE of matter and from the interaction between matter and its own self-gravitating energy, without invoking an additional non matter energy component.

In the following sections, we will demonstrate how this single correction based on first principles not only provides a concrete physical origin for dark energy, but also naturally reproduces its observed magnitude in the late universe, thereby offering a self-consistent resolution of one of the central problems in modern cosmology.

3 The Total GSE and the Structural Parameter β

As established in the previous section, the origin of dark energy in the present framework is identified with the total GSE of the universe, evaluated in a self-consistent manner. The entire construction relies on a single generalized expression for the GSE of a mass distribution, in which the structural parameter β effectively encodes the influence of internal mass distribution and relativistic corrections, without introducing any additional dynamical degrees of freedom beyond matter itself. This section provides a more detailed examination of this foundational quantity, $U_{gs} = -\beta GM^2/R$, and clarifies the physical meaning and practical role of the parameter β.

3.1 From Newtonian binding energy to a relativistic framework

The GSE U_{gs} represents the total gravitational potential energy associated with a mass distribution and arises from the mutual gravitational interaction among its constituent elements. For an object of total mass M, which may be conceptualized as an assembly of infinitesimal

[2] Here, "Matter" includes both baryonic and dark matter. The term "Matter-Only" refers to the absence of an independent dark energy fluid. The same principle applies to radiation, with the replacement $\rho_m \to \rho_r$.

mass elements satisfying $M = \sum dm_i$, this energy corresponds to the work required to assemble the system from infinite separation. It is therefore a specific and fundamental form of gravitational potential energy, commonly referred to as gravitational binding energy, with a negative sign reflecting the energy required to disperse the system [28].

Within Newtonian gravity, the GSE of a uniform sphere of mass M and radius R is given by the well known expression [29].

$$U_{gs,\text{Newton}} = -\frac{3}{5}\frac{GM^2}{R} \tag{33}$$

Although this result provides a useful reference, it is insufficient for cosmological applications where relativistic effects and strong self-gravity become relevant. In General Relativity, the evaluation of GSE for a static and spherically symmetric configuration requires integration over a curved spacetime geometry. While a closed form analytic expression is generally not available, the net result can be captured effectively by a generalized expression of the same functional form [30, 31],

$$U_{gs} = -\beta\frac{GM^2}{R} \tag{34}$$

The dimensionless coefficient β replaces the Newtonian value $3/5$ and summarizes the combined effects of internal density profile, pressure support, and relativistic corrections. Its value is not universal and depends on the structural properties of the gravitating system.

3.2 The physical interpretation and structural evolution of β

Within the MOC framework, the parameter β serves as a structural descriptor that connects simplified analytical expressions to the complex and evolving matter distribution of the universe. Importantly, β is not introduced as a free tuning parameter, but is constrained by well established physical models of self-gravitating systems and by the observed large scale structure of the universe.

3.2.1 Theoretical constraints and structural models

The admissible range of β is determined by the degree of mass concentration and by the importance of relativistic effects.

- **Lower bound from Newtonian uniformity:** For a nonrelativistic and perfectly uniform sphere, β takes the exact value $3/5 = 0.6$
- **Upper bound from relativistic compactness:** For compact objects described by General Relativity, such as neutron stars, numerical solutions of the TOV equations indicate that β typically lies in the range from approximately 1.0 up to 2.039 for highly centrally condensed configurations [20, 21].

To quantify the impact of cosmic structure formation on β, we performed a numerical integration of the gravitational potential energy for the Navarro Frenk White density profile [32], which provides an accurate description of dark matter halos. The resulting values demonstrate a systematic correlation between the halo concentration parameter c and the effective structural coefficient β [33].

- $c = 20$ corresponding to highly concentrated early structures gives $\beta \approx 1.62$
- $c = 15$ corresponding to dense galactic halos gives $\beta \approx 1.45$
- $c = 10$ corresponding to Milky Way sized halos gives $\beta \approx 1.25$

- $c = 5$ corresponding to cluster scale structures gives $\beta \approx 1.02$

These results suggest a clear evolutionary trend. An early universe that is nearly uniform and strongly self-gravitating may be characterized by relatively large values of β, approaching but not exceeding the relativistic compactness limit. As cosmic structures form hierarchically and subsequently virialize, the effective value of β decreases toward unity. Once galaxy scale halos have formed and reached approximate virial equilibrium, typically at cosmic times $t \gtrsim 0.5$ to 1 Gyr, the large scale mass distribution evolves primarily through mergers and gradual rearrangements. As a consequence, the volume averaged $\beta(t)$ is expected to vary only slowly at late times.

3.2.2 Phenomenological significance of $\beta(t)$

In the present analysis, β is treated as a time dependent but slowly varying effective parameter $\beta(t)$ that represents a cosmological average over the evolving matter distribution. It encapsulates several large scale physical effects.

- **Inhomogeneity and hierarchy:** The universe exhibits a pronounced hierarchical structure. As demonstrated by the NFW based analysis, the transition from compact early halos to extended cluster scale structures naturally drives a gradual evolution of the effective β.
- **Causality and retardation:** The parameter $\beta(t)$ implicitly reflects the finite propagation speed of gravitational interactions and associated retardation effects, which are not captured in purely static Newtonian descriptions.

Accordingly, the range of values $\beta \approx 1.0180$ for the enhanced matter model and $\beta \approx 1.4949$ for the baseline model obtained in this work is not arbitrary. These values are consistent with the polytropic model of index $n = 3$, which yields $\beta = 3/2$ and describes marginally relativistic self-gravitating systems [34]. They also quantitatively match the NFW halo profile with concentration parameter $c \approx 15$, for which $\beta \approx 1.45$ [32].

Over the cosmological time interval relevant for our simulations, namely $t \gtrsim 0.8$ Gyr, all viable MOC realizations maintain $\beta(t)$ within a narrow interval of width $\Delta\beta \sim 0.1$. This behavior indicates that the emergence of dark energy in the MOC framework is driven primarily by the geometric scaling of the total GSE with cosmic expansion, rather than by any finely tuned temporal evolution of the structural parameter itself.

3.3 $\beta(t)$ is not a free parameter and can be treated as a constant except in the early universe

It is important to clarify that the structural parameter β does not represent a new free degree of freedom in the MOC framework. Although β may be regarded as a function of cosmic time over the full history of the universe, its admissible range is tightly restricted to values of order unity, typically between $\beta \sim 1$ to 2, as dictated by well established models of self-gravitating systems. Moreover, once galaxy scale structures have formed and virialized, the large scale matter distribution evolves only slowly, and the effective cosmological value of β is expected to behave approximately as a constant.

This expectation is explicitly supported by the MOC simulations presented in Section 7.5. In particular, simulations performed with a strictly constant value of β reproduce essentially the same qualitative dark energy phenomenology as simulations allowing for mild temporal variation of β. These include an initially negative dark energy density, a sign transition at intermediate epochs, the onset of late time accelerated expansion, the appearance of a finite

maximum, and a subsequent monotonic decay. This robustness demonstrates that β is not a control parameter governing cosmic dynamics, but rather a fixed structural coefficient entering the definition of the total GSE.

In the present work, the numerical value of β is estimated using physically motivated structural models, yielding values in the range $\beta \sim 1$ to 1.5. This approach reflects practical limitations rather than conceptual freedom.

In principle, β can be determined independently through large scale N body simulations by directly comparing the simulated matter distribution with observed galactic and cluster scale structures. Such a procedure would allow β to be computed from first principles and removed entirely from the set of adjustable quantities.

Accordingly, β should be viewed not as a tunable parameter, but as a structural coefficient entering the total GSE, whose value is fixed by the large scale organization of matter in the universe.

4 The Friedmann Equations in the MOC Framework

The standard ΛCDM model successfully accounts for cosmic expansion by introducing dark energy as an independent component characterized by a negative pressure, $P_\Lambda = -\rho_\Lambda$ [3,4,8]. In contrast, the Matter-Only Cosmology framework argues that the phenomena attributed to dark energy do not arise from a new substance or exotic field, but instead emerge from the GSE of matter itself and its associated interaction energy. This section reformulates the Friedmann equations within the MOC framework.

4.1 A re-examination of the gravitational source term

The first Friedmann equation may be derived both from General Relativity and, in an intuitive manner, from Newtonian energy conservation applied to a test particle located at the boundary of an expanding homogeneous sphere (see for example [26, 27, 35] and Figure 1). The Newtonian derivation provides a useful interpretive perspective, namely that the energy density ρ appearing in the relation $H^2 \propto \rho$ is associated with the total energy content of the system, rather than solely with the rest mass of its constituent particles.

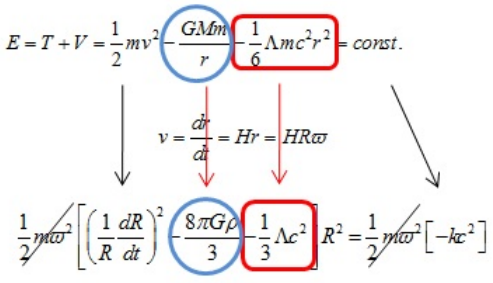

Figure 1: A schematic illustration of the derivation of the Friedmann equation from mechanical energy conservation, $E = K + U$. This construction highlights that the density term ρ originates from the total potential energy of the system, not only from its rest mass [36].

Within the Friedmann equations, all quantities denoted by ρ represent equivalent mass densities, defined as energy densities divided by c^2. As such, all ρ terms enter on equal footing as gravitational sources.

Standard cosmology has long operated on the implicit assumption that, within the matter sector, the rest-mass density ρ_m fully characterizes the gravitational source associated with matter on cosmological scales. We argue that this assumption is conceptually incomplete. The total mass density ρ_T that sources cosmic expansion in the Friedmann equations must also include the equivalent mass density associated with the GSE of matter and its self-interaction.

The total effective mass density governing cosmic expansion therefore consists of two fundamental contributions.

1) **Matter density (ρ_m):** The observable rest mass density of baryonic and dark matter. This term represents the material content of the universe and the origin of all gravitational interactions.

2) **Total GSE or dark energy (ρ_{Λ_m}):** The net equivalent mass density arising from the GSE of matter. This contribution is not an independent fluid, but an emergent effect generated by matter through its own self-gravity. As shown in previous sections, it consists of two components.

   - **Negative component ($-\rho_{gs}$):** The equivalent mass density associated with classical gravitational binding energy.
   - **Positive component ($\rho_{m\text{-}gs}$):** The equivalent mass density generated by the self-gravitation of GSE, consistent with the general relativistic principle that all forms of energy act as sources of gravity.

In the ΛCDM model, matter and dark energy are treated as separate and noninteracting components [3,4,8]. In contrast, the MOC framework interprets dark energy as the total GSE of matter, including both the classical self-binding contribution and the interaction energy between matter and its own GSE.

Accordingly, the total mass energy density entering the Friedmann equation is given by

$$\rho_T = \rho_m + \rho_{\Lambda_m} = \rho_m + \rho_{m\text{-}gs} - \rho_{gs} \tag{35}$$

This expression does not introduce new physics, but rather provides a more complete representation of the total equivalent mass density ρ_T, sometimes denoted ρ_{eq}.

Including the spatial curvature parameter k, the first Friedmann equation in the MOC framework takes the form.

$$H^2 = \frac{8\pi G}{3}\rho_T - \frac{k}{a^2} = \frac{8\pi G}{3}(\rho_m + \rho_{m\text{-}gs} - \rho_{gs}) - \frac{k}{a^2} \tag{36}$$

In the following subsections, we derive explicit realizations of this equation for both an expanding cosmological spacetime and a static self-gravitating system.

4.2 Friedmann equations in an expanding universe

In a cosmological context, it is necessary to distinguish between the scale governing gravitational interaction and the scale governing volumetric dilution. In the MOC framework, these roles are played by the particle horizon χ_p and the physical horizon radius R_{phys}, respectively.

4.2.1 Causal Interaction and Volumetric Dilution: The Roles of χ_p and R_{phys}

In the MOC framework, it is necessary to distinguish between the scale governing gravitational interaction and the scale governing volumetric dilution. These roles are played by the

comoving particle horizon χ_p and the physical horizon radius $R_{\rm phys}$, respectively. This distinction ensures that the GSE calculation remains consistent with both the causal structure of spacetime and the conservation of matter.

We introduce two characteristic radii to describe the evolution of the causal domain.

$$\chi_p(t) = \int_0^t \frac{c}{a(t')} dt' \qquad \text{(comoving particle horizon)} \tag{37}$$

$$R_{\rm phys}(t) = a(t)\chi_p(t) \qquad \text{(physical horizon radius)} \tag{38}$$

The comoving horizon $\chi_p(t)$ determines which mass elements have entered the causal network of mutual gravitational interaction by cosmic time t [37,38]. Accordingly, $\chi_p(t)$ provides the appropriate scale for calculating the accumulated gravitational potential energy. By contrast, the physical horizon $R_{\rm phys}(t)$ defines the actual spatial extent of this causal domain and serves as the scale for volumetric dilution.

To ensure physical consistency, the mass $M(t)$ participating in the gravitational interaction must be invariant regardless of the coordinate system used for its evaluation. This invariance resolves potential confusion regarding the scaling of mass in an expanding background. If we work in physical coordinates, the mass is the integral of the local physical density $\rho_m(t)$ over the physical horizon volume $V_{\rm phys}(t) = \frac{4\pi}{3} R_{\rm phys}(t)^3$.

$$M(t) = \rho_m(t)\left(\frac{4\pi}{3} R_{\rm phys}(t)^3\right) \tag{39}$$

Alternatively, in comoving coordinates, the same mass is expressed as the integral of the comoving density $\rho_m^{\rm com}(t) = a(t)^3 \rho_m(t)$ over the comoving horizon volume $V_{\rm com}(t) = \frac{4\pi}{3}\chi_p(t)^3$.

$$M(t) = \rho_m^{\rm com}(t)\left(\frac{4\pi}{3}\chi_p(t)^3\right) = \left[a(t)^3\rho_m(t)\right]\left(\frac{4\pi}{3}\chi_p(t)^3\right) \tag{40}$$

Since $R_{\rm phys}(t) = a(t)\chi_p(t)$, substituting this relation into Eq. (39) immediately yields Eq. (40). This identity demonstrates that the two definitions are mathematically equivalent and physically consistent, ensuring that $M(t)$ correctly tracks the amount of matter that has become causally connected to the observer.

The GSE $U_{gs}(t)$ is then determined by the interaction scale $\chi_p(t)$ as follows

$$U_{gs}(t) = -\beta(t)\frac{GM(t)^2}{\chi_p(t)} \tag{41}$$

While the source mass $M(t)$ is accounted for across the entire causally connected region, the interaction strength is governed by the integrated causal structure $\chi_p(t)$ rather than the instantaneous physical separation. The GSE is formed through causal interactions accumulated over cosmic history, so the appropriate interaction scale in the binding energy is the comoving particle horizon $\chi_p(t)$ rather than the instantaneous physical radius. This formulation provides a self-consistent framework for emergent dark energy. Matter generates dark energy through its own GSE, where the magnitude is determined by the causal scale χ_p and the resulting density is diluted by the physical scale $R_{\rm phys}$ [18,39].

4.2.2 Derivation of GSE densities: why interaction uses χ_p but dilution uses $R_{\rm phys}$

The GSE depends on two ingredients. The first is the amount of mass participating in mutual gravitational interaction. The second is the characteristic separation over which those interactions are established. In an expanding universe, both ingredients are constrained by causality.

The particle horizon $\chi_p(t)$ therefore provides the natural interaction scale. It represents the largest comoving separation over which gravitational information could have propagated since the initial singularity [37,38]. Accordingly, the formation of gravitational binding energy is characterized by $U_{gs}(t) \sim -\beta(t)\frac{GM(t)^2}{\chi_p(t)}$.

This choice reflects the physical fact that gravity is an infinite range interaction whose effective reach at finite cosmic time is limited not by instantaneous kinematic scales such as c/H, but by the integrated causal structure of spacetime [40, 41]. Only mass elements that have been able to exchange gravitational influence can contribute coherently to the global potential energy.

Once the total GSE is formed, its density must be defined by dividing by the physical volume occupied by the causally connected region at that epoch. This role is played by the physical horizon radius.

$$R_{\text{phys}}(t) = a(t)\chi_p(t) \tag{42}$$

which sets the actual size of the causal domain in physical units. The corresponding volume is

$$V_{\text{phys}}(t) = \frac{4\pi}{3}R_{\text{phys}}(t)^3 \tag{43}$$

Because energy densities in FRW cosmology are defined per unit physical volume, the conversion from a global energy to an equivalent mass density must involve V_{phys} [8,18]. This yields the total GSE density prescription.

$$-\rho_{gs}(t) = \frac{U_{gs}(t)}{V_{\text{phys}}(t)c^2} = -\frac{1}{\left(\frac{4\pi}{3}R_{\text{phys}}(t)^3\right)c^2}\left(\beta(t)\frac{GM(t)^2}{\chi_p(t)}\right) \tag{44}$$

A similar construction applies to the relativistic interaction component.

$$\rho_{m\text{-}gs}(t) = \frac{U_{m\text{-}gs}(t)}{V_{\text{phys}}(t)c^2} \tag{45}$$

with $U_{m\text{-}gs}(t)$ evaluated using the same causal interaction scale $\chi_p(t)$ [23].

The resulting expressions are

$$-\rho_{gs}(t) = -\frac{3\beta(t)}{4\pi}\frac{GM(t)^2}{c^2\chi_p(t)R_{\text{phys}}(t)^3} \tag{46}$$

$$\rho_{m\text{-}gs}(t) = +\frac{15\beta(t)^2}{28\pi}\frac{G^2M(t)^3}{c^4\chi_p(t)^2R_{\text{phys}}(t)^3} \tag{47}$$

$$\boxed{\rho_{\Lambda_m} = \frac{\beta\rho_m}{2}\frac{R_S}{\chi_p}\left(\frac{5\beta}{14}\frac{R_S}{\chi_p} - 1\right)} \tag{48}$$

where ρ_m is the matter density defined per unit physical volume $V_{\text{phys}} = \frac{4\pi}{3}R^3_{\text{phys}}$, and $R_S = 2GM/c^2$ is the Schwarzschild radius associated with the total mass $M = \rho_m V_{\text{phys}}$ that has become causally connected within the particle horizon χ_p.

$$\boxed{\rho_{\Lambda_m} = \frac{4\pi G}{3c^2}\beta\rho_m^2\frac{R^3_{\text{phys}}}{\chi_p}\left(\frac{20\pi G}{21c^2}\beta\rho_m\frac{R^3_{\text{phys}}}{\chi_p} - 1\right)} \tag{49}$$

Conceptually, the prescription can be summarized as follows.

The particle horizon $\chi_p(t)$ sets the scale over which gravitational binding energy is generated, because only mass elements that have been in causal contact can contribute coherently

to the accumulated GSE. By contrast, the physical horizon $R_{\text{phys}}(t)$ sets the scale over which this energy is diluted into a physical energy density.

Using R_{phys} as the interaction length would incorrectly treat gravitational binding energy as if it were determined by an instantaneous geometric separation, rather than by the causal history of gravitational interaction. Conversely, using χ_p as the dilution scale would be inconsistent with the FRW definition of energy density, which is defined per unit physical volume rather than per comoving volume [39, 42].

The MOC framework therefore assigns χ_p and R_{phys} to distinct and non-interchangeable physical roles. This separation is causally well motivated and fully compatible with relativistic cosmology.

4.2.3 General GSE Framework: The Friedmann equations in expanding space

To formalize this framework, we treat the total GSE as an effective source term in the Einstein field equations

$$G_{\mu\nu} = \frac{8\pi G}{c^4}\left(T_{\mu\nu}^{\text{matter}} + T_{\mu\nu}^{\text{GSE}}\right) \tag{50}$$

where the GSE source tensor is modeled as a perfect fluid defined by

$$T_{\mu\nu}^{\text{GSE}} = \left(\rho_{\Lambda_m} + P_{\Lambda_m}\right)u_\mu u_\nu + P_{\Lambda_m} g_{\mu\nu} \tag{51}$$

Solving these equations for the standard FLRW metric, substituting the total GSE densities and expressing them in terms of the matter density ρ_m yields the first Friedmann equation in the MOC framework.

$$\boxed{H^2 = \frac{8\pi G\rho_m}{3}\left[1 + \frac{\beta}{2}\frac{R_S}{\chi_p}\left(\frac{5\beta}{14}\frac{R_S}{\chi_p} - 1\right)\right] - \frac{k}{a^2}} \tag{52}$$

This expression explicitly reveals the scaling with the dimensionless geometric ratio R_S/χ_p, which represents the competition between the gravitational radius and the causal horizon.

The acceleration equation is derived from the total energy-momentum conservation as follows

$$\frac{\ddot{a}}{a} = -\frac{4\pi G}{3}(\rho_m + \rho_{\Lambda_m} + 3P_T) \approx -\frac{4\pi G}{3}\left[\rho_m + (1 + 3w_{\Lambda_m})\rho_{\Lambda_m}\right] \tag{53}$$

Adopting an effective equation of state $w_{\Lambda_m} \approx -1$ for the emergent dark energy component, the acceleration equation reduces to a compact form.

$$\boxed{\frac{\ddot{a}}{a} = -\frac{4\pi G\rho_m}{3}\left[1 - \beta\frac{R_S}{\chi_p}\left(\frac{5\beta}{14}\frac{R_S}{\chi_p} - 1\right)\right]} \tag{54}$$

This equation demonstrates that the sign of cosmic acceleration is governed by the evolution of the total GSE term. As the causal horizon grows and the balance between the attractive and repulsive self-interaction components shifts, the universe naturally transitions from early-time deceleration to late-time acceleration.

This result encapsulates the central thesis of the MOC framework. Matter is the sole fundamental energy source. Dark energy is not an independent physical entity but an emergent consequence of the GSE of matter and its relativistic self-interaction. In this sense, matter generates dark energy and drives cosmic acceleration through its own gravitational field.

4.2.4 Static GSE Framework: The Friedmann equations in non-expanding space

The MOC framework can also be applied to non-expanding and static systems by identifying the interaction and dilution scales such that $\chi_p = R_{\text{phys}} = R$. This identification renders the equations applicable to a wide class of self-gravitating systems beyond cosmology. In this limit, the ratio R_S/χ_p becomes R_S/R.

Substituting the explicit GSE-based expressions, the first Friedmann equation for a static system is expressed as follows

$$H^2 = \frac{8\pi G\rho_m}{3}\left[1+\frac{\beta}{2}\frac{R_S}{R}\left(\frac{5\beta}{14}\frac{R_S}{R}-1\right)\right]-\frac{k}{a^2} \tag{55}$$

Expanding the terms inside the bracket highlights the corrections to the Newtonian limit.

$$H^2 = \frac{8\pi G\rho_m}{3}\left(1-\frac{\beta}{2}\frac{R_S}{R}+\frac{5\beta^2}{28}\frac{R_S^2}{R^2}\right)-\frac{k}{a^2} \tag{56}$$

The curvature term enters in the standard geometric manner and plays the same role as in the ΛCDM model. All nontrivial dynamical effects arise solely from the GSE of the matter distribution.

The corresponding acceleration equation is derived under the assumption $w_{\Lambda_m} \approx -1$.

$$\frac{\ddot{a}}{a} = -\frac{4\pi G\rho_m}{3}\left[1-\beta\frac{R_S}{R}\left(\frac{5\beta}{14}\frac{R_S}{R}-1\right)\right] \tag{57}$$

In the strictly static limit, the first Friedmann equation reduces to a constraint equation describing the balance of energy densities.

$$\frac{8\pi G\rho_m}{3}\left[1+\frac{\beta}{2}\frac{R_S}{R}\left(\frac{5\beta}{14}\frac{R_S}{R}-1\right)\right]-\frac{k}{R^2} = 0 \tag{58}$$

This condition describes the formal equivalent of hydrostatic equilibrium in a self-gravitating sphere. The repulsive component of the GSE can counterbalance gravitational attraction and prevent gravitational collapse. The acceleration equation similarly simplifies to a form that determines the stability of the system.

$$\ddot{a} \propto -\frac{4\pi G\rho_m}{3}\left[1-\beta\frac{R_S}{R}\left(\frac{5\beta}{14}\frac{R_S}{R}-1\right)\right] \tag{59}$$

This static formulation provides a powerful analytical tool for various physical scales. For astrophysical objects such as stars or black hole interiors, it offers a framework to model internal energy density structures where repulsive GSE effects may regulate singularity formation. In elementary particle physics, it suggests a novel approach to self-energy problems by treating particles as self-contained gravitationally bound systems whose divergences are naturally regularized by their own GSE [20, 43].

4.3 Origin of negative pressure in the MOC framework

The second Friedmann equation governs cosmic acceleration. In the MOC framework, dark energy is not introduced as an independent fluid. Instead, it is identified with an effective contribution ρ_{Λ_m} generated by the GSE of matter and its associated interaction term.

In this setting, the pressure associated with ρ_{Λ_m} is not imposed axiomatically. It can be inferred from energy conservation once the total effective energy density is specified.

The total effective energy density is defined as $\rho_T = \rho_m + \rho_{\Lambda_m}$. The conservation of the total energy content is expressed by the continuity equation.

$$\dot{\rho}_T + 3H(\rho_T + P_T) = 0 \tag{60}$$

Here the total effective pressure is defined by

$$P_T = P_m + P_{\Lambda_m} \tag{61}$$

For pressureless matter one has $P_m = 0$. In addition, the matter component is separately conserved in the standard FRW sense.

$$\dot{\rho}_m + 3H\rho_m = 0 \tag{62}$$

Subtracting the matter continuity equation from the total continuity equation yields an evolution equation for the effective GSE induced component.

$$\dot{\rho}_{\Lambda_m} + 3H(\rho_{\Lambda_m} + P_{\Lambda_m}) = 0 \tag{63}$$

Solving for the effective pressure gives

$$P_{\Lambda_m} = -\rho_{\Lambda_m} - \frac{\dot{\rho}_{\Lambda_m}}{3H} \tag{64}$$

This relation implies that the effective pressure contains two contributions. The first term $-\rho_{\Lambda_m}$ is vacuum like in the sense that it reproduces the familiar relation $P = -\rho$ when ρ_{Λ_m} is constant. The second term encodes the dynamical nature of the MOC framework through the time variation of ρ_{Λ_m}.

To analyze cosmic acceleration within the MOC framework, we define an effective equation of state parameter. $w_{\Lambda_m}(t) \equiv \frac{P_{\Lambda_m}}{\rho_{\Lambda_m}}$. Combining this definition with Eq. (64) yields

$$w_{\Lambda_m}(t) = -1 - \frac{\dot{\rho}_{\Lambda_m}}{3H\rho_{\Lambda_m}} \tag{65}$$

In the MOC framework, $\rho_{\Lambda_m}(t)$ is determined by the total GSE expression given in Eq. (31). Accordingly, $w_{\Lambda_m}(t)$ is generally time dependent, reflecting the evolving balance between the attractive and repulsive contributions inside the total GSE term.

This expression provides a transparent physical interpretation of the effective equation of state. If the total GSE density varies slowly compared to the Hubble expansion rate, such that $|\dot{\rho}_{\Lambda_m}| \ll 3H|\rho_{\Lambda_m}|$, the second term is subdominant and $w_{\Lambda_m}(t)$ approaches -1. In this regime, the effective pressure satisfies $P_{\Lambda_m} \approx -\rho_{\Lambda_m}$ and the GSE contribution behaves similarly to a cosmological constant.

More generally, whenever $\rho_{\Lambda_m}(t)$ evolves monotonically with cosmic time, the second term remains finite and negative for an expanding universe. As a result, $w_{\Lambda_m}(t)$ remains negative, implying an effective negative pressure. This negative pressure is the direct dynamical origin of cosmic acceleration in the MOC framework, arising from the time dependence of the total GSE rather than from an independent vacuum component.

The continuity equation employed above is not an additional model dependent assumption. It follows from the covariant conservation law for the total energy–momentum tensor.

$$\nabla_\mu T^{\mu\nu}_{\text{total}} = 0 \tag{66}$$

which is required by general relativity.

4.4 Thermodynamic derivation of GSE pressure

In this work, we introduce an *effective* pressure associated with the total GSE-induced internal energy $U_{\text{gs-T}}$ via the thermodynamic-like relation

$$P_{\Lambda_m} \equiv -\frac{dU_{\text{gs-T}}}{dV_{\text{phys}}} = -\frac{\dot{U}_{\text{gs-T}}}{\dot{V}_{\text{phys}}} \tag{67}$$

where $V_{\text{phys}}(t) = (4\pi/3)R_{\text{phys}}(t)^3$ represents the physical coarse-graining volume over which the GSE contribution is diluted. The second equality holds provided that the cosmic time t serves as the unique parameter governing the evolution of the system [30, 39].

We emphasize that Eq. (67) should be interpreted as an effective equation-of-state identification rather than a full equilibrium thermodynamic identity. Standard thermodynamics dictates that pressure is defined as a partial derivative, $P = -(\partial U/\partial V)_{S,N,\ldots}$, taken at fixed entropy and particle number [44]. Consequently, adopting Eq. (67) implies the following idealized assumptions:

1) **Prescribed matter evolution along the horizon.** Unlike a closed thermodynamic system with fixed particle number, the causal domain in our framework is an open system where the enclosed mass M grows with the horizon scale (e.g., via the causal prescription $M(\chi_p)$). Accordingly, the derivative in Eq. (67) is evaluated along this *specific evolutionary trajectory*. It implicitly captures the combined effects of geometric expansion and the causal inflow of matter, effectively treating the horizon-enclosed region as a single dynamic entity [45].

2) **Negligible non-volumetric work.** We neglect macroscopic work channels other than effective volumetric work. This implies that contributions from chemical potential ($\mu\, dN$), anisotropic stress, or viscous dissipation are either absent or subdominant at the level of this effective description. This simplification is consistent with the standard treatment of the cosmic fluid as a perfect fluid on large scales [18, 42].

3) **Effective adiabaticity for the fluid description.** While the horizon expansion theoretically involves entropy increase (e.g., due to information inflow or horizon area growth [46]), we model the GSE component as an effective perfect fluid governed by mechanical work. Thus, the derivative in Eq. (67) is taken under the assumption that explicit entropy production terms are either subdominant or can be decoupled from the mechanical equation of state, analogous to the standard adiabatic treatment of cosmic fluids [4].

4) **Phenomenological energy exchange.** If the system exchanges energy with its surroundings (e.g., via radiation during collapse), these microscopic processes are not resolved here. Instead, their net effect is assumed to be encoded phenomenologically in the evolution of $U_{\text{gs-T}}$. Therefore, P_{Λ_m} represents the effective pressure required to reproduce the macroscopic U–V relation, rather than a locally measured microscopic pressure.

Strictly speaking, since the comoving domain constitutes an open system with causal matter inflow, the direct application of the equilibrium relation Eq. (67) faces formal limitations. However, it is instructive to examine the consequences of this thermodynamic definition as a heuristic probe. Under the assumptions outlined above, Eq. (67) serves as a valuable proxy, providing a consistent framework to estimate the sign and magnitude of the effective pressure. This exploratory analysis allows us to evaluate the effective equation-of-state parameter $w_{\Lambda_m} \equiv P_{\Lambda_m}/(\rho_{\Lambda_m}c^2)$ and its contribution to cosmic acceleration ($\rho_{\Lambda_m} + 3P_{\Lambda_m}/c^2$), offering complementary insights to the rigorous gravitational derivation.

4.4.1 Geometric volume factor

We define the physical volume of the causally connected domain as

$$V_{\text{phys}}(t) = \frac{4\pi}{3} R_{\text{phys}}(t)^3 = \frac{4\pi}{3}\big[a(t)\chi_p(t)\big]^3 \tag{68}$$

Differentiating with respect to time yields

$$\frac{dV_{\text{phys}}}{dt} = 4\pi a(t)^3 \chi_p(t)^3 \left(H(t) + \frac{\dot{\chi}_p(t)}{\chi_p(t)}\right) \tag{69}$$

Using the definition of the comoving particle horizon,

$$\chi_p(t) \equiv \int_0^t \frac{c}{a(t')}\, dt' \quad \Longrightarrow \quad \dot{\chi}_p(t) = \frac{c}{a(t)} \tag{70}$$

and noting that $\chi_p(t) = c\,\eta(t)$ (where η is the conformal time), Eq. (69) can be rewritten in a computationally convenient form.

$$\begin{aligned} \frac{dV_{\text{phys}}}{dt} &= 4\pi a(t)^3 \chi_p(t)^2 \Big(H(t)\chi_p(t) + \dot{\chi}_p(t)\Big) \\ &= 4\pi a(t)^2 \chi_p(t)^2\, c \left(1 + a(t)H(t)\eta(t)\right) \end{aligned} \tag{71}$$

Since $a > 0$, $\chi_p > 0$, and (for an expanding universe) $H > 0$ and $\dot{\chi}_p > 0$, it follows that $dV_{\text{phys}}/dt > 0$. Therefore, the sign of the effective pressure P_{Λ_m} is determined solely by the sign of the time derivative $dU_{\text{gs-T}}/dt$.

4.4.2 Time derivative of the total GSE

In the MOC framework, the total GSE is taken as

$$U_{\text{gs-T}}(t) = -\beta(t)\frac{GM(t)^2}{\chi_p(t)} + \frac{5}{7}\beta(t)^2 \frac{G^2 M(t)^3}{c^2 \chi_p(t)^2} \tag{72}$$

Here we explicitly treat the matter density as time dependent and define the enclosed mass by

$$M(t) \equiv \frac{4\pi}{3}\,\rho_m(t)\,\chi_p(t)^3 \tag{73}$$

so that

$$\dot{M}(t) = \frac{4\pi}{3}\Big(\dot{\rho}_m\,\chi_p^3 + 3\rho_m\,\chi_p^2 \dot{\chi}_p\Big) \tag{74}$$

Treating $U_{\text{gs-T}}(t) = U(\beta(t), M(t), \chi_p(t))$ as a composite function yields

$$\frac{dU_{\text{gs-T}}}{dt} = \frac{\partial U}{\partial \beta}\dot{\beta} + \frac{\partial U}{\partial M}\dot{M} + \frac{\partial U}{\partial \chi_p}\dot{\chi}_p \tag{75}$$

with

$$\frac{\partial U}{\partial \beta} = -\frac{GM^2}{\chi_p} + \frac{10}{7}\beta\,\frac{G^2 M^3}{c^2 \chi_p^2} \tag{76}$$

$$\frac{\partial U}{\partial M} = -2\beta\,\frac{GM}{\chi_p} + \frac{15}{7}\beta^2\,\frac{G^2 M^2}{c^2 \chi_p^2} \tag{77}$$

$$\frac{\partial U}{\partial \chi_p} = \beta\,\frac{GM^2}{\chi_p^2} - \frac{10}{7}\beta^2\,\frac{G^2 M^3}{c^2 \chi_p^3} \tag{78}$$

Substituting these derivatives into Eq. (75) gives the explicit result

$$\frac{dU_{\text{gs-T}}}{dt} = \left(-\frac{GM^2}{\chi_p} + \frac{10}{7}\beta\,\frac{G^2M^3}{c^2\chi_p^2}\right)\dot{\beta} + \left(-2\beta\,\frac{GM}{\chi_p} + \frac{15}{7}\beta^2\,\frac{G^2M^2}{c^2\chi_p^2}\right)\dot{M} + \left(\beta\,\frac{GM^2}{\chi_p^2} - \frac{10}{7}\beta^2\,\frac{G^2M^3}{c^2\chi_p^3}\right)\dot{\chi}_p \tag{79}$$

where $M(t)$ and $\dot{M}(t)$ are given by Eqs. (73)–(74).

4.4.3 Final pressure formula in an expanding universe

Combining Eqs. (71), and (79), the thermodynamic GSE pressure becomes

$$P_{\Lambda_m}(t) = -\frac{\left(-\frac{GM^2}{\chi_p} + \frac{10}{7}\beta\,\frac{G^2M^3}{c^2\chi_p^2}\right)\dot{\beta} + \left(-2\beta\,\frac{GM}{\chi_p} + \frac{15}{7}\beta^2\,\frac{G^2M^2}{c^2\chi_p^2}\right)\dot{M} + \left(\beta\,\frac{GM^2}{\chi_p^2} - \frac{10}{7}\beta^2\,\frac{G^2M^3}{c^2\chi_p^3}\right)\dot{\chi}_p}{4\pi a^3\chi_p^2\left(H\chi_p + \dot{\chi}_p\right)} \tag{80}$$

with

$$M(t) = \frac{4\pi}{3}\rho_m(t)\chi_p(t)^3, \qquad \dot{M}(t) = \frac{4\pi}{3}\left(\dot{\rho}_m\,\chi_p^3 + 3\rho_m\,\chi_p^2\dot{\chi}_p\right) \tag{81}$$

1) Optional specialization (dust). If one further assumes pressureless matter conservation in an FRW background,

$$\dot{\rho}_m(t) = -3H(t)\rho_m(t) \tag{82}$$

then Eq. (81) reduces to

$$\dot{M}(t) = 4\pi\rho_m(t)\chi_p(t)^2\left(\dot{\chi}_p(t) - H(t)\chi_p(t)\right) \tag{83}$$

which can be substituted into Eq. (80) to express $P_{\Lambda_m}(t)$.

2) Slow evolution of the structural parameter $\beta(t)$. In the MOC framework, β is a structural parameter encoding the geometric response of the causally connected matter distribution in the GSE functional. After the formation of large-scale galactic structure, any residual evolution of $\beta(t)$ is expected to be slow compared to the Hubble time, so that β may be approximated as constant for the purpose of the present derivation.

Accordingly, we adopt the quasi-static approximation. $\dot{\beta}(t) \simeq 0$ under which Eq. (80) simplifies to

$$P_{\Lambda_m}(t) = -\frac{\left(-2\beta\,\frac{GM(t)}{\chi_p(t)} + \frac{15}{7}\beta^2\,\frac{G^2M(t)^2}{c^2\chi_p(t)^2}\right)\dot{M}(t) + \left(\beta\,\frac{GM(t)^2}{\chi_p(t)^2} - \frac{10}{7}\beta^2\,\frac{G^2M(t)^3}{c^2\chi_p(t)^3}\right)\dot{\chi}_p(t)}{4\pi a(t)^3\chi_p(t)^2\left(H(t)\chi_p(t) + \dot{\chi}_p(t)\right)} \tag{84}$$

3) Fully expanded form in terms of $\rho_m(t)$ and $\chi_p(t)$ ($\dot{\beta} \simeq 0$). Adopting the quasi-static approximation $\dot{\beta}(t) \simeq 0$, we start from

$$P_{\Lambda_m}(t) = -\frac{\left(-2\beta\,\frac{GM}{\chi_p} + \frac{15}{7}\beta^2\,\frac{G^2M^2}{c^2\chi_p^2}\right)\dot{M} + \left(\beta\,\frac{GM^2}{\chi_p^2} - \frac{10}{7}\beta^2\,\frac{G^2M^3}{c^2\chi_p^3}\right)\dot{\chi}_p}{4\pi a^3\chi_p^2\left(H\chi_p + \dot{\chi}_p\right)} \tag{85}$$

Using the time-dependent mass definition

$$M(t)=\frac{4\pi}{3}\rho_m(t)\chi_p(t)^3,\qquad \dot{M}(t)=\frac{4\pi}{3}\Big(\dot{\rho}_m(t)\,\chi_p(t)^3+3\rho_m(t)\,\chi_p(t)^2\dot{\chi}_p(t)\Big) \tag{86}$$

we obtain the explicitly expanded pressure

$$P_{\Lambda_m}(t)=-\frac{\mathcal{N}_{\rho\chi}(t)}{4\pi\,a(t)^3\,\chi_p(t)^2\Big(H(t)\chi_p(t)+\dot{\chi}_p(t)\Big)} \tag{87}$$

with the numerator

$$\begin{aligned}\mathcal{N}_{\rho\chi}(t)=&\left[-2\beta\,G\left(\frac{4\pi}{3}\right)\rho_m\,\chi_p^2+\frac{15}{7}\beta^2\,\frac{G^2}{c^2}\left(\frac{4\pi}{3}\right)^2\rho_m^2\,\chi_p^4\right]\left(\frac{4\pi}{3}\right)\Big(\dot{\rho}_m\,\chi_p^3+3\rho_m\,\chi_p^2\dot{\chi}_p\Big)\\&+\left[\beta\,G\left(\frac{4\pi}{3}\right)^2\rho_m^2\,\chi_p^4-\frac{10}{7}\beta^2\,\frac{G^2}{c^2}\left(\frac{4\pi}{3}\right)^3\rho_m^3\,\chi_p^6\right]\dot{\chi}_p\end{aligned} \tag{88}$$

4) Equivalent representation. Collecting terms proportional to $\dot{\rho}_m(t)$ and $\dot{\chi}_p(t)$, the numerator $\mathcal{N}_{\rho\chi}(t)$ can be written in the linear form

$$\mathcal{N}_{\rho\chi}(t)=A(t)\,\dot{\rho}_m(t)+B(t)\,\dot{\chi}_p(t) \tag{89}$$

$$A(t)\equiv\left(\frac{32\pi^2}{9}\right)\beta G\rho_m\chi_p^5\left[-1+\left(\frac{10\pi G}{7c^2}\right)\beta\rho_m\chi_p^2\right] \tag{90}$$

$$B(t)\equiv(\frac{80\pi^2}{9})\beta G{\rho_m}^2{\chi_p}^4\left[-1+(\frac{4\pi G}{3c^2})\beta\rho_m{\chi_p}^2\right] \tag{91}$$

Substituting Eq. (89) into Eq. (87) yields $P_{\Lambda_m}(t)$

$$\boxed{P_{\Lambda_m}(t)=-\frac{A(t)\dot{\rho}_m+B(t)\dot{\chi}_p}{4\pi a^3{\chi_p}^2(H\chi_p+\dot{\chi}_p)}} \tag{92}$$

5) Equation-of-state form and a present-day estimate. By collecting the dimensionless factors in Eq. (92), the effective GSE pressure can be cast in the standard equation-of-state form

$$P_{\Lambda_m}(t)=w_{\Lambda_m}(t)\,\rho_{\Lambda_m}(t) \tag{93}$$

where $w_{\Lambda_m}(t)$ is identified with the (dimensionless) prefactor multiplying $\rho_{\Lambda_m}(t)$ after extracting the overall density scale. Although a closed analytic expression for $w_{\Lambda_m}(t)$ can be written down, it is algebraically lengthy and not particularly illuminating, so we do not reproduce it here.

Evaluating the expression at the present epoch using the fiducial late-time parameters $a(t_0)=1$, $\chi_p(t_0)=43.337\,\mathrm{Gly}$, $\beta(t_0)=1.4949$, $\Omega_m=0.315$, and the SH0ES value $H_0=73.04$ $\mathrm{km\,s^{-1}\,Mpc^{-1}}$ yields

$$w_{\Lambda_m}(t_0)\simeq-0.757 \tag{94}$$

This value is intriguing in light of recent discussions regarding DESI BAO constraints combined with CMB and Type Ia supernovae, which hint at possible deviations from ΛCDM, potentially favoring dynamical dark energy solutions with a present-day equation of state $w_0>-1$ (e.g., $w_0\sim-0.8$ [12]).

4.4.4 Thermodynamic origin and sign transition of GSE pressure

The effective pressure associated with the GSE induced dark energy is defined thermodynamically as Eq. (67).

In an expanding universe one has $a > 0$, $H > 0$, and $\dot{\chi}_p > 0$. Consequently $dV_{\rm phys}/dt > 0$. It follows that the sign of P_{Λ_m} is determined entirely by the sign of $dU_{\text{gs-T}}/dt$. The attractive or repulsive character of the effective pressure is therefore controlled by the internal energy structure of the total GSE and is independent of the detailed expansion history beyond the monotonic growth of the physical volume.

$$\text{sign}\big(P_{\Lambda_m}\big) = -\text{sign}\left(\frac{dU_{\text{gs-T}}}{dt}\right) \tag{95}$$

In the MOC framework, the total GSE in the static approximation is given by $U_{\text{gs-T}}$.

To inspect the structural dependence of the GSE potential $U_{\text{gs-T}}$ on the horizon scale, we adopt a scaling ansatz for the enclosed mass:

$$M(\chi_p) \approx K\,\chi_p^3 \tag{96}$$

where K represents an effective density coefficient. While the actual matter density evolves with time, this power-law relation captures the leading-order geometric scaling of the mass within the causal volume, allowing us to determine the stationary point of the potential.

Substituting Eq. (96) into Eq. (19) yields

$$U_{\text{gs-T}}(\chi_p) = -A\,\chi_p^5 + B\,\chi_p^7 \tag{97}$$

with $A \equiv \beta G K^2$, $B \equiv \frac{5}{7}\beta^2 \frac{G^2K^3}{c^2}$. Taking the derivative with respect to χ_p gives

$$\frac{dU_{\text{gs-T}}}{d\chi_p} = \chi_p^4\big(-5A + 7B\chi_p^2\big) \tag{98}$$

Since $\dot{\chi}_p > 0$, Eqs. (95) and (98) imply that the pressure changes sign when the factor in parentheses vanishes.

$$-5A + 7B\chi_p^2 = 0 \quad \Longleftrightarrow \quad \chi_{p,*}^2 = \frac{c^2}{\beta G K} \tag{99}$$

Using $M = K\chi_p^3$ and the Schwarzschild radius $R_S = 2GM/c^2$, the transition condition can be written in compact and physically transparent form.

$$\boxed{\frac{R_S}{\chi_p} = \frac{2}{\beta}} \tag{100}$$

Therefore, the effective GSE pressure satisfies

$$P_{\Lambda_m} > 0 \quad \text{for} \quad \frac{R_S}{\chi_p} < \frac{2}{\beta} \tag{101}$$

$$P_{\Lambda_m} < 0 \quad \text{for} \quad \frac{R_S}{\chi_p} > \frac{2}{\beta} \tag{102}$$

The dark energy density is defined as $\rho_{\Lambda_m} \equiv \frac{U_{\text{gs-T}}}{V_{\rm phys}c^2}$ Since $V_{\rm phys}(t) > 0$, the sign of ρ_{Λ_m} is determined by the sign of $U_{\text{gs-T}}$.

Equation (97) shows that the same competition between the negative Newtonian binding term and the positive relativistic self-interaction term governs both the sign of $U_{\text{gs-T}}$ and the

sign of its derivative. However, note that the transition epochs differ slightly due to the different exponents: the pressure turns negative (repulsive) as the system passes the potential minimum ($dU_{\text{gs-T}}/d\chi_p = 0$), whereas the energy density becomes positive later when $U_{\text{gs-T}}$ crosses zero.

In the regime where the Newtonian binding term dominates, the potential slope is negative ($dU_{\text{gs-T}}/d\chi_p < 0$), resulting in positive pressure $P_{\Lambda_m} > 0$. Once the relativistic term grows sufficiently to satisfy the condition Eq. (100), the slope turns positive ($dU_{\text{gs-T}}/d\chi_p > 0$), generating negative pressure $P_{\Lambda_m} < 0$. This repulsive phase emerges naturally from the deep relativistic structure of the gravitational self-energy.

4.4.5 Connection to the sign of the dark energy density

In MOC, the dark energy density is defined as

$$\rho_{\Lambda_m} \equiv \frac{U_{\text{gs-T}}}{V_{\text{phys}} c^2} \tag{103}$$

Since $V_{\text{phys}} > 0$, the sign of ρ_{Λ_m} is determined by the sign of $U_{\text{gs-T}}$. The total GSE contains two competing contributions. The Newtonian self-binding term is negative, while the relativistic self-interaction term is positive.

At early epochs, when the causally connected domain is small and the enclosed mass is correspondingly limited, the negative binding contribution dominates. In this regime one has

$$U_{\text{gs-T}} < 0 \quad \Longrightarrow \quad \rho_{\Lambda_m} < 0 \tag{104}$$

In the same regime, the thermodynamic pressure analysis implies $P_{\Lambda_m} > 0$. Equivalently, using the sign relation in Eq. (95) together with the monotonic growth of the particle horizon, the model yields

$$\rho_{\Lambda_m} < 0 \quad \Longrightarrow \quad P_{\Lambda_m} > 0 \tag{105}$$

As the causal domain grows and the enclosed mass increases, the positive self-interaction contribution eventually dominates the total GSE. One then finds

$$U_{\text{gs-T}} > 0 \quad \Longrightarrow \quad \rho_{\Lambda_m} > 0 \tag{106}$$

In this late time regime the same thermodynamic analysis implies $P_{\Lambda_m} < 0$.

$$\rho_{\Lambda_m} > 0 \quad \Longrightarrow \quad P_{\Lambda_m} < 0 \tag{107}$$

Equations (105) and (107) summarize a key physical feature of the MOC mechanism. The dark energy component contributes an attractive tendency when its equivalent density is negative and its effective pressure is positive. After the sign transition, it contributes a repulsive tendency once its equivalent density becomes positive and its effective pressure becomes negative. This late time behavior is the regime relevant for cosmic acceleration in MOC.

The thermodynamic derivation presented here is consistent with the continuity equation approach. Both routes lead to the same qualitative conclusion in the late universe. The effective pressure becomes negative and the corresponding equation of state approaches $w_{\Lambda_m} \simeq -1$ when the evolution of ρ_{Λ_m} is slow compared to the Hubble rate.

4.5 Applicability to the radiation era

Although the name "Matter-Only Cosmology" emphasizes that the model introduces no independent dark energy fluid, the underlying mechanism is not restricted to nonrelativistic matter. The GSE construction is an energy-budget statement and therefore applies to any dominant gravitating component that enters the Friedmann equations.

During the radiation-dominated epoch, the dominant energy component is radiation with energy density ε_r. The corresponding equivalent mass density that sources gravity is $\rho_r \equiv \frac{\varepsilon_r}{c^2}$.

In this era, the MOC framework is implemented by replacing the matter source ρ_m with the radiation source ρ_r in the GSE expressions. The total equivalent mass density retains the same structural form.

$$\rho_T = \rho_r + \rho_{\Lambda_r} \tag{108}$$

Here ρ_{Λ_r} denotes the total GSE contribution induced by the radiation source.

In direct analogy with the matter-era decomposition, it can be written as

$$\rho_{\Lambda_r} = \rho_{r\text{-}gs}(\rho_r) - \rho_{gs}(\rho_r) \tag{109}$$

where the bracket notation emphasizes that both the positive interaction contribution and the negative binding contribution are now sourced by ρ_r.

The principal differences relative to the matter-dominated case are the dilution law and the background pressure. Radiation satisfies $\rho_r \propto a^{-4}$ whereas nonrelativistic matter satisfies $\rho_m \propto a^{-3}$. In addition, the equation of state parameter is $w_r = \frac{1}{3}$ while for pressureless matter one has $w_m \simeq 0$. These differences modify the time dependence of $\chi_p(t)$, $R_{\rm phys}(t)$, and the sourced GSE densities, but do not alter the formal structure of the GSE-induced contribution itself.

Consequently, the MOC framework is formally applicable across the radiation- and matter-dominated epochs, provided the dominant source term in the GSE expressions is chosen consistently with the cosmic equation of state. In this work we focus primarily on quantitative predictions for the post-CMB epoch. The implications of the same mechanism for earlier epochs, including the transition out of inflation, are discussed in Section 10.

4.6 Theoretical consistency: Positive energy density and the origin of repulsion

A central theoretical requirement for any alternative description of cosmic acceleration is to generate repulsive dynamics without introducing known instabilities. Scenarios that rely on genuinely exotic degrees of freedom, such as phantom components with $w < -1$, can exhibit vacuum instabilities or ghostlike excitations and are therefore widely regarded as pathological [47, 48].

In this section we show that the MOC framework avoids these pathologies by maintaining a nonnegative total equivalent mass density ρ_T while producing repulsion through the effective pressure associated with the total GSE contribution.

4.6.1 Stability via nonnegative total energy density

To test whether the total density can become negative, we examine the condition

$$\rho_T = \rho_m + \rho_{\Lambda_m} < 0 \tag{110}$$

which is equivalent to $\rho_{\Lambda_m} < -\rho_m$. Substituting $\rho_m = 3M/(4\pi R^3)$ and the expression for ρ_{Λ_m} from Eq. (31) yields

$$\frac{3\beta}{4\pi}\frac{GM^2}{c^2R^4}\left(\frac{5\beta}{14}\frac{R_S}{R} - 1\right) < -\frac{3M}{4\pi R^3} \tag{111}$$

Introducing the dimensionless compactness variable, $x \equiv \frac{R_S}{R}$ and using $R_S = 2GM/c^2$ transforms Eq. (111) into the quadratic inequality.

$$\frac{5\beta^2}{28}x^2 - \frac{\beta}{2}x + 1 < 0 \tag{112}$$

The discriminant of the quadratic polynomial in Eq. (112) is

$$D = \left(-\frac{\beta}{2}\right)^2 - 4\left(\frac{5\beta^2}{28}\right) = -\frac{13\beta^2}{28} \tag{113}$$

For any real β, one has $D < 0$ and the leading coefficient is positive. Therefore the quadratic expression is strictly positive for all real x, so the inequality in Eq. (112) has no solution. Equivalently, the total density never becomes negative.

$$\rho_T(R) > 0 \qquad \text{for all } R > 0 \tag{114}$$

In regimes where ρ_{Λ_m} is negative because the binding contribution dominates, its magnitude remains bounded so that ρ_T stays positive. The same conclusion holds when ρ_{Λ_m} is expressed through the general expanding-universe prescriptions in Eqs. (46) and (47), provided M denotes the causally connected mass and R_{phys} the corresponding physical volume scale.

This result implies that the MOC background satisfies the density part of the weak energy condition in the sense that $\rho_T \geq 0$ [37,38] Accordingly, the construction avoids the most direct instability associated with a genuinely negative total energy density and is not forced into the vacuum-decay behavior typical of explicitly unstable negative-energy components [49].

4.6.2 Repulsion from effective pressure

If the total mass-energy density remains positive, the origin of acceleration must reside in the pressure sector. In an FRW background, the acceleration equation depends on the active gravitational mass density, which contains the combination $\rho + 3P/c^2$. In the MOC framework this may be written as

$$\frac{\ddot{a}}{a} = -\frac{4\pi G}{3}\left(\rho_T + \frac{3P_T}{c^2}\right) \tag{115}$$

where $P_T = P_m + P_{\Lambda_m}$ For pressureless matter one sets $P_m \simeq 0$, so $P_T \simeq P_{\Lambda_m}$.

Although ρ_T remains positive, the total GSE sector induces an effective pressure P_{Λ_m} that can become negative after the sign transition derived in Section 4.5 and Section 3. In the effective-fluid description, this negative pressure is the driver of repulsive dynamics.

Our thermodynamic and continuity-equation derivations show that, in the late universe where $\rho_{\Lambda_m} > 0$, the effective equation-of-state parameter approaches. $w_{\Lambda_m} \equiv \frac{P_{\Lambda_m}}{\rho_{\Lambda_m}} \simeq -1$ so that $P_{\Lambda_m} < 0$ holds in the same regime.

Under these conditions the active gravitational mass density contributed by the GSE sector is negative.

$$\rho_{\Lambda_m} + \frac{3P_{\Lambda_m}}{c^2} \simeq -2\rho_{\Lambda_m} < 0 \tag{116}$$

and the total combination in Eq. (115) can satisfy

$$\rho_T + \frac{3P_T}{c^2} < 0 \tag{117}$$

which yields $\ddot{a} > 0$ and therefore accelerated expansion.

This provides a mechanism for repulsive cosmological dynamics without requiring a negative total energy density or a phantom component with $w < -1$.

- **Ontological stability:** The total equivalent mass density remains positive, $\rho_T > 0$, avoiding the most direct negative-energy pathology and remaining consistent with standard energy-condition expectations for the background density [37, 38].

- **Dynamical repulsion:** The total GSE sector generates an effective negative pressure, $P_{\Lambda_m} < 0$, which can render the active gravitational mass density negative and drive acceleration in agreement with supernova evidence for late-time repulsion [1, 2].

Therefore, within the MOC framework, late-time acceleration can arise as a purely gravitational effect generated by the self-consistent energy structure of the total GSE sector, without introducing additional exotic fields and without invoking phantom instabilities.

4.7 Definition of the GSE framework

The GSE framework asserts that the total energy of a gravitating system can be decomposed into a free-state contribution and a self-gravitating contribution associated with mutual gravitational interactions among the system constituents. In particular, the framework treats the GSE as part of the system energy budget that enters its equivalent mass, consistent with the general relativistic principle that all forms of energy gravitate [16–18].

Crucially, our construction extends the conventional Newtonian binding-energy term by incorporating an additional relativistic interaction contribution that arises once the self-energy itself is included as part of the gravitational source. In other words, the effective source is obtained by replacing the bare enclosed mass with an equivalent mass that includes the self-energy contribution, which generates a second term at order $1/c^2$ in the total GSE.

Since all physical entities possess energy and thus generate gravity, the GSE framework is a universal principle applicable to all matter distributions, from elementary particles to the universe at large.

[Classification: general versus static model]

Depending on whether the background spacetime is treated as expanding or effectively time independent on the scales of interest, the framework is formulated in two regimes.

- **The General GSE model:** This formulation applies to an expanding FRW background, where the causal interaction scale is set by the particle horizon $\chi_p(t)$, while dilution into an energy density is defined with respect to the physical horizon radius $R_{\rm phys}(t)$. Because $\chi_p(t)$ and $R_{\rm phys}(t)$ can evolve differently, the GSE density acquires a nontrivial time dependence, which is the relevant regime for cosmological applications and the emergence of an dark energy component.

- **The Static GSE model:** This limiting formulation applies to gravitationally bound systems that are effectively decoupled from cosmic expansion on the scales of interest, including compact astrophysical objects such as stars and black holes, as well as more localized energy-carrying systems such as elementary particles [43]. In this regime, the characteristic interaction length is taken to be commensurate with the physical size of the system, so that the distinction between the causal interaction scale and the physical size can be neglected to leading order. Accordingly, one may set $R_{\rm phys} \simeq \chi_p \simeq R$ within the system and treat the cosmological expansion as a subleading background effect in the internal energy bookkeeping.

  This static approximation is justified not only by spatial scale separation, but also by temporal scale separation. The characteristic dynamical timescales of such bound systems are vastly shorter than the cosmological expansion timescale. As a result, the cosmological background evolves negligibly over the relevant analysis time and can be treated as

effectively constant. Background-induced corrections therefore remain parametrically small across the spatial extent of the system and are consistently neglected.

This static GSE formulation provides a simplified and self-consistent analytic description of internal structure and stability in self-gravitating configurations.

5 Observational Validation and the Evolution of β

In the preceding sections, we established the foundational equations of MOC. In this paradigm, the phenomenon conventionally attributed to dark energy arises from the total GSE of the universe, evaluated in a self-consistent manner.

$$\rho_{\Lambda_m} = \rho_{m\text{-}gs} - \rho_{gs} = \frac{3\beta GM^2}{4\pi c^2 R^4}\left(\frac{5\beta}{14}\frac{R_S}{R} - 1\right) \tag{118}$$

Here β is a structural coefficient entering the total GSE. It effectively summarizes the dependence of the self-energy on the mass distribution and relativistic compactness. In the full cosmic history β may be regarded as a slowly varying function of time. However, after the onset of substantial structure formation, its evolution is expected to be modest and can be treated as approximately constant for the late universe analysis presented in this section.

The decisive test of this framework is confrontation with empirical anchors. We therefore compare the MOC requirements with constraints from the early universe inferred from the Cosmic Microwave Background (CMB) [5] and with late universe measurements of the local distance ladder such as SH0ES [15].

In practice, the late time effective value of β is not predicted uniquely from first principles within the present analytic treatment. Instead, it is constrained by the observed present epoch energy budget and by the physically plausible range implied by gravitationally bound structures. Our strategy is therefore to determine the value of β required to reproduce the observed present day dark energy density under two baselines.[3]

We treat the present matter density parameter Ω_m as a variable to be explored rather than as a fixed input. For each baseline, we solve for the β that satisfies the present epoch matching condition.

$$\rho_{\Lambda_m}(t_0) = (1-\Omega_m)\rho_c \tag{119}$$

For the CMB baseline we adopt $H_0 = 67.4\,\mathrm{km\,s^{-1}\,Mpc^{-1}}$ [5] and for the SH0ES baseline we adopt $H_0 = 73.04\,\mathrm{km\,s^{-1}\,Mpc^{-1}}$ [15].

We repeat this procedure across a range of matter densities, including scenarios in which the effective matter abundance is modestly higher than the standard ΛCDM inference $\Omega_m \simeq 0.315$ [5].

The results are summarized in Tables 1 and 2. By comparing the required values of β with the physically plausible range inferred from gravitationally bound structures, we can assess the viability of MOC. For reference, a uniform Newtonian sphere yields $\beta = 3/5$ while relativistic compact objects can reach $\beta \sim 2$ depending on internal structure and compactness. In addition, large scale structure simulations provide complementary guidance on plausible structural states of collapsed halos and virialized matter distributions [51].

[3] In principle, the structural coefficient β can be determined independently through large-scale N-body simulations [50], by directly comparing the simulated matter distribution with observed galaxy and galaxy-cluster scale structures. Such a program would allow β to be computed from first principles and removed entirely from the set of adjustable physical quantities in the model.

Matter Incr. (%)	ρ_m ($\times 10^{-27}\,\mathrm{kg\,m^{-3}}$)	ρ_{Λ_m} (Target) ($\times 10^{-27}\,\mathrm{kg\,m^{-3}}$)	**Required β**	$\rho_{m\text{-}gs}$ ($\times 10^{-27}\,\mathrm{kg\,m^{-3}}$)	$-\rho_{gs}$ ($\times 10^{-27}\,\mathrm{kg\,m^{-3}}$)
-20	2.150	6.383	**2.2068**	12.522	-6.139
-10	2.418	6.115	**1.8597**	12.662	-6.547
0	2.687	5.846	**1.5952**	12.780	-6.934
10	2.956	5.577	**1.3879**	12.877	-7.300
20	3.224	5.309	**1.2219**	12.956	-7.648
30	3.493	5.040	**1.0863**	13.019	-7.979
40	3.762	4.771	**0.9737**	13.067	-8.296
50	4.030	4.502	**0.8791**	13.100	-8.598
60	4.299	4.234	**0.7986**	13.120	-8.886

Table 1: **Required Structural Parameter β for CMB Baseline ($H_0 = 67.4$ km/s/Mpc, $R = 46.5$ Gly, $\rho_c \approx 8.53 \times 10^{-27}$ kg/m^3)** The table lists the necessary β values to recover the precise CMB dark energy density for various matter density scenarios. The range from approximately -10% to +30% matter variation yields physically plausible β values ($1.0 \lesssim \beta \lesssim 2.0$) consistent with virialized structures.

Matter Incr. (%)	ρ_m ($\times 10^{-27}\,\mathrm{kg\,m^{-3}}$)	ρ_{Λ_m} (Target) ($\times 10^{-27}\,\mathrm{kg\,m^{-3}}$)	**Required β**	$\rho_{m\text{-}gs}$ ($\times 10^{-27}\,\mathrm{kg\,m^{-3}}$)	$-\rho_{gs}$ ($\times 10^{-27}\,\mathrm{kg\,m^{-3}}$)
-20	2.525	7.496	**2.0681**	14.706	-7.210
-10	2.840	7.180	**1.7428**	14.870	-7.690
0	3.156	6.865	**1.4949**	15.008	-8.143
10	3.472	6.549	**1.3007**	15.122	-8.573
20	3.787	6.233	**1.1450**	15.215	-8.982
30	4.103	5.918	**1.0180**	15.289	-9.371
40	4.418	5.602	**0.9125**	15.345	-9.743
50	4.734	5.287	**0.8239**	15.384	-10.098
60	5.050	4.971	**0.7484**	15.408	-10.437

Table 2: **Required Structural Parameter β for SH0ES Baseline ($H_0 = 73.04$ km/s/Mpc, $\chi_p(t_0) = R = 43.337$ Gly,$\rho_c \approx 1.002 \times 10^{-26}$ kg/m^3).** The table lists the precise β values required to recover the observed SH0ES dark energy density across varying matter density scenarios. The range from -10% to $+30\%$ corresponds to physically viable structural parameters ($1.0 \lesssim \beta \lesssim 2.039$). Specifically, the 0% ($\beta \approx 1.4949$) and +20% ($\beta \approx 1.1450$) models are particularly favored as they align well with standard astrophysical expectations.

An examination of Tables 1 and 2 reveals an important implication of the MOC matching procedure. Across a broad span of assumed matter densities, solutions for β exist that reproduce the required present epoch ρ_{Λ_m}. This indicates that the framework is not restricted to a narrowly tuned matter abundance at t_0.

For the canonical value $\Omega_m \simeq 0.315$ [5], corresponding to the 0% rows, the required values are $\beta \simeq 1.5952$ under the CMB baseline and $\beta \simeq 1.4949$ under the SH0ES baseline. These values lie within the range expected for a universe that is substantially nonuniform and structurally evolved at late times. The later universe is expected to be highly virialized and less uniform on cosmological scales, which is naturally associated with the region where β approaches 1 to 1.5.

From this perspective, scenarios yielding β in the approximate interval $1.0 \lesssim \beta \lesssim 1.5$ are especially well aligned with the physical interpretation of β as a structural coefficient associated with virialized large scale matter organization. In the tables, this interval corresponds roughly to the +0% to +20% matter enhancement cases under both baselines.

While the standard ΛCDM model does not require an increase in Ω_m relative to the Planck baseline at the present epoch, the MOC framework allows for such a possibility. In MOC this reflects the fact that the dark energy density is not an independent component but a derived quantity tied to the matter distribution through the total GSE and its structural coefficient β.

5.1 The Hubble Tension as a natural consequence of MOC

One of the most significant challenges in modern cosmology is the "Hubble tension"—the persistent discrepancy between the value of the Hubble constant (H_0) measured from the early universe and that from the local, late-time universe [11]. Measurements from the Cosmic Microwave Background (CMB) by the Planck satellite suggest $H_0 \approx 67.4$ km/s/Mpc [5], while local measurements using Type Ia supernovae from the SH0ES team indicate a higher value of $H_0 \approx 73.04$ km/s/Mpc [15]. In the standard ΛCDM model, where dark energy is an immutable constant, this disagreement presents a fundamental crisis [52–55].

However, within the MOC framework, this tension is not a crisis but a natural and predicted consequence of cosmic evolution. The key is our structural parameter, β, which is not a fundamental constant but an effective parameter reflecting the evolving structure of the universe's matter distribution.

5.1.1 The evolution of $\beta(t)$ as a record of cosmic structure formation

As the universe evolves, the large-scale matter distribution changes progressively. In the early universe (the CMB era), matter was distributed almost uniformly. As time progressed, gravitational instability caused this matter to clump together, forming the complex cosmic web of galaxies, clusters, and vast voids we see today [39]. This process of structure formation directly impacts the total GSE of the universe and, consequently, must be reflected in the value of β. A more clustered, inhomogeneous, and virialized universe is expected to have a different effective β than a smooth, uniform one.

Our analysis of the two primary cosmological datasets confirms this picture with remarkable clarity. Instead of requiring a large, unobserved matter component, MOC successfully explains the data with matter densities very close to the canonical value. We highlight two key scenarios based on our updated calculations.

- **The 0% matter-increase scenario ($\Omega_m \approx 0.315$):** To explain the universe as seen in the CMB, our model requires $\beta_{\text{CMB}} \approx 1.595$. For the local universe (SH0ES), it requires $\beta_{\text{SH0ES}} \approx 1.495$. The inferred change is $\Delta\beta \equiv \beta_{\text{SH0ES}} - \beta_{\text{CMB}} \approx -0.100$
- **The 10% matter-increase scenario ($\Omega_m \approx 0.346$):** We are also interested in the +10% material growth model, considering the recent publication of the results of studies with 12.06% material growth claims ($\Omega_m \approx 0.352$) [56]. It requires $\beta_{\text{CMB}} \approx 1.388$ for the early universe and $\beta_{\text{SH0ES}} \approx 1.301$ for the present day.

In the MOC framework, the Hubble tension is re-framed not as a crisis, but as a powerful confirmation of our model. The discrepancy in the measured values of H_0 arises because cosmologists have attempted to describe two physically distinct cosmic epochs within a single, constant dark energy model (Λ). If the dark energy density is not constant, but changes with time, this is destined to fail.

The tension is the expected signal of a universe where the apparent "dark energy" is not a constant, but a dynamic entity whose properties evolve in response to the changing structure of the cosmos. It is governed by the internal dynamics of $\beta(t)$, $\rho_m(t)$, and the cosmic scale $R(t)$. This transforms the tension from a problematic anomaly into crucial evidence for a universe where matter alone dictates its own complex, evolving destiny. The fact that two different values of H_0 are measured is not a problem for MOC; it is a core prediction.

6 Cosmic History of the MOC

6.1 Preface on methodology and limitations

Most currently adopted cosmological parameters and widely used compilation datasets are inferred within the standard ΛCDM framework which models dark energy as a constant energy density represented by a cosmological constant Λ [3, 4]. However, the MOC that we seek to build posits a significant departure from this paradigm; it features a dark energy density that evolves over time and exhibits different dynamics. A fully self-contained and precision-level formulation of MOC would therefore require an end-to-end inference pipeline and a dedicated dataset constructed within the MOC assumptions.

At present, MOC is at an early stage of development, whereas ΛCDM is supported by a mature ecosystem of observational products and inference tools. Consequently, the primary objective of this paper is not to deliver a final precision-calibrated cosmological model. The objective is to introduce the core ideas of MOC to the academic community and to test their internal consistency through controlled calculations under simplified assumptions.

Because a dedicated observational pipeline for MOC is not yet available, the analysis below necessarily uses widely adopted inputs that were originally inferred under ΛCDM. Accordingly, the numerical outputs should be interpreted as a preliminary exploration of feasibility and qualitative behavior. They should not be interpreted as a definitive measure of final precision or statistical optimality.

6.2 Methods: General framework for MOC cosmic history simulations

6.2.1 Overview: Horizon-scale separation

This work develops a MOC framework in which the dark energy density $\rho_{\Lambda_m}(t)$ arises dynamically from the total GSE of the matter sector. Unlike standard ΛCDM, where ρ_Λ is constant,

MOC treats dark energy as an emergent consequence of GSE and the evolving causal structure of the universe.

A key element of the simulations is a horizon-scale separation prescription for computing GSE densities. We distinguish the characteristic scale associated with energy formation from the scale associated with density dilution.

1) **Energy formation (causal interaction scale)** The total binding energy is determined by gravitational interactions that are limited by causal contact. Since gravitational influence is constrained by the particle horizon, the interaction scale is taken to be the comoving particle horizon $\chi_p(t)$, which encodes the comoving extent of the causally connected network [42].

2) **Density dilution (physical volume scale)** While the binding energy is generated through the causal network, the corresponding energy density is defined per unit physical volume in an expanding FRW spacetime. Therefore, the dilution scale is set by the physical horizon radius $R_{\rm phys}(t) = a(t)\chi_p(t)$, which determines the proper volume of the causally connected region at each epoch [42].

This two-scale horizon formulation captures the competition between the growth of the causally connected gravitational network and the expansion of the physical volume. It provides the operational basis for all MOC cosmic-history simulations presented in this work.

6.2.2 Constants and horizon definitions

We adopt the following constants and present-epoch anchors based on the SH0ES baseline.

- Hubble constant: $H_0 = 73.04\,\mathrm{km\,s^{-1}\,Mpc^{-1}}$
- Critical density: $\rho_c = \dfrac{3H_0^2}{8\pi G} \simeq 1.002 \times 10^{-26}\,\mathrm{kg\,m^{-3}}$
- Present age (SH0ES-based): $t_0 = 12.73\,\mathrm{Gyr}$

We define two distinct horizon scales.

$$\chi_p(t) = \int_0^t \frac{c}{a(t')}\,dt' \qquad \text{(comoving particle horizon)} \tag{120}$$

$$R_{\rm phys}(t) = a(t)\chi_p(t) \qquad \text{(physical horizon radius)} \tag{121}$$

At the present epoch, $a(t_0) = 1$, these two scales coincide.

$$\chi_p(t_0) = R_{\rm phys}(t_0) \simeq 43.337\,\mathrm{Gly} \tag{122}$$

6.2.3 Mass growth and matter density

The effective gravitational mass $M(t)$ entering the self-energy calculation is defined as the mass enclosed within the causal domain set by the particle horizon. Within our causal bookkeeping prescription, this enclosed mass scales with the comoving interaction volume.

$$M(t) = M(t_0, f)\left(\frac{\chi_p(t)}{\chi_p(t_0)}\right)^3 \tag{123}$$

Here, $M(t_0, f)$ denotes the present-epoch enclosed mass corresponding to a matter enhancement factor f relative to the canonical reference $\Omega_m = 0.315$.

By contrast, the matter density $\rho_m(t)$ is treated as a local physical density and therefore follows standard dilution in an expanding FRW background.

$$\rho_m(t) = \frac{M(t)}{V_{\text{phys}}(t)} = \frac{\rho_m(t_0, f)}{a(t)^3} \tag{124}$$

where the physical volume of the horizon region is

$$V_{\text{phys}}(t) = \frac{4\pi}{3} R_{\text{phys}}(t)^3 \tag{125}$$

$$M(t) = \rho_m^{com}(t)\left(\frac{4\pi}{3}\chi_p(t)^3\right) = \left[a(t)^3\rho_m(t)\right]\left(\frac{4\pi}{3}\chi_p(t)^3\right) = \rho_m(t)\left(\frac{4\pi}{3}R_{phys}(t)^3\right) \tag{126}$$

6.2.4 Derivation of GSE densities

The General GSE framework prescribes that the total GSE depends on the enclosed mass $M(t)$ and on the causal interaction scale $\chi_p(t)$. At the level of scaling, one has

$$U_{\text{gs-T}}(t) \sim -\frac{GM(t)^2}{\chi_p(t)} \tag{127}$$

The corresponding equivalent mass density is defined by dividing the energy by the physical volume and by c^2.

1) Negative component ($-\rho_{gs}$) This term represents the classical binding-energy contribution generalized by the structural coefficient $\beta(t)$.

$$-\rho_{gs}(t) = \frac{U_{gs}(t)}{V_{\text{phys}}(t)c^2} = -\frac{1}{\left(\frac{4\pi}{3}R_{\text{phys}}(t)^3\right)c^2}\left(\beta(t)\frac{GM(t)^2}{\chi_p(t)}\right) \tag{128}$$

Equivalently, this can be written as

$$-\rho_{gs}(t) = -\frac{3\beta(t)}{4\pi}\frac{GM(t)^2}{c^2\chi_p(t)R_{\text{phys}}(t)^3} = -\frac{\beta(t)}{2}\rho_m(t)\frac{R_S(t)}{\chi_p(t)} \tag{129}$$

2) Positive component ($\rho_{m\text{-}gs}$) This term represents the relativistic self-interaction contribution in which the GSE field itself acts as part of the gravitational source. Following the same assignment of scales, interaction on $\chi_p(t)$ and dilution over $V_{\text{phys}}(t)$, one obtains

$$\rho_{m\text{-}gs}(t) = \frac{15\beta(t)^2}{28\pi}\frac{G^2M(t)^3}{c^4\chi_p(t)^2R_{\text{phys}}(t)^3} = \frac{5\beta(t)^2}{28}\rho_m(t)\left(\frac{R_S(t)}{\chi_p(t)}\right)^2 \tag{130}$$

3) Total dark energy density The dark energy density is defined as the net total GSE contribution.

$$\rho_{\Lambda_m}(t) = \rho_{m\text{-}gs}(t) - \rho_{gs}(t) \tag{131}$$

This formulation naturally yields a dynamic evolution in which the interaction network grows through $\chi_p(t)$ while the physical dilution proceeds through $R_{\text{phys}}(t)^3$. Consequently, $\rho_{\Lambda_m}(t)$ can become dynamically relevant during epochs when the growth of causal connectivity competes most strongly with volumetric dilution.

6.2.5 Structural-parameter evolution $\beta(t)$

To model mild structural evolution, we adopt a simple linear interpolation for $\beta(t)$ between an early-epoch reference value and the present epoch. For a discrete time stepping indexed by an integer $n = 0, 1, \ldots, N$ (with $n = 0$ at $t = t_0$ and $n = N$ at the early endpoint), we take

$$\beta_n = \beta_{t_0} + \left(\beta_{\mathrm{CMB}} - \beta_{t_0}\right) \frac{n}{N} \tag{132}$$

The present-epoch value β_{t_0} is determined for each matter-enhancement factor f by imposing the flatness matching condition at $t = t_0$.

$$\rho_m(t_0, f) + \rho_{\Lambda_m}(t_0, f) = \rho_c \tag{133}$$

This boundary condition enforces exact agreement with the SH0ES critical density at $z = 0$, while the model then predicts the implied cosmic history toward earlier epochs within the adopted evolution prescription.

6.3 MOC cosmic history simulation datas

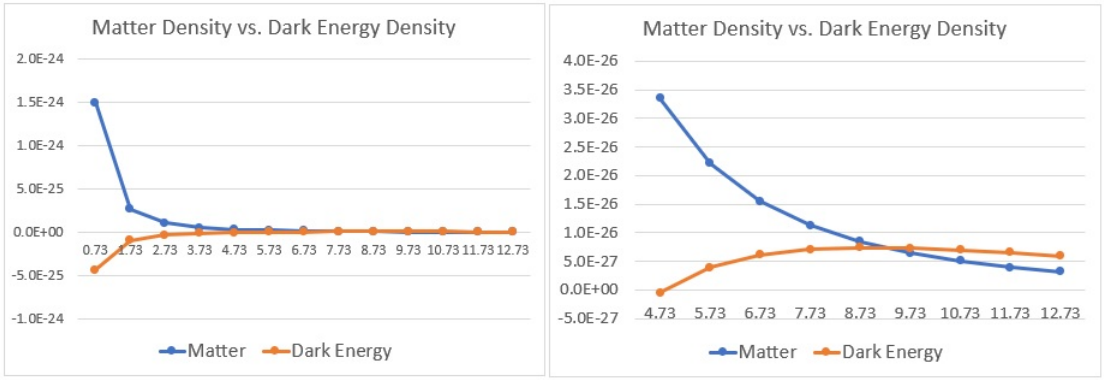

Figure 2: **Matter Density vs. Dark Energy Density (SH0ES, 0% Matter Enhancement)**: $\Omega_m = 0.315$. Dark energy density becomes negative at t< $\sim$ 4.73 Gyr, promotes the formation of galaxy structures, then accelerates the expansion of the universe from approximately t $\sim$7.0 Gyr, peaks around t=8.73 Gyr, and then monotonically decreases.

Age (Gyr)	Scale $a(t)$	Evolving $\beta(t)$	Comoving Ho. $\chi_p(t)$ (Gly)	Physical Ho. $R_{\text{phys}}(t)$ (Gly)	**Matter** $\rho_m(t)$	Repulsive $\rho_{m-gs}(t)$	Attractive $-\rho_{gs}(t)$	**Dark Energy** $\rho_{\Lambda_m}(t)$
					(10^{-27} kg m^{-3})			
0.73	0.1283	1.5952	17.080	2.191	1495.70	178.939	-612.111	**-433.172**
1.73	0.2285	1.5868	22.764	5.202	264.769	98.902	-191.466	**-92.564**
2.73	0.3111	1.5785	26.487	8.240	104.912	71.075	-102.170	**-31.096**
3.73	0.3854	1.5701	29.365	11.317	55.181	55.880	-65.702	**-9.822**
4.73	0.4552	1.5618	31.748	14.452	33.490	45.845	-46.362	**-0.517**
5.73	0.5224	1.5534	33.797	17.656	22.157	38.537	-34.574	3.963
6.73	0.5883	1.5451	35.599	20.943	15.514	32.858	-26.714	6.144
7.73	0.6540	1.5367	37.211	24.336	11.293	28.244	-21.131	7.113
8.73	0.7200	1.5283	38.668	27.841	8.463	24.415	-17.008	**7.407**
9.73	0.7871	1.5200	39.996	31.481	6.478	21.157	-13.852	7.305
10.73	0.8559	1.5116	41.214	35.275	5.038	18.348	-11.376	6.973
11.73	0.9266	1.5033	42.337	39.229	3.971	15.925	-9.408	6.516
12.73	1.0000	1.4949	43.337	43.337	3.159	13.755	-7.799	5.956

Table 3: **MOC Cosmic History Simulation (SH0ES, +0% Matter Enhancement)**: The structural parameter $\beta(t)$ evolves linearly from 1.5952to 1.4949. In the early universe ($t \lesssim 4.73$ Gyr), the dark energy density $\rho_{\Lambda_m}(t)$ is negative, enhancing deceleration and promoting the rapid formation of massive galactic structures. During the intermediate epoch, $\rho_{\Lambda_m}(t)$ transitions to positive values and drives the universe into an accelerated expansion phase around $t \approx 7.0$ Gyr, reaches a maximum near $t \approx 8.73$ Gyr, and subsequently decreases monotonically. This single, self-consistent equation for $\rho_{\Lambda_m}(t)$ simultaneously accounts for the existence of early massive galaxies, the onset of late-time acceleration, the quasi-constant behavior of dark energy, and recent indications of a mild decline in the dark energy density.

Age (Gyr)	Scale $a(t)$	Evolving $\beta(t)$	Comoving Ho. $\chi_p(t)$ (Gly)	Physical Ho. $R_{\text{phys}}(t)$ (Gly)	**Matter** $\rho_m(t)$	Repulsive $\rho_{m-gs}(t)$	Attractive $-\rho_{gs}(t)$	**Dark Energy** $\rho_{\Lambda_m}(t)$
					(10^{-27} kg m^{-3})			
0.73	0.1283	1.3879	17.080	2.191	1645.27	180.289	-644.405	**-464.116**
1.73	0.2285	1.3806	22.764	5.202	291.245	99.649	-201.568	**-101.919**
2.73	0.3111	1.3734	26.487	8.240	115.403	71.612	-107.562	**-35.950**
3.73	0.3854	1.3661	29.365	11.317	60.699	56.303	-69.169	**-12.866**
4.73	0.4552	1.3588	31.748	14.452	36.839	46.193	-48.809	**-2.616**
5.73	0.5224	1.3516	33.797	17.656	24.373	38.829	-36.399	2.430
6.73	0.5883	1.3443	35.599	20.943	17.066	33.108	-28.124	4.983
7.73	0.6540	1.3370	37.211	24.336	12.422	28.459	-22.246	6.213
8.73	0.7200	1.3298	38.668	27.841	9.309	24.600	-17.905	6.695
9.73	0.7871	1.3225	39.996	31.481	7.126	21.318	-14.583	**6.735**
10.73	0.8559	1.3152	41.214	35.275	5.542	18.488	-11.976	6.512
11.73	0.9266	1.3080	42.337	39.229	4.368	16.046	-9.905	6.141
12.73	1.0000	1.3007	43.337	43.337	3.475	13.860	-8.211	5.649

Table 4: **MOC Cosmic History Simulation (SH0ES, +10% Matter Enhancement)**: The structural parameter $\beta(t)$ evolves linearly from 1.3879 to 1.3007. In the early universe ($t \lesssim 5$ Gyr), the dark energy density $\rho_{\Lambda_m}(t)$ is negative, enhancing deceleration and promoting the formation of galactic structures. During the intermediate epoch, $\rho_{\Lambda_m}(t)$ transitions to positive values; it drives the universe into an accelerated expansion phase around $t \approx 7.73$ Gyr, reaches a maximum near $t \approx 8.73$ Gyr, and then decreases monotonically toward the present.

Age (Gyr)	Scale $a(t)$	Evolving $\beta(t)$	Comoving Ho. $\chi_p(t)$ (Gly)	Physical Ho. $R_{\text{phys}}(t)$ (Gly)	**Matter** $\rho_m(t)$	Repulsive $\rho_{m-gs}(t)$	Attractive $-\rho_{gs}(t)$	**Dark Energy** $\rho_{\Lambda_m}(t)$
					(10^{-27} kg m^{-3})			
0.8	0.1295	1.3879	17.744	2.298	1360.95	125.700	-489.386	**-363.686**
1.8	0.2226	1.3812	23.496	5.230	267.964	75.358	-168.138	**-92.780**
2.8	0.2998	1.3745	27.340	8.197	109.688	56.002	-92.735	**-36.733**
3.8	0.3694	1.3678	30.335	11.206	58.636	44.930	-60.731	**-15.801**
4.8	0.4346	1.3611	32.827	14.267	36.007	37.466	-43.458	**-5.992**
5.8	0.4972	1.3544	34.975	17.390	24.047	31.925	-32.784	**-0.859**
6.8	0.5584	1.3477	36.872	20.589	16.975	27.563	-25.594	1.969
7.8	0.6190	1.3409	38.572	23.876	12.462	23.992	-20.459	3.533
8.8	0.6796	1.3342	40.113	27.261	9.417	20.993	-16.636	4.357
9.8	0.7408	1.3275	41.522	30.759	7.270	18.421	-13.693	4.728
10.8	0.8031	1.3208	42.818	34.387	5.706	16.185	-11.371	**4.814**
11.8	0.8668	1.3141	44.017	38.154	4.538	14.230	-9.509	4.722
12.8	0.9323	1.3074	45.129	42.074	3.647	12.508	-7.992	4.516
13.8	1.0000	1.3007	46.165	46.165	2.956	10.990	-6.742	4.244

Table 5: **MOC Cosmic History Simulation (CMB, +10% Matter Enhancement)**: GSE density evolution computed on a CMB–based background ($H_0 = 67.4$) with a +10% matter enhancement and the same $\beta(t)$ profile derived from the SH0ES analysis. Unlike the SH0ES–anchored runs, here we *do not enforce* the flatness condition $\rho_m(t_0) + \rho_{\Lambda_m}(t_0) = \rho_c(H_0^{\text{CMB}})$. We intentionally retain the small mismatch between the MOC-predicted total density ($\rho_{\text{tot}} \approx 7.20$) and the standard CMB critical density ($\rho_c \approx 8.53$) as a diagnostic of how the GSE contribution compares to the canonical ΛCDM budget without ad-hoc renormalization.Dark energy is negative at t<6 Gyr, and the accelerating expansion of the universe occurs at t 9.3 Gyr.

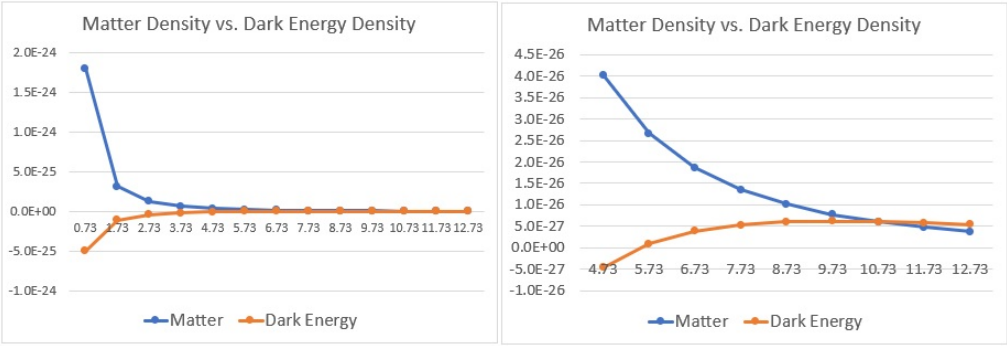

Figure 3: **Matter Density vs. Dark Energy Density (SH0ES, 20% Matter Enhancement)**: $\Omega_m = 0.378$. Dark energy density becomes negative at t< ∼ 5.73 Gyr, promotes the formation of galaxy structures, then accelerates the expansion of the universe from approximately t ∼8.4 Gyr, peaks around t=9.73 Gyr, and then monotonically decreases.

Age (Gyr)	Scale $a(t)$	Evolving $\beta(t)$	Comoving Ho. $\chi_p(t)$ (Gly)	Physical Ho. $R_{\text{phys}}(t)$ (Gly)	**Matter** $\rho_m(t)$	Repulsive $\rho_{m-gs}(t)$	Attractive $-\rho_{gs}(t)$	**Dark Energy** $\rho_{\Lambda_m}(t)$
					(10^{-27} kg m^{-3})			
0.73	0.1283	1.2219	17.080	2.191	1794.84	181.422	-675.170	**-493.749**
1.73	0.2285	1.2155	22.764	5.202	317.722	100.274	-211.190	**-110.920**
2.73	0.3111	1.2091	26.487	8.240	125.894	72.059	-112.695	**-40.635**
3.73	0.3854	1.2027	29.365	11.317	66.217	56.654	-72.469	**-15.816**
4.73	0.4552	1.1963	31.748	14.452	40.188	46.479	-51.137	**-4.658**
5.73	0.5224	1.1899	33.797	17.656	26.589	39.070	-38.135	0.935
6.73	0.5883	1.1835	35.599	20.943	18.617	33.312	-29.465	3.847
7.73	0.6540	1.1770	37.211	24.336	13.551	28.634	-23.307	5.327
8.73	0.7200	1.1706	38.668	27.841	10.156	24.751	-18.759	5.992
9.73	0.7871	1.1642	39.996	31.481	7.773	21.449	-15.278	**6.171**
10.73	0.8559	1.1578	41.214	35.275	6.046	18.601	-12.547	6.054
11.73	0.9266	1.1514	42.337	39.229	4.765	16.144	-10.377	5.767
12.73	1.0000	1.1450	43.337	43.337	3.791	13.944	-8.602	5.342

Table 6: **MOC Cosmic History Simulation (SH0ES, +20% Matter Enhancement)**: The structural parameter $\beta(t)$ evolves from 1.2219 to 1.1450. In the early universe ($t \lesssim 5.5$ Gyr), the dark energy density $\rho_{\Lambda_m}(t)$ is negative, enhancing deceleration and promoting the formation of galactic structures. During the intermediate epoch, $\rho_{\Lambda_m}(t)$ transitions to positive values; it drives the universe into an accelerated expansion phase around $t \approx 8.4$ Gyr, reaches a maximum near $t \approx 9.73$ Gyr, and then decreases monotonically toward the present. A single dark energy equation consistently explains the enhanced structure formation in the early universe, the subsequent accelerated expansion, and the recent decline in dark energy density.

Age (Gyr)	Scale $a(t)$	Evolving $\beta(t)$	Comoving Ho. $\chi_p(t)$ (Gly)	Physical Ho. $R_{\text{phys}}(t)$ (Gly)	**Matter** $\rho_m(t)$	Repulsive $\rho_{m-gs}(t)$	Attractive $-\rho_{gs}(t)$	**Dark Energy** $\rho_{\Lambda_m}(t)$
					(10^{-27} kg m^{-3})			
0.73	0.1283	1.8597	17.080	2.191	1346.13	177.291	-578.020	**-400.729**
1.73	0.2285	1.8500	22.764	5.202	238.292	97.992	-180.803	**-82.811**
2.73	0.3111	1.8402	26.487	8.240	94.421	70.421	-96.480	**-26.060**
3.73	0.3854	1.8305	29.365	11.317	49.663	55.366	-62.043	**-6.677**
4.73	0.4552	1.8207	31.748	14.452	30.141	45.424	-43.780	1.644
5.73	0.5224	1.8110	33.797	17.656	19.942	38.183	-32.649	5.534
6.73	0.5883	1.8013	35.599	20.943	13.963	32.556	-25.227	7.330
7.73	0.6540	1.7915	37.211	24.336	10.163	27.985	-19.954	8.031
8.73	0.7200	1.7818	38.668	27.841	7.617	24.190	-16.061	**8.130**
9.73	0.7871	1.7720	39.996	31.481	5.830	20.963	-13.080	7.882
10.73	0.8559	1.7623	41.214	35.275	4.534	18.180	-10.742	7.438
11.73	0.9266	1.7525	42.337	39.229	3.573	15.779	-8.885	6.894
12.73	1.0000	1.7428	43.337	43.337	2.843	13.629	-7.365	6.264

Table 7: **MOC Cosmic History Simulation (SH0ES, -10% Matter Enhancement)**: The structural parameter $\beta(t)$ evolves from 1.8597 to 1.7428. In the early universe ($t \lesssim 4.5$ Gyr), the dark energy density $\rho_{\Lambda_m}(t)$ is negative, enhancing deceleration and promoting the formation of galactic structures. During the intermediate epoch, $\rho_{\Lambda_m}(t)$ transitions to positive values; it drives the universe into an accelerated expansion phase around $t \approx 6.6$ Gyr, reaches a maximum near $t \approx 8.73$ Gyr, and then decreases monotonically toward the present.

7 Analysis of the Cosmic History using MOC

Here we analyze key simulation results derived from the MOC framework, ranging from a SH0ES–anchored matter density close to the standard ΛCDM value ($\Omega_m \approx 0.315$) to modified scenarios with matter enhancements of $\{-10\%, 0\%, +10\%, +20\%\}$ relative to this baseline (Tables 7–6).

Before proceeding to a physical interpretation of the dynamical behavior of $\rho_{\Lambda_m}(t)$, it is important to clarify the meaning of the cosmic age used in the present analysis. The often-quoted present age $t_0 \simeq 12.73\,\mathrm{Gyr}$ is not a direct observable, but rather a derived quantity obtained by adopting the SH0ES value of the Hubble constant ($H_0 = 73.04\,\mathrm{km\,s^{-1}\,Mpc^{-1}}$) within the standard ΛCDM framework. As such, this value is intrinsically model dependent.

In the MOC framework, the Hubble parameter is not treated as a fixed external input, and the dark energy density $\rho_{\Lambda_m}(t)$ is generated dynamically by the GSE of matter. In particular, $\rho_{\Lambda_m}(t)$ becomes negative in the early universe, contributing an additional attractive component that enhances the overall deceleration relative to ΛCDM. Consequently, for a given late-time value of H_0, a longer cosmic time is naturally required to reach the present expansion state.

Therefore, while the SH0ES-based ΛCDM model yields $t_0 \simeq 12.73\,\mathrm{Gyr}$, the physically relevant age of the universe in the MOC framework is expected to be larger. A conservative expectation is that the true cosmic age lies between the SH0ES ΛCDM value and the Planck-based estimate of $t_0 \simeq 13.8\,\mathrm{Gyr}$.

A coherent picture emerges across all simulated cases. In contrast to the standard ΛCDM scenario, where dark energy is a static cosmological constant, the MOC framework predicts a dynamical matter–induced dark energy density $\rho_{\Lambda_m}(t)$ with a characteristic *three–phase* evolution.

1) an early phase with **negative** $\rho_{\Lambda_m}(t)$, acting as an additional attractive component that enhances structure formation;

2) an intermediate phase in which $\rho_{\Lambda_m}(t)$ transitions through zero and becomes positive, eventually dominating the acceleration;

3) a late phase in which positive $\rho_{\Lambda_m}(t)$ varies only mildly and behaves quasi–constantly on Gyr timescales.

Below we quantify this behavior and connect it to current cosmological tensions and anomalies.

7.1 The competition of two GSE components

The central dynamical mechanism of the MOC framework is the competition between two distinct GSE contributions: the attractive self–energy density ($-\rho_{gs}$) and the repulsive interaction energy density ρ_{m-gs}. The dark energy density is defined as

$$\rho_{\Lambda_m}(t) = \rho_{m-gs}(t) - \rho_{gs}(t) \tag{134}$$

and its sign determines its gravitational role. A positive ρ_{Λ_m} carries negative effective pressure and drives accelerated expansion, whereas a negative ρ_{Λ_m} acts as an additional attractive component, effectively strengthening gravity.

The relative importance of these two GSE terms evolves over cosmic time. While $-\rho_{gs}$ scales primarily with the square of the matter density and dominates in dense, early time configurations, the interaction term ρ_{m-gs} becomes increasingly important as the horizon grows

and the cosmic matter distribution evolves. The time dependence of the structural parameter $\beta(t)$ further modulates this balance, encoding the transition from a nearly homogeneous early universe to a highly structured late–time cosmic web.

As a consequence, the MOC framework generically predicts a sign change in $\rho_{\Lambda_m}(t)$ during cosmic evolution, providing a natural transition from an early gravity–enhanced phase to a late time repulsive regime. The physical implications of this transition for early structure formation and late time cosmic acceleration are discussed in the following subsection.

7.2 The emergence of quasi-constant and weakening dark energy

A key quantitative outcome of the MOC simulations is the emergence of a positive dark energy density at late times with only mild evolution on multi-Gyr timescales. Across all four matter scenarios, once ρ_{Λ_m} becomes positive it grows to a maximum in the range $t \simeq 8$–$10\,\mathrm{Gyr}$ and then decreases slowly thereafter. This is precisely the type of behavior required by recent indications of dynamical dark energy [12, 13, 56]: the dark energy is not strictly constant, but its variation is modest and occurs over long timescales.

[Quantitative late-time behavior]

In the baseline ($f = 0\%$) case (Table 3), ρ_{Λ_m} becomes positive between $t = 4.73$ and $5.73\,\mathrm{Gyr}$, reaches its maximum value.

$$\rho_{\Lambda_m}^{\max} \simeq 7.41 \times 10^{-27}\,\mathrm{kg\,m^{-3}}$$

at $t \simeq 8.73\,\mathrm{Gyr}$, and then declines to

$$\rho_{\Lambda_m}(t_0) \simeq 5.96 \times 10^{-27}\,\mathrm{kg\,m^{-3}}$$

at $t = 12.73\,\mathrm{Gyr}$.

The same qualitative pattern holds in every matter-enhancement scenario (all values below are in units of $10^{-27}\,\mathrm{kg\,m^{-3}}$).

- $f = -10\%$ (Table 7): peak $\rho_{\Lambda_m} \simeq 8.13$ at $t = 8.73\,\mathrm{Gyr}$, decreasing to 6.26 at $t = 12.73\,\mathrm{Gyr}$
- $f = +10\%$ (Table 4): peak $\rho_{\Lambda_m} \simeq 6.74$ at $t = 9.73\,\mathrm{Gyr}$, decreasing to 5.65 at $t = 12.73\,\mathrm{Gyr}$
- $f = +20\%$ (Table 6): peak $\rho_{\Lambda_m} \simeq 6.17$ at $t = 9.73\,\mathrm{Gyr}$, decreasing to 5.34 at $t = 12.73\,\mathrm{Gyr}$

In all four cases, once the peak is reached, the subsequent decline over the last ~ 4–5 Gyr is only at the $\mathcal{O}(10\%)$ level, illustrating the quasi-constant but gently weakening character of dark energy in the late universe within MOC.

[Onset of accelerated expansion]

The onset of accelerated expansion can be approximately identified by the condition

$$\rho_m(t) - 2\rho_{\Lambda_m}(t) < 0 \tag{135}$$

which follows directly from the standard Friedmann acceleration equation in ΛCDM, assuming a pressureless matter component ($w_m = 0$) and an effective dark energy component with equation of state close to $w \simeq -1$ once ρ_{Λ_m} becomes positive. In this sense, the above criterion provides a useful and physically well-motivated diagnostic for the onset of cosmic acceleration, even though $\rho_{\Lambda_m}(t)$ is dynamically generated rather than strictly constant in the MOC framework.

Applying this diagnostic to the four SH0ES-based simulations yields a consistent picture.

- $f = -10\%$: accelerating expansion begins $t_{\rm acc} \approx 6.6\,\mathrm{Gyr}$
- $f = \quad 0\%$: accelerating expansion begins $t_{\rm acc} \approx 7.3\,\mathrm{Gyr}$
- $f = +10\%$: accelerating expansion begins $t_{\rm acc} \approx 7.7\,\mathrm{Gyr}$
- $f = +20\%$: accelerating expansion begins $t_{\rm acc} \approx 8.4\,\mathrm{Gyr}$

Thus, while the exact onset time shifts with the assumed matter content, all four simulations exhibit accelerated expansion beginning within a relatively narrow window of $t_{\rm acc} \sim 6.6$ to 8.4 Gyr. This demonstrates that the acceleration epoch is not a fragile or finely tuned feature of a particular parameter choice, but a robust consequence of the GSE dynamics under the MOC model: as the matter density increases, the onset of acceleration is systematically delayed to later cosmic times.

7.3 Resolving early–universe anomalies (JWST and Euclid)

One of the most striking features of the MOC simulations is the appearance of a **negative** dark energy density in the early universe. This regime can contribute an additional attractive component beyond the standard matter density. It therefore offers a natural pathway to **enhanced early structure growth**, which may help alleviate several early-structure anomalies, including the unusually rapid assembly of massive galaxies reported by JWST [57, 58] and the tensions in structure-growth measurements indicated by Euclid, KiDS, and related surveys [59, 60].

In all four SH0ES–based scenarios, the early–time values of ρ_{Λ_m} (at $t = 0.73\,\mathrm{Gyr}$) are significantly negative.

- $f = -10\%$: $\rho_{\Lambda_m} \simeq -4.01 \times 10^{-25}\,\mathrm{kg\,m^{-3}}$
- $f = \quad 0\%$: $\rho_{\Lambda_m} \simeq -4.33 \times 10^{-25}\,\mathrm{kg\,m^{-3}}$
- $f = +10\%$: $\rho_{\Lambda_m} \simeq -4.64 \times 10^{-25}\,\mathrm{kg\,m^{-3}}$
- $f = +20\%$: $\rho_{\Lambda_m} \simeq -4.94 \times 10^{-25}\,\mathrm{kg\,m^{-3}}$

These values represent a non–negligible attractive contribution in addition to the standard matter density. Physically, this phase of negative dark energy deepens gravitational potential wells and **accelerates the formation of massive bound structures.**

As a result, the MOC model allows for the efficient early assembly of large galaxies and supermassive black holes, even at high redshift [57, 58, 61–63], without invoking exotic new matter components or finely tuned early dark energy sectors. At the same time, the subsequent sign change and late–time positive ρ_{Λ_m} naturally supply the repulsive component required for present–day cosmic acceleration. Thus, within a GSE–based framework, the MOC scenario provides a unified mechanism that can both enhance early structure growth and reproduce the observed late–time acceleration, turning several apparent crises of ΛCDM into potential evidence for matter–induced dark energy.

7.4 The cosmological constant coincidence problem

A long–standing conceptual puzzle in the standard ΛCDM framework is the **Cosmological Constant Coincidence Problem** (CCCP) [3, 4, 8]: why is the dark energy density observed today of the same order of magnitude as the matter density, despite their fundamentally different origins and vastly different redshift scalings? In ΛCDM, this near equality occurs only within a narrow temporal window. This has motivated either fine-tuned initial conditions or anthropic reasoning in parts of the literature [3, 8].

In the MOC framework, the same observation is not a coincidence that demands a separate explanation. The dark energy density $\rho_{\Lambda_m}(t)$ does not represent an independent vacuum component, but arises dynamically from the GSE of matter itself. As a result, $\rho_{\Lambda_m}(t)$ is intrinsically linked to the matter density $\rho_m(t)$ and to the growth of the particle horizon, rather than being a fixed external constant.

Because both ρ_m and ρ_{Λ_m} originate from the same underlying matter distribution, their magnitudes remain comparable over a substantial fraction of cosmic history. This behavior is explicitly demonstrated in the SH0ES–based simulations (Fig. 3), where the matter density and the dark energy density track each other closely throughout the late universe, crossing and diverging only mildly as the universe transitions into and out of its accelerated phase.

From this perspective, the apparent coincidence $\rho_m \sim \rho_{\Lambda_m}$ at the present epoch is not accidental. Instead, it constitutes one of the strongest empirical signatures of a matter–induced dark energy scenario. What appears as an unnatural coincidence in ΛCDM emerges naturally in the MOC framework as a direct consequence of GSE dynamics, providing a compelling resolution of the cosmological constant coincidence problem without invoking fine tuning or anthropic reasoning.

7.5 Describes the dynamics of the universe without new free parameters or fields

Age (Gyr)	Scale $a(t)$	Evolving $\beta(t)$	Comoving Ho. $\chi_p(t)$ (Gly)	Physical Ho. $R_{\text{phys}}(t)$ (Gly)	**Matter** $\rho_m(t)$	Repulsive $\rho_{m\text{-}gs}(t)$	Attractive $-\rho_{gs}(t)$	**Dark Energy** $\rho_{\Lambda_m}(t)$
					(10^{-27} kg m^{-3})			
0.8	0.1295	1.3879	17.744	2.298	1360.95	125.700	-489.386	**-363.686**
1.8	0.2226	1.3879	23.496	5.230	267.964	76.092	-168.955	**-92.863**
2.8	0.2998	1.3879	27.340	8.197	109.688	57.100	-93.640	**-36.539**
3.8	0.3694	1.3879	30.335	11.206	58.636	46.262	-61.625	**-15.363**
4.8	0.4346	1.3879	32.827	14.267	36.007	38.958	-44.315	**-5.357**
5.8	0.4972	1.3879	34.975	17.390	24.047	33.526	-33.595	**-0.070**
6.8	0.5584	1.3879	36.872	20.589	16.975	29.234	-26.358	2.876
7.8	0.6190	1.3879	38.572	23.876	12.462	25.701	-21.175	4.526
8.8	0.6796	1.3879	40.113	27.261	9.417	22.715	-17.305	5.411
9.8	0.7408	1.3879	41.522	30.759	7.270	20.135	-14.316	5.819
10.8	0.8031	1.3879	42.818	34.387	5.706	17.870	-11.948	5.922
11.8	0.8668	1.3879	44.017	38.154	4.538	15.873	-10.043	5.831
12.8	0.9323	1.3879	45.129	42.074	3.647	14.096	-8.484	5.612
13.8	1.0000	1.3879	46.450	46.450	2.956	12.820	-7.283	5.537

Table 8: **MOC Cosmic History Simulation (CMB-Based, + 10% Matter Enhancement).** This table shows dark energy density evolution assuming a 10% higher matter density ($\Omega_m \approx 0.347$) while matching the standard ΛCDM current horizon (46.45 Gly). Under these conditions, a constant structural parameter $\beta = 1.3879$ is sufficient to satisfy the flatness condition ($\Omega_{tot} \approx 1$) and reproduce the observed dark energy density at the present epoch. The transition from deceleration to acceleration ($\rho_{\Lambda_m} > \rho_m/2$) occurs around $t \approx 7.8$–8.8 Gyr. The dark energy density reaches a finite maximum near $t \approx 10.8$ Gyr and then decreases slowly at late times, which is consistent with recent observational indications of mildly evolving dark energy [12]. Overall, the simulation illustrates that the qualitative sequence of early negative density, sign transition, and late time weakening emerges without introducing new fields and without requiring fine tuning of a time dependent dark energy sector.

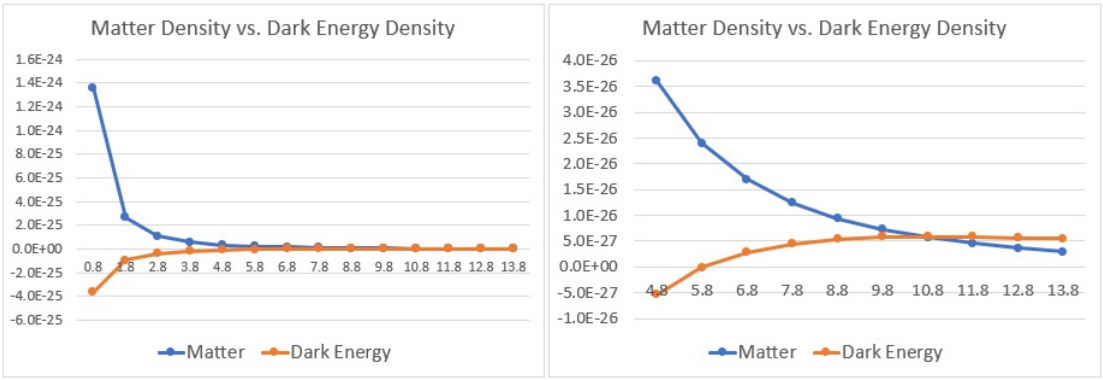

Figure 4: **Matter Density vs. Dark Energy Density (CMB-Based, + 10% Matter Enhancement, β=1.3879 = const.):** $\Omega_m = 0.347$. Dark energy density becomes negative at t< $\sim$ 5.8Gyr, promotes the formation of galaxy structures, then accelerates the expansion of the universe from approximately t $\sim$8.3 Gyr, peaks around t=10.8 Gyr, and then monotonically decreases.

The MOC framework explains the observed dark energy phenomenology without introducing new fundamental fields or additional phenomenological fluids. In this framework the dark energy density arises from the total GSE of matter and its large scale organization. The key point is that the qualitative cosmic behavior of $\rho_{\Lambda_m}(t)$ is not obtained by selecting a time dependent dark energy sector, but follows from the geometric scaling of the GSE terms.

The temporal variation of the structural parameter β remains modest, at the level of $\mathcal{O}(0.1)$ over the entire evolutionary history considered. **In fact, even when β is fixed to a constant value, the dark energy density exhibits the same qualitative behavior**: it is negative in the early universe, undergoes a sign transition at intermediate epochs, drives accelerated expansion in the late universe, reaches a finite maximum, and subsequently decreases monotonically.

This demonstrates that, within the MOC framework, the dark energy phenomenology is not sensitively dependent on the detailed evolution of structural parameters, but instead arises robustly from the geometric scaling of GSE.

This implies that β is not the driver of cosmic dynamics but simply the coefficient inherent to the GSE formulation, bringing the theory significantly closer to a parameter-free description of dark energy.

In particular, **large scale N body simulations of structure formation [50, 51], directly compared with observed galaxy and cluster scale statistics, provide a well defined route to computing β from first principles and removing it from the set of adjustable inputs.**

8 Effective Equation of State $w_{\Lambda_m}(t)$ and Key Transition Points in the MOC

8.1 Effective equation of state $w_{\Lambda_m}(t)$

In the MOC framework, the effective equation of state of matter–induced dark energy is not fixed at $w = -1$ but evolves dynamically with cosmic time. Using the updated SH0ES baseline simulation (+0% matter enhancement; Table 3), we estimate the time-dependent equation of state from the continuity relation for the dark energy component.

Assuming that w_{Λ_m} varies slowly across a single time step, a finite-difference estimator is

$$w_{\Lambda_m}(t_i) \approx -1 - \frac{1}{3}\frac{\ln[\rho_{\Lambda_m}(t_{i+1})/\rho_{\Lambda_m}(t_i)]}{\ln[a(t_{i+1})/a(t_i)]} \tag{136}$$

Since $\rho_{\Lambda_m} < 0$ before the sign crossover, the equation of state is undefined for $t \lesssim 4.8\,\mathrm{Gyr}$. After the transition to positive values, $w_{\Lambda_m}(t)$ becomes meaningful and can be tracked through the subsequent evolution.

Cosmic Age (Gyr)	**Estimated $w_{\Lambda_m}(t)$**
5.73	≈ -2.2 (strongly phantom–like; rapid growth)
6.73	≈ -1.5
7.73	≈ -1.1
8.73	≈ -1.1
9.73	≈ -0.95
10.73	≈ -0.82
11.73	≈ -0.72
12.73	≈ -0.61

Table 9: Estimated $w_{\Lambda_m}(t)$ for the SH0ES baseline (+0% matter) simulation. Shortly after ρ_{Λ_m} becomes positive near $t \simeq 4.8$–$5.0\,\mathrm{Gyr}$, the dark energy density grows rapidly with $w_{\Lambda_m} < -1$. As $\rho_{\Lambda_m}(t)$ approaches its maximum, w_{Λ_m} remains close to -1. Once $\rho_{\Lambda_m}(t)$ begins to decline, w_{Λ_m} crosses into the regime $w_{\Lambda_m} > -1$ at late times.

As summarized in Table 9, the effective equation of state is highly dynamic. Immediately after the sign change, the dark energy density increases rapidly between $t \approx 5.7$ and $7.7\,\mathrm{Gyr}$, corresponding to a clearly phantom–like regime ($w < -1$). Near the epoch at which $\rho_{\Lambda_m}(t)$ reaches its maximum ($t \simeq 8.7\,\mathrm{Gyr}$), the inferred values remain close to -1. Subsequently, as $\rho_{\Lambda_m}(t)$ begins to decline, the equation of state crosses the cosmological–constant boundary and moves into the quintessence regime, reaching $w \approx -0.6$ by $t = 12.73\,\mathrm{Gyr}$.

This late-time evolution corresponds to a gradual reduction of the effective repulsive influence associated with the dark energy component. Within the MOC interpretation, this suggests that the universe may be moving away from its most strongly accelerated phase at late times. This qualitative trend is consistent with recent observational analyses that allow for a weakening of dark energy [56].

8.2 Key transition points in the MOC model

Using the updated SH0ES-anchored simulations, we identify two transition epochs that characterize the late-time emergence of matter-induced dark energy. Transition times are obtained via linear interpolation between discrete simulation points. Importantly, the emergence of repulsive dark energy does not immediately lead to cosmic acceleration.

The early negative phase ($t \lesssim 4.8\,\mathrm{Gyr}$) enhances structure formation by providing an additional gravitationally attractive contribution to the cosmic energy budget. However, the mere appearance of positive dark energy does not immediately induce cosmic acceleration. Only after the condition $\rho_{\Lambda_m} \gtrsim 0.5\rho_m$ is met at $t \approx 7.25\,\mathrm{Gyr}$ does the universe transition into an accelerating phase. In the updated simulation, the dark energy density increases up to a maximum at $t \approx 8.7\,\mathrm{Gyr}$ and then slowly declines, exhibiting a gradual flattening that is consistent with a slowly varying dark energy component rather than a strict cosmological constant.

Transition	Definition	Interval	t (Gyr)	z	Notes
Sign Crossover	$\rho_{\Lambda_m} = 0$	4.73→5.73	≈ 4.85	≈ 1.2	Dark energy changes sign from attractive to repulsive.
Acceleration Onset	$\rho_{\Lambda_m} \approx \frac{1}{2}\rho_m$	6.73→7.73	≈ 7.25	≈ 0.6	Repulsive dark energy becomes strong enough to dominate over matter and trigger global acceleration.

Table 10: Key transition epochs for the SH0ES baseline (**+0% matter enhancement**). A characteristic feature of the MOC model is the delay between the onset of repulsive dark energy ($z \approx 1.2$) and the onset of accelerated expansion ($z \approx 0.6$). The resulting transition redshift lies within the broad range of model–independent observational estimates for the onset of cosmic acceleration.

Transition	Definition	Interval	t (Gyr)	z	Notes
Sign Crossover	$\rho_{\Lambda_m} = 0$	4.73→5.73	≈ 5.25	≈ 1.0	Dark energy changes sign from attractive to repulsive.
Acceleration Onset	$\rho_{\Lambda_m} \approx \frac{1}{2}\rho_m$	6.73→7.73	≈ 7.73	≈ 0.53	Repulsive dark energy becomes strong enough to compete with matter and trigger global acceleration.

Table 11: Key transition epochs for the SH0ES baseline (**+10% matter enhancement**). Compared to the baseline case (+0%), both the sign change of ρ_{Λ_m} and the onset of acceleration are shifted to slightly later times ($t \approx 5.25$ Gyr and $t \approx 7.73$ Gyr, respectively), illustrating how an increased matter content delays the onset of dark energy driven acceleration.

The same qualitative pattern appears in the other SH0ES–based scenarios. For +10% and +20% matter enhancements, the sign crossover of ρ_{Λ_m} occurs slightly later ($t \approx 5.0$ and 5.5 Gyr, respectively), and the acceleration onset is shifted to $t \sim 7.7$–8.4 Gyr, while the peak dark energy density moves toward $t \approx 9$–9.7 Gyr (Tables 4, 6). In the −10% matter case, both the sign crossover and acceleration onset occur earlier (around $t \approx 4.5$ Gyr and $t \approx 6.6$ Gyr, respectively; Table 7), and the peak of ρ_{Λ_m} is reached near $t \approx 8.7$ Gyr. Despite these shifts, all cases exhibit the same three-phase sequence of (negative) attraction, growth to a positive maximum, and a slowly declining repulsive phase in the late universe.

9 The Future of the Universe in the MOC

In the MOC framework, the long-term fate of the universe is governed not by a fixed vacuum energy, but by the dynamical structure of the total GSE. Unlike ΛCDM, where dark energy is introduced as an independent constant [3, 4, 8], the MOC model treats the dark energy density as an emergent quantity determined by the interplay between physical dilution and causal structure. In particular, the dark energy density depends explicitly on the matter density ρ_m and the dimensionless geometric ratio R_S/χ_p as follows

$$\rho_{\Lambda_m} = \frac{\beta \rho_m}{2} \frac{R_S}{\chi_p} \left(\frac{5\beta}{14} \frac{R_S}{\chi_p} - 1 \right) \tag{137}$$

This expression follows directly from the generalized horizon formulation of the GSE densities. Here $R_S = 2GM/c^2$ is the Schwarzschild radius associated with the total mass $M = \rho_m V_{\text{phys}}$ contained within the causally connected region, while the particle horizon χ_p sets the causal

interaction scale governing the formation of GSE.

The sign of cosmic acceleration is therefore determined by the evolution of the combination $\rho_m(R_S/\chi_p)$. While the matter density scales as $\rho_m \propto a^{-3}$ in an expanding universe [18, 42], the Schwarzschild radius R_S grows with the total mass enclosed within the particle horizon as $R_S \propto \chi_p^3 \rho_m \propto \chi_p^3 a^{-3}$. Consequently, the term R_S/χ_p scales as $\chi_p^2 a^{-3}$. During the epoch of late-time acceleration, the growth of the particle horizon $\chi_p(t)$ is logarithmic or slower relative to the scale factor $a(t)$. This implies that the factor $\rho_m(R_S/\chi_p)$ will eventually decrease monotonically in the far future, suggesting that the repulsive phase defined by $\rho_{\Lambda_m} > 0$ cannot persist indefinitely. A future transition toward a weaker dark energy density is therefore a structural necessity of the model.

Quantitatively, the SH0ES–based simulations indicate that the current repulsive phase is already past its maximum strength. Across all four matter realizations (−10%, 0%, +10%, +20%), the dark energy density $\rho_{\Lambda_m}(t)$ increases after its sign transition, reaches a broad maximum in the interval $t \simeq 8.7$–$9.7\,\mathrm{Gyr}$, and then decreases toward the present epoch. At $z = 0$, the predicted values converge to $\rho_{\Lambda_m}(t_0) \simeq (5.3\text{–}6.3) \times 10^{-27}\,\mathrm{kg\,m^{-3}}$, consistent with the expectation that the late-time dynamics is relatively insensitive to detailed microphysical parameters [3, 4].

Although the present simulation window does not yet show a full turnover to negative ρ_{Λ_m}, the post-peak decline is clearly visible in all cases. This behavior implies that the effective equation of state has already crossed into the quintessence regime ($w > -1$) and is evolving away from the de Sitter limit [8]. The gradual decrease of ρ_{Λ_m} provides physical motivation for a future transition toward weaker acceleration and potentially toward deceleration in a later epoch.

9.1 Self-regulation of cosmic expansion: A natural feedback cycle

A key structural feature of the MOC framework is the feedback between the expansion history and the GSE term itself. This feedback is mediated by the distinct evolution of the matter density ρ_m and the geometric ratio R_S/χ_p. Such feedback mechanisms are generic in nonlinear gravitational systems [39, 42].

- During **accelerated expansion**, the rapid growth of the scale factor $a(t)$ strongly dilutes the matter density ρ_m. This suppression of the factor $\rho_m(R_S/\chi_p)$ weakens the repulsive GSE contribution. In the simulations, this behavior appears as a flattening and eventual decline of $\rho_{\Lambda_m}(t)$ after it reaches a finite maximum.
- During **decelerated expansion**, the dilution of ρ_m is slower while the time evolution of the particle horizon $\chi_p(t)$ can become comparatively more effective. Consequently, the quantity $\rho_m(R_S/\chi_p)$ decreases less rapidly than in the accelerated phase, allowing the repulsive GSE component to recover relative importance. This process pushes $\rho_{\Lambda_m}(t)$ back toward more positive values and can re-enable acceleration.

This qualitative feedback structure resembles that of a damped oscillator. The system can overshoot the neutral point defined by $\rho_{\Lambda_m} = 0$, while the amplitude of each excursion is reduced as the overall energy scale continues to dilute in an expanding background [3, 42].

9.2 Entry into a decelerating phase in the near future

The MOC framework links the sign of cosmic acceleration to the evolution of the same controlling combination that appears in the total GSE expression. Equivalently, the sign of ρ_{Λ_m} is

governed by the bracketed factor

$$\frac{5\beta}{14}\frac{R_S}{\chi_p} - 1 \tag{138}$$

As the universe accelerates, the rapid increase in the physical volume and the subsequent dilution of ρ_m cause the ratio R_S/χ_p to decrease, leading the above factor toward zero. The simulations indicate that the sign transition $\rho_{\Lambda_m} = 0$ occurred in the past at $t \simeq 4.5$–8.7, Gyr depending on the matter content. All models subsequently exhibit a finite maximum of ρ_{Λ_m} followed by a gradual decline.

These trends suggest that the universe may enter a new decelerating expansion phase within the next few billion years if $\rho_{\Lambda_m}(t)$ continues to decrease from its post-peak values.

This expectation is reinforced by the decline of the quantity $\rho_m(R_S/\chi_p)$ in the late-time regime [18, 39] and by the intrinsic feedback between the expansion history and the GSE term.

9.3 Long-term behavior: Damped oscillatory evolution

Because ρ_{Λ_m} depends on the evolving quantity $\rho_m(R_S/\chi_p)$, the MOC framework naturally allows repeated sign changes of the GSE contribution. Once the feedback between the expansion history and the horizon scales becomes active, this can give rise to alternating phases of accelerated and decelerated expansion. As the matter density continues to dilute, each successive cycle is expected to exhibit a smaller amplitude. The characteristic timescale of the oscillation may also increase at late epochs, as the effective driving term evolves more slowly. This behavior is typical of a damped dynamical system, analogous to the feedback mechanisms discussed in nonlinear cosmic structure formation [3, 42].

Importantly, the early stages of this damped evolution are, in principle, observationally testable. In particular, a gradual weakening of dark energy, a transition toward $w > -1$, and the eventual onset of a decelerating phase constitute concrete predictions of the MOC framework. Future high-precision measurements of $w(a)$ and its time dependence, for example from LSST, DESI, and Euclid, can therefore directly probe this regime.

The universe thus evolves toward a damped, slowly varying expansion history, rather than eternal acceleration or an abrupt recollapse. The oscillatory description here should be understood as an effective characterization of the intermediate and late-time dynamics, prior to the exhaustion of causal structure formation.

9.4 Ultimate fate of the universe after horizon saturation

Beyond the observationally accessible regime, the MOC framework also provides a well-defined prediction for the ultimate fate of the universe. This fate is governed by the saturation of the comoving particle horizon and the consequent termination of causal matter inflow.

Once the particle horizon approaches its asymptotic limit,

$$\chi_p(t); \rightarrow; \chi_{\mathrm{lim}}; \approx; 62\text{–}64\ \mathrm{Gly} \tag{139}$$

no additional comoving matter shells can enter the causally connected region [35, 45]. As a direct consequence, the total mass enclosed within the particle horizon, $M(t)$, asymptotically approaches a finite maximum value M_∞.

While the mass sourcing the GSE ceases to grow, the scale factor $a(t)$ continues to increase due to the inertia of the cosmic expansion [4]. Since the Schwarzschild radius R_S is proportional to the enclosed mass, it also approaches a constant value $R_{S,\infty}$. However, the matter

density ρ_m continues to dilute as a^{-3}. As a result, the controlling combination $\rho_m(R_S/\chi_p)$ decreases monotonically in the post-saturation regime.

Within the MOC dark energy expression, this monotonic decrease inevitably drives the bracketed factor controlling the sign of ρ_{Λ_m} toward negative values. The repulsive phase of matter-induced dark energy therefore cannot persist indefinitely. After the current post-peak epoch, the universe must transition into a purely decelerating expansion phase. This deceleration does not imply a recollapse or a Big Crunch scenario. Because the total enclosed mass remains finite and the expansion rate remains positive, the universe continues to expand, albeit with steadily decreasing acceleration. The expansion asymptotically approaches a slow, matter-dominated dilution rather than a reversal.

The long-term cosmological outcome in the MOC framework is thus neither eternal acceleration nor catastrophic collapse, but a gradual approach to a thermodynamically cold and dilute state. In this sense, the ultimate fate of the universe resembles a form of cosmic heat death, characterized by ever-expanding physical scales, diminishing interaction rates, and a vanishingly small dark energy density. The same GSE mechanism that generates cosmic acceleration at intermediate epochs therefore also guarantees its eventual shutdown once causal structure formation is exhausted.

10 A Unified Physical Origin for Cosmic Acceleration

The standard ΛCDM model treats primordial inflation and late-time acceleration as disconnected phenomena, typically driven by independent scalar fields [64–68]. The GSE framework in MOC unifies both via a single, intuitive principle. The dark energy density arises from the total GSE of the contents of the causal horizon, expressed elegantly in terms of its compactness ratio as follows

$$\rho_{\Lambda_m} = \frac{\beta\rho_m}{2}\frac{R_S}{\chi_p}\left(\frac{5\beta}{14}\frac{R_S}{\chi_p} - 1\right) \tag{140}$$

In the General GSE framework, this single equation reveals a fundamental **Density-Scale Duality**. Repulsive gravity ($\rho_{\Lambda_m} > 0$) is driven by extreme density at small scales during inflation and by extreme scale geometric factors at low densities in the late-time dark energy epoch.

10.1 Inflation: Acceleration at extreme density

We quantify the dark energy density at the Planck epoch. In the radiation-dominated early universe, the causal scale χ_p and the physical scale R_{phys} are tightly coupled and comparable such that $R_{\text{phys}} \approx \chi_p \approx R$. Under these conditions, the MOC expression becomes a function of the local density and the compactness ratio.

$$\rho_{\Lambda_m} \approx \frac{\beta\rho_m}{2}\frac{R_S}{R}\left(\frac{5\beta}{14}\frac{R_S}{R} - 1\right) \tag{141}$$

We take $\rho_m \simeq \rho_{\text{pl}}$ and $R \simeq l_{\text{pl}}$ at this epoch. Since the early universe is expected to be extremely dense and highly structured in terms of quantum fluctuations, we assume a structural parameter close to its upper bound, $\beta \simeq 2$.

The compactness ratio at the Planck scale is calculated using the Planck density as follows

$$\frac{R_S}{R} = \frac{2GM}{c^2R} = \frac{2G(\frac{4}{3}\pi R^3\rho_{pl})}{c^2R} = \frac{8\pi G\rho_{pl}l_{pl}^2}{3c^2} = \frac{8\pi}{3} \approx 8.38 \tag{142}$$

Substituting these values into the MOC expression for ρ_{Λ_m} yields.

$$\rho_{\Lambda_m} \approx \frac{2\rho_{\rm pl}}{2}(8.38)\left(\frac{5(2)}{14}(8.38)-1\right) \approx 8.38\times(5.99-1) \tag{143}$$

This calculation gives a dark energy density of

$$\rho_{\Lambda_m} \approx 8.38\times 4.99 \approx 41.8\rho_{\rm pl} \tag{144}$$

To assess whether this GSE-induced dark energy drives accelerated expansion, we use the general FRW acceleration equation as a diagnostic tool

$$\frac{\ddot{a}}{a} = -\frac{4\pi G}{3}\sum_i \left(\rho_i + 3p_i/c^2\right) \tag{145}$$

For radiation, the equation of state is $p_r = \rho_r c^2/3$, so that

$$\rho_r + 3p_r/c^2 = 2\rho_r \tag{146}$$

For the GSE dark energy component, we adopt an effective equation of state $p_{\Lambda_m} \simeq -\rho_{\Lambda_m}c^2$ over the relevant interval, yielding

$$\rho_{\Lambda_m} + 3p_{\Lambda_m}/c^2 \approx -2\rho_{\Lambda_m} \tag{147}$$

The acceleration equation therefore reduces to

$$\frac{\ddot{a}}{a} \approx -\frac{8\pi G}{3}\left(\rho_r - \rho_{\Lambda_m}\right) \tag{148}$$

Assuming an effective equation of state $w \approx -1$ for this dark energy component, the acceleration equation at the Planck epoch becomes

$$\frac{\ddot{a}}{a} \approx -\frac{8\pi G}{3}(\rho_{\rm pl} - \rho_{\Lambda_m}) = -\frac{8\pi G}{3}(\rho_{\rm pl} - 41.8\rho_{\rm pl}) > 0 \tag{149}$$

This strongly negative effective density results in a powerful accelerated expansion, which provides a natural mechanism to solve the horizon and flatness problems without the need for additional scalar fields.

Energy Density & Hierarchy With $\rho_{\rm pl} \simeq 5.16\times 10^{96}\,\mathrm{kg/m^3}$, the calculated dark energy density is

$$\rho_{\Lambda_m} \approx 2.16\times 10^{98}\,\mathrm{kg/m^3} \tag{150}$$

$$E_{\Lambda_m} = \rho_{\Lambda_m}c^2 \approx 1.94\times 10^{115}\,\mathrm{J/m^3} \tag{151}$$

$$E_{\Lambda_m}^{(\mathrm{Planck})} \sim 10^{115}\ \mathrm{J/m^3} \tag{152}$$

which naturally matches the canonical "Planck vacuum" magnitude required for inflation.

Using the observed late-time dark energy density $\rho_{\Lambda\text{-obs}} \simeq 7\times 10^{-27}\,\mathrm{kg/m^3}$ (i.e., $E_{\Lambda\text{-obs}} \simeq 6\times 10^{-10}\,\mathrm{J/m^3}$),

$$\frac{\rho_{\Lambda_m}^{(\mathrm{Planck})}}{\rho_{\Lambda\text{-obs}}} \approx \frac{2.16\times 10^{98}}{7\times 10^{-27}} \simeq 3\times 10^{124} \tag{153}$$

Equivalently $E_{\Lambda_m}^{(\mathrm{Planck})}/E_{\Lambda\text{-obs}} \sim 10^{124}$. Thus, MOC naturally attains the colossal inflationary scale while explaining the late-time tiny value through the same density–size GSE mechanism, without fine-tuning or new fields.

10.2 Inflation triggered by GSE: Consistency with standard inflation scales

In the MOC framework, primordial inflation is not postulated as an independent dynamical sector. Instead, inflation can emerge when the matter-induced dark energy generated by total GSE becomes comparable to the dominant radiation component.

10.2.1 Acceleration condition in a radiation background

For a radiation component with equation of state $w_r = 1/3$ and a dark energy-like component with $w_{\Lambda_m} \simeq -1$ during the repulsive phase, the acceleration equation reduces to

$$\frac{\ddot{a}}{a} \approx -\frac{8\pi G}{3}\left(\rho_r - \rho_{\Lambda_m}\right) \tag{154}$$

Inflation begins when the right-hand side becomes positive, which is approximately the condition

$$\rho_{\Lambda_m} = \rho_r \tag{155}$$

10.2.2 Causal regime at very early times

At sufficiently early times, causality enforces a single characteristic scale for the size of the causally connected region. Independently of whether accelerated expansion has already started, one can take

$$\chi_p \approx R_{\text{phys}} \approx R \tag{156}$$

and, at the level of an order-of-magnitude trigger estimate, adopt

$$R \approx ct \tag{157}$$

In this causal regime, the MOC GSE expression can be written in terms of the compactness ratio as

$$\rho_{\Lambda_m} = \frac{\beta\rho_r}{2}\frac{R_S}{R}\left(\frac{5\beta}{14}\frac{R_S}{R} - 1\right) \tag{158}$$

where the Schwarzschild radius is defined by $R_S = \frac{2GM}{c^2}$. And the enclosed mass within radius R is approximated by

$$M = \frac{4\pi}{3}R^3\rho_r \tag{159}$$

10.2.3 Ratio form and the time–density trigger

Dividing Eq. (158) by ρ_r gives

$$\frac{\rho_{\Lambda_m}}{\rho_r} = \frac{\beta}{2}\frac{R_S}{R}\left(\frac{5\beta}{14}\frac{R_S}{R} - 1\right) \tag{160}$$

For the early-universe configuration emphasized in this paper, we take $\beta \simeq 2$, which yields

$$\frac{\rho_{\Lambda_m}}{\rho_r} \approx \frac{R_S}{R}\left(\frac{5}{7}\frac{R_S}{R} - 1\right) \tag{161}$$

Using Eq.(159), the compactness ratio becomes

$$\frac{R_S}{R} = \frac{2GM}{c^2R} = \frac{8\pi G}{3}\frac{R^2\rho_r}{c^2} \tag{162}$$

With the causal estimate $R \approx ct$, this simplifies to

$$\frac{R_S}{R} \approx \frac{8\pi G}{3} t^2 \rho_r \tag{163}$$

Substituting Eq. (163) into Eq. (161) gives

$$\frac{\rho_{\Lambda_m}}{\rho_r} \approx \frac{8\pi G}{3} t^2 \rho_r \left(\frac{40\pi G}{21} t^2 \rho_r - 1 \right) \tag{164}$$

Imposing the inflation condition $\rho_{\Lambda_m} = \rho_r$ from Eq. (155) yields a quadratic equation for the combination $t^2\rho_r$. The physically relevant solution can be written as

$$\boxed{t^2 \rho_r \simeq 3.71 \times 10^9} \tag{165}$$

10.2.4 Numerical implications at $t \simeq 10^{-36}\,\mathrm{s}$ and $t \simeq 10^{-35}\,\mathrm{s}$

Equation (165) implies the following two equivalent interpretations.

Inflation time ⇒ density scale. If inflation begins at

$$t \simeq 10^{-36}\,\mathrm{s} \tag{166}$$

then Eq. (165) predicts

$$\rho_r \simeq 3.71 \times 10^{81}\,\mathrm{kg\,m^{-3}} \tag{167}$$

which lies within the standard inflationary onset window commonly discussed in early inflationary models [65–67].

Likewise, if one considers a later onset time

$$t \simeq 10^{-35}\,\mathrm{s} \tag{168}$$

the required density decreases as $\rho_r \propto t^{-2}$, giving

$$\rho_r \simeq 3.71 \times 10^{79}\,\mathrm{kg\,m^{-3}} \tag{169}$$

Density scale ⇒ inflation time. Conversely, if the early universe is characterized by a nearly homogeneous radiation density of order $\rho_r \sim 10^{81}\,\mathrm{kg\,m^{-3}}$, then Eq. (165) implies that the GSE trigger $\rho_{\Lambda_m} = \rho_r$ is reached automatically at $t \sim 10^{-36}\,\mathrm{s}$.

The MOC GSE trigger relation in Eq. (165) provides a direct mapping between a characteristic inflation onset time and a characteristic early-universe mean radiation density. In this sense, the MOC framework can reproduce the usual inflationary scale window without introducing an additional inflaton field or a fine-tuned potential. Inflation emerges as a gravitational phenomenon driven by the compactness of the causally connected region and the resulting total GSE.

10.2.5 Why $\rho_r \sim 10^{79}$–$10^{81}\,\mathrm{kg\,m^{-3}}$ is physically motivated in standard inflation

In standard inflationary phenomenology, the relevant scale is often expressed by the inflationary potential energy density V. A conventional relation links the energy scale $V^{1/4}$ to the tensor-to-scalar ratio r, schematically yielding $V^{1/4}$ in the ballpark of 10^{15}–$10^{16}\,\mathrm{GeV}$ for observationally allowed r values [64, 69]. Because an energy scale $V^{1/4} \sim 10^{15}$–$10^{16}\,\mathrm{GeV}$ corresponds to an enormous energy density $V \sim (10^{15}\text{–}10^{16}\,\mathrm{GeV})^4$, this translates to mass-density scales of order 10^{79}–$10^{81}\,\mathrm{kg\,m^{-3}}$ when converted to SI units.

Therefore, the density level required by the GSE trigger relation in Eq. (**??**) is not an ad hoc insertion. It lies in the same broad magnitude range that is typically invoked when one parametrizes inflation by a high inflationary energy scale, constrained by the observed amplitude of primordial perturbations and the upper bounds on primordial tensor modes [69].

10.2.6 Initial near-thermal state and its implications for early accelerated expansion

The conventional "horizon problem" is often phrased as a causal objection to the near-uniform CMB temperature observed across widely separated directions on the sky [65–67]. Here we adopt a different viewpoint that is natural within a matter-only, GSE-driven cosmology.

If the universe originates from a single underlying physical mechanism, it is not compelling to assume that widely separated regions are "prepared" with substantially different temperatures or macroscopic states at birth. Rather, in the absence of detailed information about microscopic initial conditions, the most natural macroscopic description of the primordial state is a near-thermal configuration, with deviations that are small and statistically characterized [18].

In this picture, the early accelerated expansion driven by the total GSE proceeds from an initially hot, nearly equilibrated state. As the universe expands and the interactions effectively differentiate through successive dynamical processes, including gravitational instability and phase transitions, the system generically departs from perfect equilibrium. The observed CMB anisotropy at the level of $\Delta T/T \sim 10^{-5}$ is then interpreted not as evidence for a highly non-thermal primordial preparation, but as the expected residual imprint of a nearly equilibrated origin that becomes gradually perturbed by subsequent dynamics [5].

Under this near-thermal initial condition, the conceptual role of primordial acceleration is altered. In contrast to the standard inflationary argument, the accelerated expansion is not required to enforce global causal contact across the entire last-scattering surface. Instead, accelerated expansion occurs because the total GSE energy is positive. The initial accelerated phase (inflation) is therefore a natural dynamical response that relieves the negative pressure associated with the GSE.

The resulting dynamics naturally suppress primordial curvature, dilute relic abundances, and establish initial conditions compatible with the observed near scale-invariant perturbation spectrum [65, 66, 69], without invoking any teleological principle. In this framework, the conventional single-patch requirement is relaxed. If the primordial state is already characterized by a nearly uniform thermal configuration, the number of e-folds required during the early accelerated phase is not dictated by the need to causally synchronize the entire observable universe. Rather, it is determined by dynamical considerations such as the onset of perturbation generation, the stabilization of spatial flatness, and the smooth transition into the subsequent radiation-dominated epoch.

Consequently, a moderately reduced amount of accelerated expansion, compared to that assumed in standard inflationary scenarios, is sufficient within the MOC framework. The accelerated phase driven by the total GSE acts to preserve and gently amplify an already near-equilibrated initial state, rather than to manufacture large-scale homogeneity from an initially uncorrelated configuration.

Because the universe remains hot throughout this process and transitions smoothly into the radiation-dominated phase, the role traditionally played by excessive exponential expansion is replaced by thermal continuity and causal evolution.

As a result, MOC inflation does not need to generate an arbitrarily large number of e-folds. The required expansion factor is fixed by the adiabatic cooling needed to connect the inflationary exit temperature, $T_{\rm end} \sim 10^{15}$–10^{16} GeV, to the onset of Big Bang Nucleosynthesis at $T_{\rm BBN} \sim 10^{9}$ K. This corresponds to a finite expansion of order 10^{19}–10^{20}, which is sufficient to establish the observed thermal history without invoking superfluous exponential growth.

10.3 The self-terminating mechanism of MOC inflation

A longstanding difficulty in standard inflationary cosmology is the graceful-exit and reheating problem [70, 71]. In conventional models, inflation is driven by an external scalar inflaton field whose potential energy dominates the cosmic energy budget. Once inflation ends, the universe is left in a supercooled state due to the enormous exponential expansion required to solve the horizon and flatness problems. Recovering a hot, radiation-dominated universe therefore necessitates an additional reheating phase, in which the inflaton field decays into standard model particles through model-dependent microphysical processes.

In the MOC framework, this entire structure is replaced by a single gravitational mechanism. Inflation is not sourced by an independent scalar field but emerges dynamically when the matter-induced dark energy generated by total GSE becomes comparable to, and then exceeds, the radiation density. As a consequence, the termination of inflation is not a separate dynamical event but follows directly from the same gravitational term that initiates the accelerated expansion.

The sign and magnitude of the dark energy density in MOC are governed by the dimensionless factor

$$\Gamma(R) \equiv \left(\frac{5\beta}{14}\frac{R_S}{R} - 1\right) = \left(\frac{5\beta}{14}\frac{2GM}{c^2 R} - 1\right) \tag{170}$$

which appears explicitly in the total GSE contribution.

Using the mass-density relation $M = \frac{4\pi}{3}R^3\rho$, this factor can be rewritten as

$$\Gamma(R) = \left(\frac{20\pi\beta G}{21c^2}\rho R^2 - 1\right) \tag{171}$$

During this initial phase, the universe is radiation-dominated, meaning its energy density scales with the size of the causal patch R as $\rho \propto R^{-4}$. Substituting this scaling relation $\rho(R) = \rho_i(R_i/R)^4$ into the equation reveals the inherent evolution of the acceleration driver.

$$\Gamma(R) = \left(\frac{20\pi\beta G}{21c^2}\rho_{\rm i} R_i^4 \frac{1}{R^2} - 1\right) \equiv \left(\frac{C}{R^2} - 1\right) \tag{172}$$

where C is a positive constant fixed by the initial conditions.

This expression makes the termination mechanism transparent. At extremely early times, corresponding to the high-density regime emphasized in standard inflationary phenomenology, the compactness of the causally connected region ensures $\Gamma(R) \gg 0$. The resulting positive dark energy density generates strong repulsive gravity and drives rapid accelerated expansion. However, the same expansion that characterizes inflation inevitably increases the characteristic scale R. Because the leading contribution to $\Gamma(R)$ scales as R^{-2}, the repulsive term decays monotonically as the universe expands.

At a finite value of R, the condition $\Gamma(R) = 0$ is reached. Beyond this point, $\Gamma(R)$ becomes negative, causing the effective matter-induced dark energy density ρ_{Λ_m} to change sign from positive to negative. The repulsive gravitational effect therefore shuts off automatically and is replaced by an attractive contribution. Inflation thus terminates smoothly as a direct consequence of the expansion itself, without invoking an external decay channel or additional tuning. This provides a built-in graceful-exit mechanism that is absent in conventional inflaton-based models.

10.4 A solution to the reheating problem

The resolution of the reheating problem in the MOC framework must be discussed consistently with the inflationary trigger scale established in the preceding section. As shown above,

the onset and termination of inflation occur naturally when the matter-induced dark energy becomes comparable to the radiation background at

$$t \sim 10^{-36}\,\mathrm{s}, \qquad \rho_r \sim 10^{79}\text{–}10^{81}\,\mathrm{kg\,m^{-3}} \tag{173}$$

which coincides with the characteristic energy-density window usually invoked in standard inflationary phenomenology [65–67, 69].

In conventional inflation, the exponential expansion following this epoch typically dilutes the universe to an extremely cold and effectively empty state. A separate reheating phase is therefore introduced, in which the inflaton field decays into standard model particles through model-dependent microphysics [70, 71]. In this picture, the temperature after inflation is not determined by the expansion history itself but by the efficiency of inflaton decay.

In contrast, inflation in the MOC framework corresponds to an early phase of accelerated but finite power-law expansion driven by total GSE. Once the compactness condition governing the sign of ρ_{Λ_m} is no longer satisfied, the effective repulsive contribution automatically shuts off and the universe transitions smoothly into a radiation-dominated expansion. No separate decay or reheating mechanism is required.

The thermal evolution after the end of MOC inflation therefore follows directly from adiabatic expansion. Taking the characteristic temperature at the onset of inflation to be

$$T_{\mathrm{end}} \sim 10^{15}\text{–}10^{16}\,\mathrm{GeV} \tag{174}$$

consistent with the density scale derived at $t \sim 10^{-36}\,\mathrm{s}$, the subsequent cooling proceeds continuously toward the Big Bang Nucleosynthesis scale,

$$T_{\mathrm{BBN}} \sim 10^{9}\,\mathrm{K} \tag{175}$$

For adiabatic expansion of a radiation-dominated plasma, the temperature scales as $T \propto a^{-1}$. The required expansion factor between the end of inflation and the onset of nucleosynthesis is therefore

$$\frac{T_{\mathrm{end}}}{T_{\mathrm{BBN}}} \sim 10^{19}\text{–}10^{20} \tag{176}$$

This corresponds to a decrease in radiation energy density of

$$\frac{\rho_{\mathrm{end}}}{\rho_{\mathrm{BBN}}} \sim \left(\frac{T_{\mathrm{end}}}{T_{\mathrm{BBN}}}\right)^4 \sim 10^{76}\text{–}10^{80} \tag{177}$$

which is fully consistent with the standard thermal history connecting the inflationary epoch to Big Bang Nucleosynthesis.

Neither the exponential expansion factor in standard inflation ($e^{60} \sim 10^{26}$ [64–67]) nor the finite expansion factor in MOC ($\sim 10^{19}-10^{20}$) is directly observed. Both represent model-dependent requirements needed to connect the early universe to the observed cosmological state. The difference is that in MOC the required expansion is determined internally by GSE and thermal continuity, rather than imposed to solve horizon-scale problems.

MOC inflation does not cool the universe to a vacuum state. It ends while the universe is still extremely hot, and the subsequent adiabatic expansion alone naturally connects the inflationary epoch to Big Bang Nucleosynthesis.

The hot Big Bang does not arise from a reheating event but is the direct continuation of the post-inflationary radiation-dominated expansion. The same total GSE term that triggers inflation at early times also ensures its termination and guarantees a smooth thermal connection to the standard cosmological evolution [72].

10.5 Dark Energy: Acceleration at extreme scale

In the late matter-dominated era, the same total GSE framework governs the cosmic dynamics. However, the physical origin of acceleration is now controlled by extreme scale rather than extreme density. The relevant dimensionless compactness factor appearing in the GSE term can be written as

$$\frac{5\beta}{14}\frac{R_S(t)}{\chi_p(t)} = \frac{5\beta}{14}\frac{2GM(t)}{c^2\chi_p(t)} \propto \beta(t)\rho_m(t)\frac{R_{\text{phys}}(t)^3}{\chi_p(t)} \tag{178}$$

where $M(t) = \frac{4\pi}{3}\rho_m(t)R_{\text{phys}}(t)^3$ is the total mass contained within the causally connected region.

At late times, a competition emerges between two opposing effects. The matter density $\rho_m(t)$ decreases as $a(t)^{-3}$ due to cosmic expansion, while the geometric factor $R_{\text{phys}}(t)^3/\chi_p(t)$ grows monotonically as the causal domain expands. This dual-scale structure reflects the separation between the interaction scale $\chi_p(t)$ and the volumetric dilution scale $R_{\text{phys}}(t)$ inherent to the GSE framework.

Our numerical simulations show that after an initial period in which the attractive component dominates, the growth of the scale-dependent factor eventually overcomes the decay of the matter density. As a result, the effective GSE contribution crosses the critical threshold and becomes repulsive. This transition marks the onset of late-time cosmic acceleration.

In this regime, the dark energy density evolves slowly and remains close to a quasi-constant value. Rather than representing a true cosmological constant, the observed dark energy is interpreted as the outcome of a slowly varying balance in which the combination $\beta\rho_m(t)[R_{\text{phys}}(t)^3/\chi_p(t)]$ maintains a small net repulsive contribution over cosmological timescales.

10.6 Two accelerations, one physical origin

The total GSE framework provides a unified physical explanation for both primordial inflation and late-time cosmic acceleration. In the early universe, accelerated expansion arises whenever the total GSE becomes positive within a causally connected region. This condition is controlled by the local energy density and does not single out a unique microscopic timescale.

Instead, accelerated expansion can naturally occur at any early epoch between the Planck scale and the standard inflationary window, provided that the radiation density satisfies the GSE trigger condition derived in Sec. 10.2. In this sense, MOC is capable of reproducing inflationary behavior at the conventional $t \sim 10^{-36}$–10^{-35} s scale, while remaining equally consistent with earlier onset times approaching the Planck regime.

Primordial inflation in MOC is therefore not tied to a uniquely specified moment in time, but is a density-driven phenomenon. The onset time is selected dynamically by the value of the radiation density rather than imposed by an external field or a fine-tuned potential. The same underlying mechanism can accommodate a continuous range of early-universe conditions, from Planck-scale densities to those conventionally associated with standard inflation.

In contrast, late-time cosmic acceleration emerges from the identical GSE mechanism operating at extreme scale rather than extreme density, when the causally connected region has grown to cosmological dimensions of order $R \sim 43$ Gly. The density–scale duality of the GSE is thus encoded in a single dimensionless compactness ratio that governs the sign and magnitude of the total GSE. At early times this ratio is driven by high density, while at late times it is controlled by the growth of the causal scale.

The enormous hierarchy between the Planck-scale vacuum energy density and the present-day effective dark energy, often quoted as $\sim 10^{124}$, arises naturally from evaluating the same

physical quantity at different points along cosmic evolution. In this picture, primordial inflation and late-time acceleration are not separate phenomena but two limits of a single gravitational mechanism.

Unlike other unified dark energy models [73], the MOC framework introduces no new fields and requires no modification of General Relativity. It offers a predictive and falsifiable description of cosmic acceleration grounded entirely in the GSE of matter.

11 Resolution of the Black Hole Singularity in MOC

One of the most profound challenges in modern physics is the singularity predicted to exist at the heart of a black hole [40, 41, 46]. MOC offers a novel and consistent resolution to this problem. Here, we extend the GSE framework from the cosmos to the core of a collapsing star, demonstrating that the same physical principle that drives cosmic acceleration naturally averts the formation of a singularity.

11.1 Gravitational dynamics in a collapsing object

While the TOV equation describes static stellar structures [30,31], the dynamic collapse within a black hole's event horizon is more fundamentally described by the Friedmann equations. Unlike the TOV equation, which applies strictly to static configurations, the dynamical interior of a collapsing object can be effectively described by a Friedmann-type evolution equation under the assumption of spherical symmetry and homogeneous radial collapse. This correspondence is well established by the Oppenheimer-Snyder solution, which shows that the interior of a pressureless collapsing sphere is mathematically equivalent to a time-reversed Friedmann universe [31]. Accordingly, we adopt the Friedmann acceleration equation as an effective tool to analyze whether the collapse proceeds toward a singularity or is dynamically halted.

Unlike the expanding universe where the effective mass depends on the evolving particle horizon, a collapsing star is a localized system residing well within the cosmic causal limit ($R \ll \chi_p$). In the compact regime relevant for a collapsing object, the matter component is pressureless to leading order, $P_m \approx 0$, while the GSE-induced component satisfies an effective equation of state $w_{\Lambda_m} \approx -1$. The active gravitational source term in the acceleration equation therefore reduces to

$$\rho_T + 3P_T \approx \rho_m - 2\rho_{\Lambda_m} \tag{179}$$

The sign of this term dictates the net gravitational force. To analyze it, we use the GSE-derived expression (141) for ρ_{Λ_m} specialized to a compact object of radius R.

$$\rho_{\Lambda_m} \approx \frac{\beta\rho_m}{2}\frac{R_S}{R}\left(\frac{5\beta}{14}\frac{R_S}{R} - 1\right) \tag{180}$$

11.2 The critical threshold and the emergence of repulsion

Equation (180) reveals a critical threshold in the dynamics of gravitational collapse, determined by the ratio of the object's radius R to its Schwarzschild radius R_S. The crossover point occurs when the term in the parentheses vanishes.

$$\frac{5\beta}{14}\frac{R_S}{R} - 1 = 0 \quad \Rightarrow \quad R_{critical} = \frac{5\beta}{14}R_S \tag{181}$$

Given that the collapsing core represents an extremely dense and centrally concentrated configuration, we adopt a structural parameter value $\beta \approx 1.5$. This choice is consistent with relativistic self-gravitating systems near maximal compactness and lies within the theoretically

allowed range established by TOV solutions and our cosmological analysis of high-density epochs. In this regime, the critical radius becomes $R_{critical} \approx \frac{7.5}{14} R_S \approx 0.54 R_S$.

- **Phase 1: Accelerated collapse ($R > R_{critical}$)**
  For a collapsing object with $R > R_{critical}$, the bracketed term is negative, making $\rho_{\Lambda_m} < 0$. This means the dark energy acts as an attractive force, enhancing gravity. Thus, in the MOC framework, the initial stages of black hole formation are more rapid and violent than predicted by standard gravity.

- **Phase 2: The repulsive transition ($R = R_{critical}$)**
  At the specific radius $R \approx 0.54 R_S$ (assuming $\beta \approx 1.5$), the dark energy density vanishes. This marks the boundary between the attractive exterior and the repulsive interior.

- **Phase 3: The repulsive core ($R < R_{critical}$)**
  As the collapse proceeds past this critical radius, ρ_{Λ_m} flips sign and becomes positive. The active gravitational source term now contains a powerful repulsive component. Considering the equation of state inferred from cosmic acceleration observations ($w \approx -1$), or indeed any negative pressure condition ($w < -1/3$), this positive energy density generates a repulsive gravitational effect that counteracts the collapse. The repulsive contribution scales more steeply with decreasing radius than the attractive matter term. Specifically, the dominant GSE repulsive term grows as R^{-5}, while the matter contribution scales as R^{-3}. This difference in scaling ensures that, below a finite radius, the repulsive effect inevitably dominates, independently of the total mass of the collapsing object. A singularity, which requires attraction to dominate down to $R = 0$, is therefore fundamentally forbidden in this framework. The formation of a stable, non-singular core eliminates the spacetime singularity and removes the primary obstruction to unitary evolution. This provides a natural pathway toward resolving the black hole information problem within the MOC framework, without invoking quantum gravity effects at the Planck scale.

11.3 The equilibrium point: A singularity averted

The collapse is halted when the net gravitational force on the collapsing matter becomes zero. For simplicity, we can approximate the equilibrium condition using the general relativistic constraint for accelerated expansion, $\rho_m + \rho_{\Lambda_m} + 3P_{\Lambda_m} = 0$. Using the approximation $w_{\Lambda_m} \approx -1$ for the GSE component, this simplifies to $\rho_m \approx 2\rho_{\Lambda_m}$.

We can now solve for the equilibrium radius, R_{eq}. Substituting the expressions for ρ_m and our GSE-derived ρ_{Λ_m} (Eq. 180), we derive a quadratic equation for the dimensionless variable $X = R_S/R$.

$$\frac{5\beta^2}{14} X^2 - \beta X - 1 = 0 \tag{182}$$

Solving for the positive root gives the equilibrium ratio.

$$\frac{R_S}{R_{\text{eq}}} = \frac{14\beta + \sqrt{196\beta^2 + 280\beta^2}}{10\beta^2} = \frac{7 + \sqrt{119}}{5\beta} \tag{183}$$

Therefore, the equilibrium radius is

$$R_{\text{eq}} = \left(\frac{5\beta}{7 + \sqrt{119}} \right) R_S \approx 0.28 \beta R_S \tag{184}$$

Assuming $\beta \approx 1.5$ for the high-density core environment, we find

$$R_{\text{eq}} \approx 0.42 R_S \tag{185}$$

The collapse is thus stabilized at a finite radius of approximately $0.42R_S$, well inside the event horizon but long before the Planck scale. For a stellar black hole of 3 solar masses ($R_S \approx 9$ km), our model predicts its core would stabilize at a macroscopic equilibrium radius of $R_{\text{eq}} \approx 3.8$ km. **This demonstrates that the singularity is resolved not at the mysterious Planck scale, but at a concrete, astrophysical scale through classical GSE dynamics alone.**

11.4 Observational validation: The cosmic connection

A common objection to any proposal about black hole interiors is that the relevant physics is hidden behind an event horizon and is therefore not testable. In the MOC framework, the situation is fundamentally different. The mechanism responsible for singularity avoidance is not introduced as an ad hoc ingredient that acts only inside black holes. It is the same total GSE contribution that is already required to account for the observed acceleration of the universe.

In the cosmological setting, the GSE-induced dark energy density takes the explicit form

$$\rho_{\Lambda_m} = \frac{3\beta}{4\pi} \frac{G_N M^2}{c^2 \chi_p R_{\text{phys}}^3} \left(\frac{5\beta}{14} \frac{R_S}{\chi_p} - 1 \right) \tag{186}$$

where χ_p denotes the particle (comoving) horizon and R_{phys} is the corresponding physical horizon scale. The sign of the dark energy density is governed entirely by the dimensionless compactness factor

$$\frac{5\beta}{14} \frac{R_S}{\chi_p} \tag{187}$$

which directly measures the gravitational compactness of the causally connected universe.

For the representative value $\beta = 1.5$ adopted throughout this work, the sign transition of ρ_{Λ_m} occurs when

$$\left(\frac{5\beta}{14} \frac{R_S}{\chi_p} - 1 \right) = 0 \tag{188}$$

corresponding to a critical scale

$$\chi_p^{\text{crit}} \simeq 0.54 R_S \tag{189}$$

This result demonstrates that the emergence of the repulsive GSE contribution in cosmology is governed by gravitational physics at a sub-horizon scale, $\chi_p \simeq 0.54 R_S$, well inside the Schwarzschild radius.

The observational fact that the universe is currently undergoing accelerated expansion implies that the cosmological evolution has entered the regime in which the GSE-induced component satisfies $w_{\Lambda_m} < -1/3$ [1, 2, 56, 68]. Within MOC, this observation empirically confirms the existence and sign of the same GSE mechanism whose Schwarzschild-scale transition is responsible for halting gravitational collapse inside black holes.

Cosmological observations fix the allowed parameter regime of the GSE contribution, including the sign transition near $\chi_p \sim 0.54 R_S$. Because the same dimensionless compactness structure governs both cosmology and compact objects, the prediction of a repulsive, non-singular black hole core follows as a derived and testable consequence of the same equations. Remarkably, cosmic acceleration occurs because we exist inside a cosmological black hole.

In this sense, **the accelerating universe and the non-singular black hole are two manifestations of a single Schwarzschild-scale gravitational mechanism.**

11.5 A singularity-free core and the Information Paradox

The MOC framework naturally resolves the black hole singularity. Instead of a point of infinite density, the model predicts a dynamically stabilized core of finite, macroscopic size at the heart of the black hole. As matter collapses past the critical repulsive transition radius ($R \approx 0.54R_S$), the powerful repulsive force generated by the positive ρ_{Λ_m} grows until it precisely counterbalances the attractive force of matter at $R_{eq} \approx 0.42R_S$, creating a stable equilibrium structure.

By replacing the singularity with a stable, physical structure, this model offers a compelling resolution to the black hole information paradox [46, 74, 75]. The paradox arises because the destruction of information at a singularity violates the fundamental principle of unitarity in quantum mechanics. In our model, this conflict is entirely avoided. Information falling into the black hole is not destroyed; it is encoded in the physical state of this **non-singular black hole core**.

Because causality is preserved within this finite, macroscopic structure, the principles of quantum mechanics remain intact throughout the black hole's life and eventual evaporation. The information can, in principle, be returned to the universe as the black hole radiates away its mass via Hawking radiation, ensuring that the process is unitary. MOC thus provides a classical, MOC mechanism that removes one of the deepest paradoxes in modern physics, offering a complete and self-consistent picture of a black hole from its event horizon to its very core.

12 Observational Tests and Falsifiability of MOC

12.1 Test 1: The sign-switch of dark energy

Prediction. A generic prediction of the MOC framework is that the dark energy density was negative (attractive) during an extended early epoch. Using the updated SH0ES-based simulations (Tables 7–6), the transition to positive values occurs in the range

$$t_{\rm crit} \approx 4.5\text{–}5.5 \text{ Gyr}, \qquad z_{\rm crit} \approx 1.0\text{–}1.2$$

depending on the assumed matter enhancement scenario. This contrasts sharply with the ΛCDM expectation of a strictly positive and constant ρ_Λ at all redshifts.

Test. This prediction can be tested through model-independent reconstructions of $H(z)$ and $\rho_{\rm DE}(z)$ using supernovae (Pantheon+), BAO, and cosmic chronometers [12, 76, 77]. MOC would be falsified if future data from DESI, Euclid, or LSST demonstrate with high statistical confidence that $\rho_{\rm DE}(z)$ has remained strictly positive for all epochs $z \lesssim 1.5$ (corresponding to cosmic times $t \gtrsim 4$ Gyr), with no indication of an earlier attractive phase.

12.2 Test 2: Enhanced early structure growth

Prediction. Because ρ_{Λ_m} is negative for all $t \lesssim 4.5$–5.5 Gyr (i.e., $z \gtrsim 1.0$), the early universe experiences an additional attractive contribution to the energy budget. This is expected to enhance the growth of density perturbations and to yield a systematically larger value of the growth-rate observable $f\sigma_8(z)$ at intermediate and high redshifts relative to ΛCDM.

Test. Measurements of $f\sigma_8(z)$ from RSD [54, 55] and weak-lensing surveys provide a direct probe of this prediction [78]. If high-redshift data ($z \gtrsim 1.0$) from DESI or Euclid find a growth history fully consistent with, or weaker than, the ΛCDM expectation [59], the MOC prediction of an early attractive phase would be strongly disfavored.

12.3 Test 3: The post–crossover evolution of ρ_{Λ_m}

Prediction. In all updated SH0ES-based simulations, $\rho_{\Lambda_m}(t)$ exhibits a rapid increase immediately after the sign-switch, reaches a peak in the range $t \approx 8$–10 Gyr (depending on the matter enhancement scenario), and subsequently shows a gradual decline toward the present epoch. Recall the dark energy density derived in Eq. (48).

$$\rho_{\Lambda_m} = \frac{\beta \rho_m}{2} \frac{R_S}{\chi_p} \left(\frac{5\beta}{14} \frac{R_S}{\chi_p} - 1 \right) \tag{190}$$

This characteristic "rise-and-fall" behavior follows directly from this expression, which ties the dark energy density to the evolving combination $\rho_m(R_S/\chi_p)$.

During the post-crossover era, the enclosed mass and thus R_S increase only slowly, while the matter density $\rho_m(t)$ continues to dilute as the universe expands and the particle horizon $\chi_p(t)$ grows. As a result, the combination $\rho_m(R_S/\chi_p)$ initially increases, reaches a maximum, and eventually begins to decrease.

This naturally generates a finite peak in $\rho_{\Lambda_m}(t)$, followed by a gradual decline once the dilution of matter and the growth of $\chi_p(t)$ dominate over the increase in R_S. Thus MOC predicts a dynamic dark energy density that is distinct both from the constant ρ_Λ of the standard ΛCDM model and from the simple monotonic evolution typical of quintessence scenarios [3, 68].

Test. Reconstruction of $\rho_{\rm DE}(z)$ using SNe, BAO, and cosmic chronometers can reveal whether dark energy flattens or begins to weaken at late times ($z \lesssim 0.5$) [77]. MOC would be falsified if the reconstructed $\rho_{\rm DE}(z)$ shows a strictly monotonic increase for all $z \lesssim 1.0$ with no sign of flattening or turnover, or if it remains exactly constant to high precision across the entire redshift range. Conversely, any detected late-time evolution of dark energy density (i.e., $w > -1$ at low z), as tentatively suggested by recent Dark Energy Survey (DES) [13] and Dark Energy Spectroscopic Instrument (DESI) analyses [12], would strongly support the MOC scenario.

12.4 Test 4: Extensive falsifiability from an explicit functional origin

The Prediction: Unlike phenomenological dark energy models, MOC provides a fully explicit functional origin for the dark energy density ρ_{Λ_m}, specifying its dependence on cosmic variables (e.g., ρ_m, R, β) in analytic form. This functional transparency renders the model highly and systematically falsifiable in principle: any discrepancy in the detailed time/redshift evolution, scale dependence, or internal parameter relationships can serve as a direct test of the theory.

The Test: The analytical form of $\rho_{\Lambda_m}(t)$ is known, enabling comprehensive comparisons with high-precision observations for all detailed properties of functional evolution, as well as global features (sign conversion, peak, decline). Future advances in reconstructing the cosmic expansion history, horizon scale, and matter density (from DESI, Euclid, JWST, SKA, and beyond) will allow a continually expanding set of new and increasingly precise tests of the model. This falsifiability, made possible by MOC's explicit predictive formalism, sets it apart from existing approaches and provides a transparent link between theory and observation.

13 Discussion

In this work, we have presented a mechanism in which the GSE of matter reproduces the phenomenology normally attributed to dark energy. While our primary analysis focused on

the β-normalized model (where the interaction term scales with β^2), it is crucial to examine the robustness of this result against alternative choices of interaction coefficients and to address current observational uncertainties.

13.1 Role of the structural parameter β and model robustness

In deriving the interaction energy between the matter distribution and the equivalent negative mass associated with the GSE, we introduced the structural parameter β not as an independent dynamical degree of freedom, but as a geometric coefficient to describe the physical state of matter. Since the cosmic matter distribution is neither perfectly uniform nor static, the calculation of the GSE within any given shell inherently depends on this structural descriptor, as defined via $U_{gs}(r) = -\beta GM(r)^2/r$. This single parameter naturally encompasses the geometric distribution of mass, from $\beta \approx 2.0$ for nearly uniform spheres to lower values ($\beta \approx 1.0$) for strongly virialized structures.

Our simulations demonstrate that once galaxy-scale structures have formed ($t \gtrsim 1\,\mathrm{Gyr}$), the evolution of β becomes very slow, effectively acting as a quasi-constant coefficient for the remainder of cosmic history. This implies that the detailed time-evolution of $\beta(t)$ is not critical for the emergence of cosmic acceleration; rather, β primarily sets the overall normalization of the GSE interaction strength.

Consequently, the choice of how the interaction term scales with β (e.g., linear β vs. quadratic β^2) becomes a question of matching the effective coupling strength to the assumed background matter density. In our β^2–scaled formulation, which propagates the structural information consistently, the SH0ES–based MOC solutions with matter enhancements of $\{-10\%, 0\%, +10\%, +20\%\}$ yield present-epoch coefficients in the range $\beta(t_0) \simeq 1.145$ (+20% model), 1.301 (+10% model), 1.495 (0% model), 1.743 (−10% model). All comfortably within the theoretically motivated range for virialized cosmic structures ($\beta \approx 1.0$–2.0).

By contrast, adopting a linear scaling (replacing β^2 with β) would require a substantially larger effective coefficient, $\beta \simeq 7.37$, to reproduce the observed acceleration given the current SH0ES baseline ($\Omega_m = 0.315$). This suggests that the linear model would only be viable if the true cosmic matter density were significantly higher ($\Omega_m \gtrsim 0.35$), in which case the required β would fall back into the physically standard range ($\beta \sim 1$–2). Therefore, if future observations become more precise and demonstrate a significant increase in the cosmic matter density, the linear model may also be considered a viable alternative formulation.

13.2 Observational uncertainties and future constraints

First, there is a significant tension in the value of Ω_m across different dataset combinations. As highlighted in recent analyses [56], the inferred matter density can vary substantially, spanning $\Omega_m \approx 0.21$ to $\Omega_m \approx 0.36$, depending on whether SN Ia age-bias corrections are applied and which probes (CMB, BAO, SNe) are combined. Because the structural parameter β is defined through the matter distribution, this observational scatter in Ω_m directly propagates into an uncertainty range for β. The four SH0ES–anchored MOC simulations with matter modifications of $\{-10\%, 0\%, +10\%, +20\%\}$ demonstrate the corresponding inferred values of $\beta(t_0)$ as Ω_m varies. In all of these scenarios, however, $\beta(t)$ remains quasi-constant after the epoch of early structure formation, and the MOC model continues to reproduce the observed expansion history even under substantial matter-enhancement variations.

Second, and perhaps more fundamentally, nearly all existing cosmological datasets are reduced and calibrated under the assumption of the standard ΛCDM model. There is currently no comprehensive dataset processed specifically within the context of the MOC. Since the MOC

model fundamentally reinterprets the source of cosmic acceleration as a GSE effect rather than a vacuum energy, it may ultimately require a re-analysis of raw observational data.

As the MOC framework is in its initial stage, we anticipate that future studies, building dedicated datasets and likelihoods grounded in this alternative paradigm, will be able to break these degeneracies. Once such datasets are established, the MOC framework can be subjected to more stringent observational tests, allowing its viability as a physically motivated alternative to ΛCDM to be assessed more conclusively.

14 Conclusion: A Unified Cosmology from Total Gravitational Self-Energy

The standard cosmological model treats inflation and late-time acceleration as conceptually disconnected phenomena, typically driven by independent scalar fields [64–68]. The GSE framework in Matter-Only Cosmology (MOC) unifies both via a single, intuitive principle. The matter-induced dark energy density arises from the total GSE of the contents of the causal horizon. Within the General GSE framework, this is expressed as

$$\rho_{\Lambda_m} = \frac{\beta \rho_m}{2} \frac{R_S}{\chi_p} \left(\frac{5\beta}{14} \frac{R_S}{\chi_p} - 1 \right) \tag{191}$$

where ρ_m is the matter density diluted over the physical volume V_{phys}, and $R_S = 2GM/c^2$ is the Schwarzschild radius associated with the total matter mass $M = \rho_m V_{\text{phys}}$ contained within the causally connected physical volume within the interaction scale χ_p. This single equation encapsulates a fundamental **density–scale duality**: repulsive gravity ($\rho_{\Lambda_m} > 0$) is driven by extreme density at small scales (inflation) and by the extreme growth of the physical scale relative to the causal horizon at low densities (dark energy).

In essence, the dynamical interactions governed by this single GSE principle determine the entire history of cosmic expansion, from the onset and natural termination of inflation, to the long epoch of deceleration, to the acceleration phase we observe today, and potentially to a future era of damped oscillatory stability.

By rigorously accounting for the **GSE of matter and its contribution to the source of gravity**, MOC offers a more complete, self-consistent, and physically motivated description of our universe. It replaces a series of disconnected puzzles with a unified framework and provides a rich set of falsifiable predictions. The road ahead is clear: to put this model to the test against the wealth of forthcoming observational data. The journey into the dark sector may not require new particles or new forces, but a return to a deeper understanding of gravitational self-interaction within General Relativity.

Finally, the universality of the GSE principle suggests implications beyond cosmology. Furthermore, the validity of this self-energy principle is not confined to the macroscopic cosmos. When applied to the microscopic realm, the source renormalization mechanism ($M \to M_{eq}$) inherently suppresses the gravitational interaction strength near the Planck scale. This suggests that the same framework resolving black hole singularities may also eliminate ultraviolet divergences (UV completion), offering a unified pathway toward the long-sought and definitive "**Completion of Quantum Gravity**" [43, 79].

Puzzle	MOC's Resolution	Key Prediction / Feature
Dark Energy	Replaced the static Λ with a dynamic dark energy density $\rho_{\Lambda_m}(t)$ born from the GSE of matter.	Predicts a dynamic life cycle: **early negative energy (attractive)**, current positive energy (repulsive), and a future return to deceleration due to the evolving horizon ratio.
Hubble Tension	Reframed as a measurement of the evolving cosmic structure, encapsulated in a time-varying structural parameter, $\beta(t)$.	Naturally explains why CMB ($z \sim 1100$) and local ($z \sim 0$) measurements of H_0 differ, as they probe different epochs with different β values.
Unification of Inflation & Dark Energy	The same GSE mechanism drives both **inflation (high-density repulsion)** and **late-time acceleration (large-scale repulsion)**.	Naturally explains the 10^{124} energy scale hierarchy between the two epochs via the geometric scaling of GSE with the expanding horizon.
Cosmic Fate	**Dynamics governed by the competition between matter dilution and horizon growth.**	Predicts a **damped oscillatory evolution**, preventing eternal acceleration and leading to a stabilized, slowly varying expansion.

Table 12: Summary of cosmological puzzles resolved by MOC. The simulations demonstrate the robustness of these predictions, including a robust prediction of a future transition to a decelerating phase.

A Appendix A: A Re-examination of the Energy Components of a Gravitating System

Theoretical motivation

In this paper, we have developed a cosmological model based on a fundamental principle of General Relativity: *all forms of energy, including gravitational potential energy, must act as sources of gravity [17, 18]*. Standard cosmological models typically treat the mass density ρ_m as the sole source of gravity, implicitly assuming that the self-energy of the system is either negligible or already absorbed into the matter sector. However, on cosmological scales, the GSE of the universe becomes significant and cannot be ignored.

We argue that the process of assembling mass M naturally induces a negative GSE component ($-M_{gs}$) and, consequently, a mutual interaction energy ($+M_{m-gs}$) between the matter distribution and its own GSE field. This appendix introduces an approach that explicitly demonstrates that the ρ_{m-gs} term derived from the GSE mechanism is an interaction term between the matter and equivalent mass of GSE.

$$\rho_{\Lambda_m} = \rho_{m-gs} - \rho_{gs} = \frac{3\beta}{4\pi}\frac{GM^2}{c^2R^4}\left(\frac{5\beta}{14}\frac{R_S}{R} - 1\right) \tag{192}$$

Here, the term $-\rho_{gs}$ represents the traditional negative GSE density, while ρ_{m-gs} represents the positive gravitational energy density arising from the coupling between the matter M and the equivalent negative mass associated with its GSE, $-M_{gs}$. This decomposition reveals that

what we observe as “dark energy” is not an exotic addition, but an intrinsic property of a self-gravitating system.

A.1 Total energy components of a gravitating system

In conventional energy accounting of a physical system, it is typically assumed that all forms of energy are implicitly incorporated into an equivalent-mass representation. However, a more careful examination reveals that a dynamical system composed of an extended mass distribution is not a simple single-body system. Instead, it is effectively a composite system that includes an additional negative equivalent mass, $-M_{gs}$, arising from the system's own gravitational potential energy.

A crucial physical effect arises here: when two distinct energy components coexist, there necessarily appears a mutual gravitational interaction term U_{m-gs}.

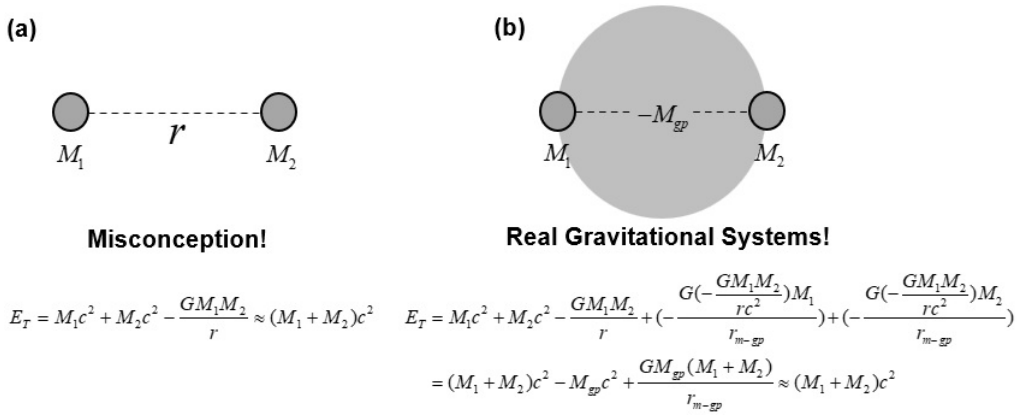

Figure 5: Conceptual diagram illustrating the composite nature of a gravitating system. The system consists of the free mass M_{fr} and the negative equivalent mass of its GSE, $-M_{gs}$. This configuration necessitates an interaction energy term U_{m-gs}, which manifests as a positive energy density.

The total mass-energy of the system is thus

$$M_T \approx M_{fr} + \frac{U_{gs}}{c^2} + \frac{U_{m-gs}}{c^2} = M_{fr} + (-M_{gs}) + M_{m-gs} \tag{193}$$

where $-M_{gs}$ and $+M_{m-gs}$ are the equivalent masses of the GSE and the interaction energy (GPE), respectively.

Since the gravitational potential energy between a positive mass ($+M_{fr}$) and a negative equivalent mass ($-M_{gs}$) takes a positive form (repulsive interaction), the interaction energy is given by

$$U_{m-gs} = -\frac{G(+M_{fr})(-M_{gs})}{r} = +\frac{GM_{fr}M_{gs}}{r} > 0 \tag{194}$$

Consequently, the equivalent mass density obtained by dividing this interaction energy by volume, $+\rho_{m-gs}$, carries a positive energy density. The total mass density of the object is therefore

$$\rho_{Total} = \rho_{fr} + \rho_{m-gs} - \rho_{gs} \approx \rho_m + \rho_{m-gs} - \rho_{gs} \tag{195}$$

1) **Matter (ρ_m):** Strictly speaking, ρ_m is a net result of the free-state mass density (ρ_{fr} minus its GSE term ($-\rho_{gs}$) and interaction term($+\rho_{m-gs}$). Thus, $\rho_m = \rho_{fr} - (\rho_{m-gs} - \rho_{gs})$. In a weak field, $(\rho_{m-gs} - \rho_{gs})$ is negligible, thus $\rho_m \approx \rho_{fr}$. This matter distribution is the ultimate source of all subsequent gravitational effects.

2) **GSE ($-\rho_{gs}$):** The mass-equivalent of the system's own negative binding energy (U_{gs}). In relation to the expansion of the universe, the positive dark energy term is linked to negative pressure, and the negative dark energy density plays an attractive role. In cosmology, rather than interpreting the $-\rho_{gs}$ term alone, it is thought more appropriate to understand the characteristics based on $\rho_{\Lambda_m} = \rho_{m-gs} - \rho_{gs}$.

3) **Interaction energy ($+\rho_{m-gs}$):** The mass-equivalent of the positive GPE that arises from the interaction between the matter field (M) and its own negative GSE field ($-M_{gs}$). In relation to the expansion of the universe, the positive dark energy term is connected to negative pressure, and since the positive dark energy density plays a repulsive role. In cosmology, rather than interpreting the ρ_{m-gs} term alone, it is thought more appropriate to define the characteristics based on $\rho_{\Lambda_m} = \rho_{m-gs} - \rho_{gs}$.

In standard astrophysical contexts, the term $(\rho_{m-gs} - \rho_{gs})$ is negligible compared to ρ_m, justifying the approximation $\rho_{Total} \approx \rho_m$. However, on the cosmological scale, these terms are no longer negligible. The net contribution of the GPE terms, $\rho_{\Lambda_m} = \rho_{m-gs} - \rho_{gs}$, becomes the dominant component driving cosmic acceleration.

$$\rho_{\Lambda_m} = \rho_{m-gs} - \rho_{gs} \tag{196}$$

A.2 Derivation of the matter-induced dark energy density

Having established the conceptual basis of MOC and the General GSE Framework, we now derive the explicit form of the dark energy density, ρ_{Λ_m}. The derivation leverages a physical model where gravitational potential energy is generated over the causal scale (the comoving horizon χ_p), while its density is diluted over the physical volume (V_{phys}) [18, 39, 42].

The total energy density entering the Friedmann equation is given by $\rho_T = \rho_m + \rho_{m-gs} - \rho_{gs}$. The latter two terms, arising purely from gravitational interactions, constitute the matter-induced dark energy density.

The entire derivation originates from the GSE of the total mass $M(t)$ contained within the causal horizon. While the classical form scales as $1/R$, in our General GSE framework, the characteristic interaction length scale is the comoving horizon $\chi_p(t)$.

$$U_{gs,\text{General}} = -\beta(t)\frac{GM(t)^2}{\chi_p(t)} \tag{197}$$

Here, $\beta(t)$ encapsulates the necessary relativistic and structural corrections, evolving as the universe transitions from homogeneity to a structured state.

A.2.1 The negative-energy component: $-\rho_{gs}$

The first component $-\rho_{gs}$, represents the equivalent mass-density of the system's own gravitational binding energy. This binding energy corresponds to a mass defect, effectively creating a negative mass component, $-M_{gs}$, within the total energy budget [17, 37, 38].

$$-M_{gs} = \frac{U_{gs,\text{General}}}{c^2} = -\frac{\beta GM(t)^2}{c^2\chi_p(t)} \tag{198}$$

Distributing this negative mass over the physical volume $V_{\text{phys}}(t) = \frac{4\pi}{3}R_{\text{phys}}(t)^3$ yields the negative energy density component.

$$-\rho_{gs}(t) = \frac{-M_{gs}}{V_{\text{phys}}(t)} = -\frac{3\beta(t)}{4\pi}\frac{GM(t)^2}{c^2\chi_p(t)R_{\text{phys}}(t)^3} \tag{199}$$

A.2.2 The positive-energy component: $+\rho_{m-gs}$

The existence of the negative equivalent mass component ($-M_{gs}$), within the space containing the positive mass M, necessitates an interaction term. The interaction energy U_{m-gs} arises from the gravitational coupling between the matter distribution M and the effective mass ($-M_{gs}$) distribution. Here, we make a critical choice for the interaction coefficient.

A.2.3 A Note on the Interaction Coefficient

In Newtonian mechanics, the GSE of a uniform sphere is $U_{self} = -(3/5)GM^2/R$. However, in General Relativity, this is modified to $U_{self} = -\beta GM^2/R$, where β encapsulates relativistic effects. A parallel question arises for the interaction energy between two overlapping distributions. The general relativistic form of the interaction energy is complex and model-dependent. It might be characterized by a new coefficient β_2, not necessarily equal to β.

Faced with this ambiguity, we adopt $\beta_2 = 1$ as our working assumption in this specific derivation. This choice is motivated by physical reasoning: it is the natural value for stable, virialized systems and is consistent with the fact that the primary relativistic correction is already encapsulated within the M_{gs} term, which includes β. Since the form containing β^2 was covered in the main text, there is also a need to analyze the case in which the interaction coefficient is unity.

With this assumption, the interaction energy in the General GSE framework becomes

$$U_{m-gs} \approx -\frac{GM(t)(-M_{gs})}{\chi_p(t)} = +\frac{GM(t)M_{gs}}{\chi_p(t)} \tag{200}$$

Substituting our definition of $M_{gs} = \beta GM^2/(c^2\chi_p)$, we obtain

$$U_{m-gs} = +\beta\frac{G^2M(t)^3}{c^2\chi_p(t)^2} \tag{201}$$

This leads to the positive equivalent mass-density.

$$\rho_{m-gs}(t) = \frac{U_{m-gs}}{V_{\text{phys}}(t)c^2} = \frac{3\beta(t)}{4\pi}\frac{G^2M(t)^3}{c^4\chi_p(t)^2R_{\text{phys}}(t)^3} \tag{202}$$

A.3 The complete expression for ρ_{Λ_m}

Combining the positive and negative energy density components, we arrive at the final expression for the dark energy density in this specific model ($\beta_2 = 1$).

$$\rho_{\Lambda_m}(t) = \rho_{m-gs}(t) - \rho_{gs}(t) = \frac{3\beta}{4\pi}\frac{G^2M^3}{c^4\chi_p^2R_{\text{phys}}^3} - \frac{3\beta}{4\pi}\frac{GM^2}{c^2\chi_pR_{\text{phys}}^3} \tag{203}$$

To reveal its physical significance, we can factor this equation. Expressing the term in the parenthesis using the Schwarzschild radius of the total causal mass, $R_S(t) = 2GM(t)/c^2$.

$$\rho_{\Lambda_m}(t) = \frac{3\beta(t)}{4\pi}\frac{GM(t)^2}{c^2\chi_p(t)R_{\text{phys}}(t)^3}\left(\frac{GM(t)}{c^2\chi_p(t)} - 1\right) \tag{204}$$

$$\rho_{\Lambda_m}(t) = \frac{\beta\rho_m}{2}\frac{R_S}{\chi_p}\left(\frac{1}{2}\frac{R_S}{\chi_p} - 1\right) \tag{205}$$

This result demonstrates that under the assumption of a unity interaction coefficient ($\beta_2 = 1$), the condition for the onset of cosmic acceleration is governed purely by the ratio of the Schwarzschild radius to the comoving horizon, $\frac{R_S}{2\chi_p} > 1$, without an additional β factor inside the parenthesis. This provides a simpler, more fundamental criterion for the transition to dark energy dominance.

A.4 Observational validation and the evolution of β

Here we briefly recall the role of the structural coefficient β entering the total GSE. It effectively summarizes the dependence of the GSE on the mass distribution and relativistic compactness. Over the full cosmic history, β is expected to vary slowly with time. However, after the onset of substantial structure formation, its evolution is expected to be modest and can be treated as approximately constant for the late universe analysis presented in this section.

An important consistency check of this framework is confrontation with empirical anchors. We therefore compare the MOC requirements with early universe constraints inferred from the Cosmic Microwave Background (CMB) [5], as well as with late universe measurements from the local distance ladder such as SH0ES [15].

In practice, the effective late time value of β is not predicted uniquely from first principles within the present analytic treatment. Instead, it is constrained by the observed present epoch energy budget and by the physically plausible range implied by gravitationally bound structures. Our strategy is therefore to determine the value of β required to reproduce the observed present day dark energy density under two baselines.[4]

The results of this analysis, summarized in Tables 13 and 14, reveal the required values of β across a spectrum of possible universes. By comparing these required β values to the physically plausible range derived from gravitationally bound structures and stellar structure considerations ($\beta \approx 0.6 - 2$), we can assess the viability of the MOC framework and gain insight into the structural evolution of our universe.

Matter Incr. (%)	ρ_m ($\times 10^{-27}$ kg/m^3)	ρ_{Λ_m}	**Required β**	$\rho_{m\text{-}gs}$ ($\times 10^{-27}$ kg/m^3)	$-\rho_{gs}$
-20	2.150	6.383	**10.2792**	35.186	-28.803
-10	2.419	6.114	**4.6990**	24.264	-18.150
+0	2.688	5.845	**2.6295**	18.573	-12.728
+10	2.957	5.576	**1.6388**	15.001	-9.425
+20	3.225	5.308	**1.0824**	12.520	-7.212
+30	3.494	5.039	**0.7445**	10.684	-5.645
+40	3.763	4.770	**0.5269**	9.262	-4.492
+50	4.032	4.501	**0.3808**	8.132	-3.631

Table 13: CMB baseline ($H_0 = 67.4$ km/s/Mpc, $R = 46.5$ Gly). Required β and GSE components computed from $\rho_{\Lambda_m} = \beta \left(\frac{4\pi G}{3c^2}\rho_m^2 R^2\right)\left(\frac{4\pi G}{3c^2}\rho_m R^2 - 1\right)$.

A.5 Computer simulation data

[4] In principle, the structural coefficient β can be determined independently through large-scale N-body simulations, by directly comparing the simulated matter distribution with observed galaxy and galaxy-cluster scale structures. Such a program would allow β to be computed from first principles and removed entirely from the set of adjustable physical quantities in the model.

Matter Incr. (%)	ρ_m ($\times 10^{-27}$ kg/m^3)	ρ_{Λ_m}	**Required β**	$\rho_{m\text{-}gs}$ ($\times 10^{-27}$ kg/m^3)	$-\rho_{gs}$
-20	2.525	7.495	**7.0184**	30.893	-23.398
-10	2.841	7.178	**3.5026**	21.961	-14.783
+0	3.156	6.864	**2.0267**	17.419	-10.555
+10	3.472	6.548	**1.2738**	14.577	-8.029
+20	3.788	6.232	**0.8469**	12.586	-6.354
+30	4.103	5.917	**0.5868**	11.083	-5.166
+40	4.419	5.601	**0.4185**	9.874	-4.273
+50	4.734	5.286	**0.3057**	8.869	-3.583

Table 14: SH0ES baseline ($H_0 = 73.04$ km/s/Mpc, $R = 43.337$ Gly). Required β and GSE components computed form $\rho_{\Lambda_m} = \beta\left(\frac{4\pi G}{3c^2}\rho_m^2 R^2\right)\left(\frac{4\pi G}{3c^2}\rho_m R^2 - 1\right)$.

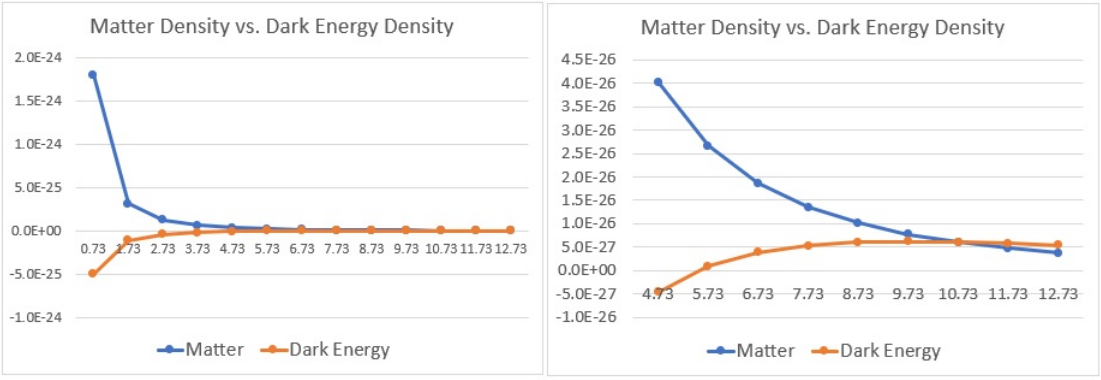

Figure 6: **Matter Density vs. Dark Energy Density (SH0ES baseline, Model-2, 10% Matter Enhancement)**: $\Omega_m = 0.347$. In the early universe, dark energy was negative and promoted structure formation. It transitioned to positive around 4 Gyr, contributing to the accelerated expansion of the universe. At approximately t=7.5 Gyr, matter density and dark energy density became equal, and dark energy density peaked at approximately 8 Gyr and then gradually decreased.

Age (Gyr)	Scale $a(t)$	Evolving $\beta(t)$	Comoving Ho. $\chi_p(t)$ (Gly)	Physical Ho. $R_{\text{phys}}(t)$ (Gly)	**Matter** $\rho_m(t)$	Repulsive $\rho_{m-gs}(t)$	Attractive $-\rho_{gs}(t)$	**Dark Energy** $\rho_{\Lambda_m}(t)$
					(10^{-27} kg m^{-3})			
0.73	0.1283	1.6388	17.080	2.191	1645.27	214.737	-760.898	**-546.161**
1.73	0.2285	1.6084	22.764	5.202	291.245	117.716	-234.819	**-117.103**
2.73	0.3111	1.5780	26.487	8.240	115.403	83.876	-123.586	**-39.710**
3.73	0.3854	1.5476	29.365	11.317	60.699	65.364	-78.356	**-12.992**
4.73	0.4552	1.5171	31.748	14.452	36.839	53.136	-54.495	**-1.359**
5.73	0.5224	1.4867	33.797	17.656	24.373	44.243	-40.039	4.204
6.73	0.5883	1.4563	35.599	20.943	17.066	37.352	-30.467	6.885
7.73	0.6540	1.4259	37.211	24.336	12.422	31.779	-23.725	8.054
8.73	0.7200	1.3955	38.668	27.841	9.309	27.179	-18.790	8.389
9.73	0.7871	1.3651	39.996	31.481	7.126	23.293	-15.052	8.241
10.73	0.8559	1.3346	41.214	35.275	5.542	19.970	-12.153	7.817
11.73	0.9266	1.3042	42.337	39.229	4.368	17.126	-9.877	7.249
12.73	1.0000	1.2738	43.337	43.337	3.475	14.610	-8.041	6.569

Table 15: **MOC Cosmic History Simulation (SH0ES baseline, Model-2, +10% Matter Enhancement)**. Results using the alternative interaction coefficient assumption ($\beta_2 = 1$) discussed in the Appendix. The structural parameter evolves linearly from $\beta(0.73\,\text{Gyr}) = 1.6388$ to $\beta(12.73\,\text{Gyr}) = 1.2738$. Even with the reduced magnitude of the repulsive term (proportional to β^1 rather than β^2), the model successfully reproduces the transition from negative to positive dark energy at $t \approx 5.0$ Gyr, demonstrating the robustness of the GSE-driven acceleration mechanism.

Age (Gyr)	Scale $a(t)$	Evolving $\beta(t)$	Comoving Ho. $\chi_p(t)$ (Gly)	Physical Ho. $R_{\text{phys}}(t)$ (Gly)	**Matter** $\rho_m(t)$	Repulsive $\rho_{m-gs}(t)$	Attractive $-\rho_{gs}(t)$	**Dark Energy** $\rho_{\Lambda_m}(t)$
					(10^{-27} kg m^{-3})			
0.73	0.1283	1.0824	17.080	2.191	1794.84	184.134	-598.089	**-413.955**
1.73	0.2285	1.0628	22.764	5.202	317.722	100.984	-184.655	**-83.672**
2.73	0.3111	1.0432	26.487	8.240	125.894	71.987	-97.229	**-25.242**
3.73	0.3854	1.0235	29.365	11.317	66.217	56.125	-61.674	**-5.549**
4.73	0.4552	1.0039	31.748	14.452	40.188	45.648	-42.914	2.734
5.73	0.5224	0.9843	33.797	17.656	26.589	38.027	-31.546	6.481
6.73	0.5883	0.9647	35.599	20.943	18.617	32.122	-24.018	8.104
7.73	0.6540	0.9450	37.211	24.336	13.551	27.345	-18.713	8.632
8.73	0.7200	0.9254	38.668	27.841	10.156	23.400	-14.829	8.571
9.73	0.7871	0.9058	39.996	31.481	7.773	20.066	-11.886	8.180
10.73	0.8559	0.8862	41.214	35.275	6.046	17.214	-9.603	7.611
11.73	0.9266	0.8665	42.337	39.229	4.765	14.773	-7.810	6.963
12.73	1.0000	0.8469	43.337	43.337	3.791	12.611	-6.363	6.248

Table 16: **MOC Cosmic History Simulation (SH0ES baseline, Model-2, +20% Matter Enhancement)**. Results using the Model-2 assumption ($\beta_2 = 1$). The structural parameter evolves linearly from $\beta(0.73) = 1.0824$ to $\beta(12.73) = 0.8469$. This model exhibits an early transition to accelerated expansion at $t \approx 4.0$ Gyr, driven by the enhanced matter density. The dark energy density peaks around $t \approx 8$ Gyr and then slowly decreases, consistent with the dynamic nature of the GSE mechanism.

References

[1] A. G. Riess *et al.* (Supernova Search Team), "Observational Evidence from Supernovae for an Accelerating Universe and a Cosmological Constant," Astron. J. **116**, 1009 (1998).

[2] S. Perlmutter *et al.* (Supernova Cosmology Project), "Measurements of Ω and Λ from 42 High-Redshift Supernovae," Astrophys. J. **517**, 565 (1999).

[3] P. J. E. Peebles and B. Ratra, "The cosmological constant and dark energy," Rev. Mod. Phys. **75**, 559 (2003).

[4] S. Dodelson and F. Schmidt, *Modern Cosmology*, 2nd ed. (Academic Press, 2020).

[5] N. Aghanim *et al.* (Planck Collaboration), "Planck 2018 results. VI. Cosmological parameters," Astron. Astrophys. **641**, A6 (2020).

[6] P. Bull *et al.*, "Beyond ΛCDM: Problems, solutions, and the road ahead," Phys. Dark Universe **12**, 56 (2016).

[7] S. Weinberg, "The cosmological constant problem," Rev. Mod. Phys. **61**, 1 (1989).

[8] S. M. Carroll, "The Cosmological Constant," Living Rev. Relativ. **4**, 1 (2001).

[9] I. Zlatev, L. M. Wang, and P. J. Steinhardt, "Quintessence, Cosmic Coincidence, and the Cosmological Constant," Phys. Rev. Lett. **82**, 896 (1999).

[10] P. J. Steinhardt, "A quintessential introduction to dark energy," Phil. Trans. R. Soc. A **361**, 2497 (2003).

[11] E. Di Valentino *et al.*, "In the realm of the Hubble tension—a review of solutions," Class. Quantum Grav. **38**, 153001 (2021).

[12] A. G. Adame *et al.* (DESI Collaboration), "DESI 2024 VI: Cosmological Constraints from the Measurements of Baryon Acoustic Oscillations," (2024) [arXiv:2404.03002].

[13] T. M. C. Abbott *et al.* (DES Collaboration), "Dark Energy Survey Year 3 Results: Cosmological Constraints from Galaxy Clustering and Weak Lensing," Phys. Rev. D **109**, 042001 (2024).

[14] M. Vincenzi *et al.* (DES Collaboration), "The Dark Energy Survey: Cosmology Results With Type Ia Supernovae from the Full Five-Year Dataset," (2024) [arXiv:2401.02929].

[15] A. G. Riess *et al.*, "Large Magellanic Cloud Cepheid standards for a 1% determination of the Hubble constant," Astrophys. J. **876**, 85 (2019).

[16] C. W. Misner, K. S. Thorne, and J. A. Wheeler, *Gravitation* (W. H. Freeman, 1973).

[17] A. Einstein, "Die Grundlage der allgemeinen Relativitätstheorie," Ann. Phys. **354**, 769 (1916).

[18] S. Weinberg, *Gravitation and Cosmology: Principles and Applications of the General Theory of Relativity* (John Wiley & Sons, 1972).

[19] H. C. Ohanian and R. Ruffini, *Gravitation and Spacetime*, 3rd ed. (Cambridge University Press, 2013).

[20] H. Choi, "Sphere Theory: Completing Quantum Gravity through Gravitational Self-Energy," (2025). Available at: https://www.researchgate.net/publication/388995044.

[21] J. M. Lattimer and M. Prakash, "Neutron Star Structure and the Equation of State," Astrophys. J. **550**, 426 (2001).

[22] H. Choi, "Dark Energy is Gravitational Potential Energy or Energy of the Gravitational Field," (2022). Available at: https://www.researchgate.net/publication/360096238.

[23] S. Chandrasekhar, "The Post-Newtonian Equations of Hydrodynamics in General Relativity," Astrophys. J. **142**, 1488 (1965).

[24] H. A. Buchdahl, "General Relativistic Fluid Spheres," Phys. Rev. **116**, 1027 (1959).

[25] M. S. R. Delgaty and K. Lake, "Physical Acceptability of Isolated, Static, Spherically Symmetric, Perfect Fluid Solutions of Einstein's Equations," Comput. Phys. Commun. **115**, 395 (1998).

[26] E. A. Milne, "A Newtonian Gravitational Universe," Q. J. Math. **5**, 64 (1934).

[27] W. H. McCrea and E. A. Milne, "Newtonian Universes and the Curvature of Space," Q. J. Math. **5**, 73 (1934).

[28] S. L. Shapiro and S. A. Teukolsky, *Black Holes, White Dwarfs, and Neutron Stars: The Physics of Compact Objects* (John Wiley & Sons, 1983).

[29] J. Binney and S. Tremaine, *Galactic Dynamics*, 2nd ed. (Princeton University Press, 2008).

[30] R. C. Tolman, "Static Solutions of Einstein's Field Equations for Spheres of Fluid," Phys. Rev. **55**, 364 (1939).

[31] J. R. Oppenheimer and G. M. Volkoff, "On Massive Neutron Cores," Phys. Rev. **55**, 374 (1939).

[32] J. F. Navarro, C. S. Frenk, and S. D. M. White, "A Universal Density Profile from Hierarchical Clustering," Astrophys. J. **490**, 493 (1997).

[33] A. A. Dutton and A. V. Macciò, "Cold dark matter haloes in the Planck era: evolution of structural parameters," Mon. Not. R. Astron. Soc. **441**, 3359 (2014).

[34] S. Chandrasekhar, *An Introduction to the Study of Stellar Structure* (University of Chicago Press, 1939).

[35] B. Ryden, *Introduction to Cosmology* (Addison-Wesley, 2003).

[36] H. Choi, "On Problems and Solutions of General Relativity (Commemoration of the 100th Anniversary of General Relativity)," (2015). Available at: https://www.researchgate.net/publication/286935998.

[37] S. W. Hawking and G. F. R. Ellis, *The Large Scale Structure of Space-Time* (Cambridge University Press, 1973).

[38] R. M. Wald, *General Relativity* (University of Chicago Press, 1984).

[39] P. J. E. Peebles, *Principles of Physical Cosmology* (Princeton University Press, 1993).

[40] R. Penrose, "Gravitational Collapse and Space-Time Singularities," Phys. Rev. Lett. **14**, 57 (1965).

[41] S. W. Hawking and R. Penrose, "The Singularities of Gravitational Collapse and Cosmology," Proc. R. Soc. Lond. A **314**, 529 (1970).

[42] V. F. Mukhanov, *Physical Foundations of Cosmology* (Cambridge University Press, 2005).

[43] H. Choi, "The Klein-Gordon-Choi Equation: A Unified Resolution of the Divergences in Quantum Gravity and QED," (2025). Available at: https://www.researchgate.net/publication/398285103.

[44] H. B. Callen, *Thermodynamics and an Introduction to Thermostatistics*, 2nd ed. (John Wiley & Sons, 1985).

[45] T. M. Davis and C. H. Lineweaver, "Expanding Confusion: Common Misconceptions of Cosmological Horizons and the Superluminal Expansion of the Universe," Publ. Astron. Soc. Aust. **21**, 97 (2004), [arXiv:astro-ph/0310808].

[46] S. W. Hawking, "Breakdown of predictability in gravitational collapse," Phys. Rev. D **14**, 2460 (1976).

[47] S. M. Carroll, M. Hoffman, and M. Trodden, "Can the dark energy be a phantom?," Phys. Rev. D **68**, 023509 (2003).

[48] J. M. Cline, S. Jeon, and G. D. Moore, "The Phantom menaced: Constraints on phantom dark energy from particle physics," Phys. Rev. D **70**, 043543 (2004).

[49] R. V. Buniy and S. D. H. Hsu, "Instabilities and the null energy condition," Phys. Lett. B **632**, 543 (2006).

[50] M. Boylan-Kolchin, V. Springel, S. D. M. White, A. Jenkins, and G. Lemson, "Resolving cosmic structure formation with the Millennium-II Simulation," Mon. Not. R. Astron. Soc. **398**, 1150 (2009).

[51] A. Pillepich *et al.*, "First results from the IllustrisTNG simulations: the stellar mass content of groups and clusters of galaxies," Mon. Not. R. Astron. Soc. **475**, 648 (2018).

[52] A. G. Adame *et al.* (DESI Collaboration), "DESI 2024 VI: Cosmological Constraints from the Measurements of Baryon Acoustic Oscillations," (2024) [arXiv:2404.03002].

[53] E. Abdalla *et al.*, "Cosmology intertwined: A review of the particle physics, astrophysics, and cosmology associated with the cosmological tensions and anomalies," J. High Energy Astrophys. **34**, 49 (2022).

[54] A. Amon *et al.* (DES Collaboration), "Dark Energy Survey Year 3 results: Cosmology from cosmic shear and robustness to modeling uncertainty," Phys. Rev. D **105**, 023514 (2022).

[55] R. C. Nunes and S. Vagnozzi, "Arbitrating the S_8 tension with the Hubble tension," Mon. Not. R. Astron. Soc. **505**, 5427 (2021).

[56] Y.-W. Lee *et al.*, "A revised local matter density from Type Ia supernovae and its implication for the Hubble tension," Mon. Not. R. Astron. Soc. **546**, L1 (2025).

[57] I. Labbé *et al.*, "A population of red candidate massive galaxies at $z > 10$," Nature **616**, 266 (2023).

[58] M. Boylan-Kolchin, "Stress Testing ΛCDM with High-redshift Galaxy Candidates," Nat. Astron. **7**, 731 (2023).

[59] T. Saifollahi *et al.* (Euclid Collaboration), "Euclid: Early Release Observations – Globular clusters in the Fornax galaxy cluster," Astron. Astrophys. **686**, A1 (2024).

[60] M. Brouwer *et al.* (KiDS-1000 Collaboration), "KiDS-1000 cosmology: Constraints from density split statistics," Astron. Astrophys. **669**, A69 (2023).

[61] X. Fan *et al.*, "Constraining the Evolution of the Ionizing Background and the Epoch of Reionization with $z \sim 6$ Quasars," Astron. J. **132**, 117 (2006).

[62] K. Inayoshi, E. Visbal, and Z. Haiman, "The Assembly of the First Massive Black Holes," Annu. Rev. Astron. Astrophys. **58**, 27 (2020).

[63] Y. Harikane *et al.*, "Evidence for an Active Galactic Nucleus in a Galaxy at $z \simeq 10$," Astrophys. J. Lett. **959**, L24 (2023).

[64] A. A. Starobinsky, "A new type of isotropic cosmological models without singularity," Phys. Lett. B **91**, 99 (1980).

[65] A. H. Guth, "Inflationary universe: A possible solution to the horizon and flatness problems," Phys. Rev. D **23**, 347 (1981).

[66] A. D. Linde, "A new inflationary universe scenario: A possible solution of the horizon, flatness, homogeneity, isotropy and primordial monopole problems," Phys. Lett. B **108**, 389 (1982).

[67] A. Albrecht and P. J. Steinhardt, "Cosmology for Grand Unified Theories with Radiatively Induced Symmetry Breaking," Phys. Rev. Lett. **48**, 1220 (1982).

[68] J. A. Frieman, M. S. Turner, and D. Huterer, "Dark Energy and the Accelerating Universe," Annu. Rev. Astron. Astrophys. **46**, 385 (2008).

[69] D. Baumann, "TASI Lectures on Inflation," arXiv:0907.5424.

[70] L. Kofman, A. D. Linde, and A. A. Starobinsky, "Reheating after inflation," Phys. Rev. Lett. **73**, 3195 (1994).

[71] B. A. Bassett, S. Tsujikawa, and D. Wands, "Inflation dynamics and reheating," Rev. Mod. Phys. **78**, 537 (2006).

[72] R. Allahverdi, R. Brandenberger, F.-Y. Cyr-Racine, and A. Mazumdar, "Reheating in Inflationary Cosmology: Theory and Applications," Annu. Rev. Nucl. Part. Sci. **60**, 27 (2010).

[73] S. Nojiri and S. D. Odintsov, "Unifying phantom inflation with late-time acceleration: Scalar phantom-non-phantom transition phase and generalized holographic dark energy," Gen. Relativ. Gravit. **38**, 1285 (2006).

[74] J. Preskill, "Do black holes destroy information?," (1992) [arXiv:hep-th/9209058].

[75] L. Susskind, L. Thorlacius, and J. Uglum, "The Stretched Horizon and Black Hole Complementarity," Phys. Rev. D **48**, 3743 (1993) [arXiv:hep-th/9306069].

[76] D. Scolnic *et al.* (Pantheon+ Collaboration), "The Pantheon+ Analysis: The Full Data Set and Cosmological Constraints," Astrophys. J. **938**, 113 (2022).

[77] R. Jimenez and A. Loeb, "Constraining Cosmological Parameters with the Age of Old Galaxies," Astrophys. J. **573**, 37 (2002).

[78] N. Kaiser, “Clustering in real space and in redshift space,” Mon. Not. R. Astron. Soc. **227**, 1 (1987).

[79] H. Choi, “The Physical Origin of the Planck Scale Cutoff and Completion of Perturbative Quantum Gravity,” (2025). Available at: https://www.researchgate.net/publication/397952460.